R. & M. No. 3633

MINISTRY OF TECHNOLOGY

AERONAUTICAL RESEARCH COUNCIL
REPORTS AND MEMORANDA

Studies of the Turbulent Boundary Layer on a Waisted Body of Revolution in Subsonic and Supersonic Flow

By K. G. WINTER, J. C. ROTTA and K. G. SMITH

LONDON: HER MAJESTY'S STATIONERY OFFICE
1970
PRICE £2 0*s* 0*d* NET

Studies of the Turbulent Boundary Layer on a Waisted Body of Revolution in Subsonic and Supersonic Flow

By K. G. WINTER*, J. C. ROTTA** and K. G. SMITH***

Reports and Memoranda No. 3633†
August, 1968

Summary.

The object of the study was to determine the influence of Mach number, pressure gradients and streamline convergence and divergence on the development of turbulent boundary layers. Measurements were made of pressure distribution, local skin friction and boundary-layer profiles along the body, at Mach numbers between 0·6 and 2·8 and Reynolds numbers, based on the length of the body, between 5×10^6 and 2×10^7. The results of comparative calculations based on simultaneous integration of the momentum and kinetic energy equations are generally in fair agreement with the experiments except at the two higher Mach numbers (2·4 and 2·8). The study was a result of collaboration between the Aerodynamische Versuchsanstalt, Göttingen and the Royal Aircraft Establishment, Bedford.

LIST OF CONTENTS

*Royal Aircraft Establishment, Bedford.
**Aerodynamische Versuchsanstalt, Göttingen.
***Formerly at R.A.E. Bedford now at University of Queensland.
†Replaces R.A.E. Technical Report 68 215—A.R.C. 30 935.

---

1. *Introduction.*

For a slender wing supersonic transport aircraft skin friction may contribute about a third of the total drag. Engines are likely to be installed on the wings and their intake design and performance will be strongly influenced by the local boundary-layer conditions on the wing surface. A detailed knowledge of the boundary-layer development over the wings is thus essential.

Following the ideas of Spence[1], methods of calculation for turbulent boundary layers at supersonic speeds on slender wings were developed by Cooke[2]. One of the assumptions in this work was that the relationships between skin friction and Reynolds number based on local boundary-layer momentum thickness could be taken to be the same as on a flat plate, and in fact a power law was used. Calculations of this nature were found inadequate in predicting skin-friction coefficients measured on a cambered delta wing[3]. The inference taken from Ref. 3 was that the skin-friction law used was of a too simple form. The measurements showed that though the total skin-friction drag was fairly close to that of a flat plate, local values as low as half that on a flat plate at the same length Reynolds number were found. These low values occurred in regions where there was convergence of the flow combined with a mild adverse pressure gradient. In Ref. 3, skin friction only was measured and knowledge of the local boundary-layer profiles was clearly required to make any progress in understanding the flow. To avoid the experimental difficulties of boundary-layer exploration on the wing, which would arise from the crossflows, the present study was undertaken.

The main aim of the study was to produce an axisymmetric converging flow with an adverse pressure gradient. At the same time, it was appreciated that general information on the behaviour of turbulent boundary layers in compressible flows with pressure gradients could be of great value in developing and checking methods of calculation, which, in the present state of knowledge, must generally be based upon empirical correlations.

The study was a joint effort of the Aerodynamische Versuchsanstalt Göttingen and the Royal Aircraft Establishment Bedford. The measurements were made in the RAE 8ft × 8ft wind tunnel. A brief description of the work is contained in Ref. 4 and a more complete account in German in Ref. 5.

2. *Model Design.*

The obvious simple example of a supersonic flow with an adverse pressure gradient and converging streamlines is the aft end of a parabolic body of revolution. However, the convergence for a parabolic body increases as the tail is approached, and a more nearly constant value of the convergence parameters was felt to be desirable. (It was, in fact, visualised initially that a series of bodies with various values of convergence and divergence might be studied.) The starting point for the model design was thus a body approximating to a parabolic body over the forepart but with concavity introduced over the aft end. By adding a flare to the body it was hoped to obtain a diverging flow, whilst retaining for some part the adverse pressure gradient.

On the delta wing model of Ref. 3 the convergence of the external flow measured was about 0·04 radian per inch, and values of divergence up to 0·08 radian per inch were found. Since the intended model was to be of the same length (60 in.) as the delta wing and to be tested at the same conditions, it was reasonable to use the same dimensional values of convergence and divergence. This was taken to be 0·05 radian per inch, i.e.

$$\frac{1}{R}\frac{dR}{dX} = \pm 0{\cdot}05 \qquad (2.1)$$

when R and X the body radius and distance from the nose are measured in inches. Equation (2.1) implies an exponential variation of radius with distance but it was found that a cubic equation would give a sensibly constant value of $\frac{1}{R}\frac{dR}{dX}$ over the regions of interest.

The final shape of the model is shown in Fig. 1. Its shape is specified in five sections with continuity of ordinate, slope and curvature at the junctions of the sections except at the end of the conical part of the nose where the curvature is discontinuous. The conical nose has an included angle of 40 degrees, being the largest angle to give an attached shock wave at the lowest supersonic speed of the test ($M_\infty = 1{\cdot}4$). This is followed by a shape defined by a quartic curve which joins the cubic giving approximately constant convergence. A mirror image of this cubic provides the final flare and a quartic fairing curve joins the converging and diverging regions.

The non-dimensional divergence parameter $\frac{\eta'}{\eta}$ where $\eta = \frac{R}{l}$ and the prime denotes differentiation with respect to $x = \frac{X}{l}$, is shown in Fig. 2, together with the non-dimensional longitudinal curvature. The pressure distribution is shown in Fig. 3, and by comparison with Fig. 2, it can be seen that combinations of streamline convergence or divergence, and sign of pressure gradient as in the following table are obtained.

Supersonic speeds

x	0–0·142	0·142–0·3	0·3–0·4	0·4–0·7	0·7–1·0
Streamlines	divergent	divergent	convergent	convergent	divergent
Pressure gradient	zero	favourable	favourable	adverse	slightly adverse

Subsonic speeds

x	0–0·3	0·3–0·7	0·7–1·0
Streamlines	divergent	convergent	divergent
Pressure gradient	favourable	adverse	favourable

All four possible combinations, the last only marginally, are obtained at supersonic speeds but only two at subsonic speed.

Fig. 4 compares the calculated pressure distribution at $M_\infty = 1{\cdot}4$, using linear theory[6], with the measured pressures. Despite the absence of any boundary-layer displacement correction in the calculations the comparison is good.

3. *Experimental Details.*

3.1. *Model Construction.*

The model was constructed of fibreglass skin and bulkheads assembled over a steel core, and filled with foamed resin. The skin and bulkheads were 0·25 inch thick. Pressure tubes were built into the skin and emerged at the model base. 29 tubes were provided along each of two generators 30 degrees apart ($\varphi = 0$ and $\varphi = 30°$) and extra holes at 90 degrees intervals were added at $X = 6, 24, 42, 59$ inches. The pressure holes were 0·03 inch diameter. The hole at $X = 9$ inches $\varphi = 0$ became blocked early in the experiment and could not be cleared.

3.2. *Skin-Friction Measurement.*

Skin friction was measured by the razor blade technique described in Ref. 7. The portions of razor blade (about 0·2 inch square) were mounted over the row of holes at $\varphi = 30$ degrees, and the pressure difference taken from the static pressure measured on the row of holes at $\varphi = 0$ degrees. The height of the razor blades was approximately 0·005 inch. That the presence of the razor blades did not influence the results was checked by repeating measurements with alternate blades removed. The calibration used differed from that given in Ref. 7 being based upon measurements taken during the tests of Ref. 8 in which surface shear was measured directly.

3.3. *Velocity Profiles.*

Boundary-layer profiles were measured using the standard tunnel flow survey equipment. This is illustrated in Figs. 5a and b. Four remotely controlled motions are available with this equipment, a primary rotation coaxial with the model support sting, a secondary rotation about a parallel offset axis at the end of the primary arm, a tertiary rotation about an axis at the end of the secondary arm and a longitudinal motion along this axis. In addition the secondary arm can be adjusted manually through ± 10 degrees about two axes to change the direction of the longitudinal motion. The movement used for profile measurements was the tertiary rotation with an arm of length 3 inches. The probe thus traversed along circular arcs but the distance used in defining the profiles was the radial distance from the body. The survey probe used had five pitot tubes of 0·0195 inch outside diameter and 0·0103 inch inside diameter spaced 0·1 inch apart. The use of multiple tubes enabled a check to be made on any interference and backlash effects by repeating readings at a given point with different tubes, and also of course diminished the time necessary for a traverse. The angular setting was measured in steps of 0·05 degree, i.e. the error was less than or equal to 0·025 degree so that the positional accuracy was 0·0013 inch. The small backlash present in the gear train would give an error in excess of this. The backlash was however largely eliminated by using the surface of the model as datum, and little change in aerodynamic load on the probes would occur during the course of a traverse. Contact was determined electrically by using silver paint on the model surface and a sensitive relay circuit.

The fore and aft travel of the probe is limited to 24 inches so that different extension pieces were required for the forward and rearward parts of the body. Because of the shape of the body it was not possible to align the probes with the local direction of a generator of the body. The misalignment generally was about 5 degrees except for traverses in the waist of the body ($x = 0{\cdot}7$) when it was 11 degrees.

The pressures from the probes were measured using a strain gauge pressure transducer mounted in a pressure switch at the base of the secondary arm. The pressure switch had 24 ways with the connections arranged in four sequences of six each giving five pressures, from the five pitot tubes, plus either a calibration pressure or a zero. Velocities were evaluated from the measured pressures assuming the static pressure to be constant across the boundary-layer thickness*. At subsonic speeds the measured pressure at the wall was used. At supersonic speeds the static pressure was determined from the Mach number evaluated from the pitot reading at the assumed edge of the boundary layer using normal shock relations. A calculated total-pressure loss through the nose shock of the body was taken into account. For the temperature distribution the parabolic formula,

$$\frac{T}{T_\delta} = 1 + r\frac{\gamma - 1}{2} M_\delta^2 \left[1 - \left(\frac{u}{u_\delta} \right)^2 \right] \tag{3.1}$$

was used, and both $r = 1$ (constant total temperature) and $r = 0{\cdot}89$ were taken. For the profiles measured by Nothwang[9] the use of equation (3.1) with $r = 0{\cdot}89$ has been found to give values of momentum thickness which are too high by about 9 per cent at $M = 3$ compared with using his measured temperature distribution. Taking $r = 1$ gives momentum thickness correctly to within about 1 per cent. For the present results Tables 3a and b show a difference at $M_\infty = 2{\cdot}8$ of 6 to 7 per cent for the two assumptions. Similar results are found in Ref. 8. It is interesting to note that the results of Ref. 8 show that the important parameter H_{12}^i has more nearly the correct value by taking $r = 0{\cdot}89$; the error at $M = 2{\cdot}8$ is about $-0{\cdot}3$ per cent compared with $-1{\cdot}1$ per cent for $r = 1$.

The various integral properties of the boundary layer, as defined in the list of symbols, were calculated taking into account the radius of the body. This of course is necessary in order that the quantities in the momentum integral equation do satisfy the equation. The application of the factor $1 + \frac{y}{R}$ in the integrands of quantities such as δ_1^i (*see* Section 5) may be questioned, since in some respects these quantities may be regarded merely as descriptive geometric parameters of the boundary-layer profiles. However, the correlation given in Ref. 8 for compressible boundary-layer profiles on the basis of similarity of 'incompressible' profiles implies some physical significance of the various δ^i. Accordingly the factor $1 + \frac{y}{R}$ in the integrals has been applied consistently throughout. In fact the influence of the factor on the shape parameters used is small.

3.4. *Transition Trip.*

For all experiments a transition trip was attached 1·5 inches from the nose of the body. The trip was of Ballotini of size 0·005 inch. The size proved to be inadequate at Mach numbers above 1·4. Using the criterion of Ref, 10 (established after the initial experiments) a trip of size, 0·013 inch would be required to bring transition forward to the roughness band at $M_\infty = 2{\cdot}8$ and a unit Reynolds number of 1 million per foot.

3.5. *Range of Measurements.*

The range of nominal conditions for the experiments are given in the following tables.

Skin friction

M_∞	0·6	0·8	1·4	1·7	2·0	2·4	2·8
$10^{-6} Re_l$	10	10	5 10 20	10	5 10 17	10	5 10

*Some comment on the effect of normal pressure gradients on the measured profiles is offered in Section 7.3.

Profiles

M_∞	0·6	1·4	1·7	2·0	2·4	2·8
$10^{-6}\,Re_l$	10	10 20	10	10	10	10

Profiles were measured at $x = 0{\cdot}4$, 0·475, 0·55, 0·7, 0·833, 0·983 except for $M_\infty = 1{\cdot}7$, 2·4, 2·8 where $x = 0{\cdot}475$ was omitted.

3.6. *Accuracy.*

For a Reynolds number of 10^7 the pressure coefficients are estimated to have an accuracy of about $\pm 0{\cdot}005$, about half of which arises from possible systematic error and about half from random error. Assuming that the razor blade calibration used is applicable to the conditions of the experiment, the skin-friction coefficients are estimated to be accurate to within $\pm 0{\cdot}0002$. Part of this error is due to inaccuracies in measurement and part due to incorrect fore and aft positioning of the blades with respect to the static holes. The errors will be smaller at the higher Reynolds numbers and larger at the lower Reynolds numbers.

As noted in Section 3.3 the resolution of the system for measuring probe position was about 0·0013 inch. Since the wall was used as datum the accuracy of the distance from the wall was about 0·0026 inch.

The model shape was correct to within 0·01 inch with the slope maintained within 0·001 inch/inch. The maximum eccentricity was 0·006 inch.

4. *Experimental Results.*

Table 1 gives details of pressure, local Mach number and skin-friction distributions along the body. The pressure coefficient is referred to free stream static pressure and kinetic pressure but the skin-friction coefficient is referred to local kinetic pressure.

Table 2 lists the Mach numbers and velocity ratios in the boundary layers against the distance from the wall, y, measured in inches, with data evaluated both for $r = 1$ and $r = 0{\cdot}89$ in the parabolic temperature distribution (equation (3.1)). The assumed edge of the boundary layer is indicated but some points are given beyond the edge. These points are included because they show normal gradients exist in the flow for supersonic speeds. (Pitot pressure outside the boundary layer is, of course, constant in principle for subsonic speeds.) The points are however incorrect because of the assumption of constant static pressure. For example at $M_\infty = 2{\cdot}8$ and $x = 0{\cdot}7$ if the total pressure outside the boundary layer is taken as constant the Mach number rises from 2·759 to 2·812 between $y = 0{\cdot}630$ and $y = 1{\cdot}193$ inches instead of falling from 2·759 to 2·695 as shown in the tabulation. Integral properties of the boundary layers are listed in Table 3.

The velocity profiles are plotted in Fig. 7 and the main results are summarised in Figs. 15 to 26 where comparisons with calculations are made.

5. *Boundary-Layer Properties.*

The experimental results are summarised in Fig. 6 which also illustrates the basic problem that the experiment was designed to study. In the figure, the measured values of local skin-friction coefficient are plotted against Reynolds number based on momentum thickness, with both expressed in intermediate temperature form, using the expression due to Eckert[11], which for zero heat transfer is

$$T^* = 0{\cdot}28\,T_\delta + 0{\cdot}72\,T_w\,. \tag{5.1}$$

For flat plate boundary layers the effects of compressibility are taken into account to within a small percentage by the intermediate temperature hypothesis. It will be seen that for the present model the measurements at the model base fall within ± 10 per cent of the Prandtl-Schlichting line, and for Mach numbers of 1·4, 1·7 and 2·0 the measurements at $x = 0{\cdot}4$ also fall near the line. For $M_\infty = 0{\cdot}6$ the value at $x = 0{\cdot}4$ is low but this might be expected since at subsonic speeds the adverse pressure gradient starts at $x = 0{\cdot}3$. It is however surprising that the values for $x = 0{\cdot}4$ fall well below the line at $M_\infty = 2{\cdot}4$ and 2·8.

The main point of interest is the low values of skin-friction coefficient at the waist of the model. For all Mach numbers tested the value is approximately half that for a flat plate, and it is this feature particularly that the experiment was designed to study.

Velocity profiles are shown in Fig. 7. The profiles for Mach numbers up to 2 are as would be anticipated from Fig. 6, in that hollow profiles are obtained where the skin friction is low. At the highest two Mach numbers, however, the profiles remain full along the whole body.

For incompressible flows the Ludwieg-Tillmann[12] formula relates skin friction to the velocity profile shape by expressing local skin-friction coefficient c_f as a function of Reynolds number based on momentum thickness $\frac{u_\delta \delta_2}{\nu}$ and shape parameter $H_{12} = \frac{\delta_1}{\delta_2}$ where δ_1, δ_2 are displacement and momentum thickness. This relationship cannot be used directly for compressible flows because H_{12} is strongly dependent upon the density distribution through the boundary layer. Walz[13] has suggested instead the use of a parameter $H^i_{12} = \delta^i_1/\delta^i_2$ where δ^i_1, δ^i_2 are evaluated from the velocity profiles as though the flow were incompressible, i.e. ignoring density terms. Walz also suggested that the Reynolds number based on momentum thickness should be modified by using a value of viscosity evaluated at wall conditions. The modified form of the Ludwieg-Tillmann formula is then

$$c_f = 0{\cdot}246 \left(\frac{\rho_\delta u_\delta \delta_2}{\mu_w} \right)^{-0{\cdot}268} 10^{-0{\cdot}678 H^i_{12}} \times k \tag{5.2}$$

where Walz takes $k = \frac{\delta_2}{\delta^i_2}$.

Fig. 8a shows k determined from the measurements of Ref. 8 at Reynolds numbers of the order of 50×10^6. At such high Reynolds numbers the Ludwieg-Tillmann formula gives low values of c_f but the results are nearly parallel to a line with twice the slope of the prediction of Walz, i.e.

$$k = 2\frac{\delta_2}{\delta^i_2} - 1\,. \tag{5.3}$$

(There is obviously an upper limit to the Mach number for which the formula holds, otherwise at high Mach number negative skin friction would be predicted.) Fig. 8b shows the results on the body and though there is considerable scatter the same correlation is roughly applicable. In Fig. 8b the momentum thickness values used are evaluated in accord with the expression for a body of revolution and with the temperature distribution of equation (3.1) with $r = 0{\cdot}89$.

Walz[14] has utilised power law profiles together with a parabolic temperature distribution to calculate relationships between various profile parameters for compressible boundary layers and has suggested approximate general formulae fitting the results of his calculations. It is of interest to see how far his correlations can be applied to the present results. The use also of results of Ref. 8 gives a useful guide to the applicability of the correlations to flat plate conditions. The assumption of power law profiles implies that

$$H^i_{32} = \frac{4 H^i_{12}}{3 H^i_{12} - 1} \tag{5.4}$$

where $H^i_{32} = \frac{\delta^i_3}{\delta^i_2}$, the ratio of kinetic energy thickness to momentum thickness for constant density.

Fig. 9a shows that the flat plate profiles of Ref. 8 (which can be collapsed very closely by a summation of a logarithmic velocity distribution plus a constant wake term) can in fact also be represented well by power laws. The exponent is between 1/7 and 1/9. For the profiles on the body (Fig. 9b) there is much greater disparity with the power law line, particularly at the two higher Mach numbers (note change of scale between Figs. 9a and 9b). At other Mach numbers the points only at both ends of the body are far from the power law line.

In order to derive the compressible shape parameter H_{32} from the 'incompressible' value H_{32}^i Walz has suggested the approximation.

$$H_{32} = H_{32}^i\,[1+(2-H_{32}^i)\,b\,] \tag{5.5}$$

where b is primarily a function of Mach number but also from calculations shows a weak dependence upon H_{32}^i. Walz suggested as an approximation that

$$b = 0{\cdot}004\,M_\delta+0{\cdot}0075\,M_\delta^2-0{\cdot}00018\,M_\delta^4\,. \tag{5.6}$$

Fig. 10a shows that for flat plate profiles a better fit is obtained if the linear term is omitted, i.e.

$$b = 0{\cdot}0075\,M_\delta^2-0{\cdot}00018\,M_\delta^4 \tag{5.7}$$

and the results on the body Fig. 10b are in fair agreement with equation (5.7).

For the ratio of 'incompressible' momentum thickness to actual momentum thickness the suggested correlation is

$$\frac{\delta_2^i}{\delta_2} = 1+r\frac{\gamma-1}{2}M_\delta^2\,H_{32}\,(2-H_{32}^i)\,a \tag{5.8}$$

where r is the recovery factor and a is a function both of H_{32}^i and M_δ, but with b, is only weakly dependent upon H_{32}^i and the dependence can be ignored. Fig. 11 shows that a better fit to both flat plate data and to the results on the body is obtained with

$$a = 1-0{\cdot}043\,M_\delta \tag{5.9}$$

rather than the form suggested by Walz. An even better fit would be obtained with a formula for which a tends to about 0·97 as $M_\delta \to 0$, as also given by the calculations of Ref. 5.

6. *Details of Calculations.*

The calculations are based upon the simultaneous integration of the momentum and kinetic energy equations of the boundary layer. For an isentropic flow over a surface with zero heat transfer these equations may be written

$$d\frac{\delta_2/l}{dx}+\frac{\delta_2}{l}\left[\frac{H_{12}+2}{u_\delta}\frac{du_\delta}{dx}+\frac{1}{\rho_\delta}\frac{d\rho_\delta}{dx}+\frac{1}{\eta}\frac{d\eta}{dx}\right] = \frac{c_f}{2} \tag{6.1}$$

$$d\frac{\delta_3/l}{dx}+\frac{\delta_3}{l}\left[\frac{3}{u_\delta}\frac{du_\delta}{dx}+(2-\gamma)\frac{1}{\rho_\delta}\frac{d\rho_\delta}{dx}+\frac{1}{\eta}\frac{d\eta}{dx}\right] = c_D \tag{6.2}$$

where lengths have been non-dimensionalised by dividing by the body length l. Strictly the streamwise distance should be measured along the body surface. The error involved in using the axial distance has been accepted. Providing the shape factor H_{12}, skin-friction coefficient c_f and dissipation coefficient c_D can be determined, the integration of the two equations can be performed. The basis for the determination of H_{12} is the set of relationships between the various parameters outlined in the preceding section. With the addition of the equation

$$H_{12} = H^i_{12}\frac{\delta^i_2}{\delta_2}+\frac{\gamma-1}{2}M^2_\delta H_{32} \tag{6.3}$$

which is exact for a flow with zero heat transfer, H_{12} can be determined from the values of δ_2, δ_3 obtained from the integration. The skin-friction coefficient is given by the modified Ludwieg-Tillmann formula (equation (5.2)). There remains to be obtained an exprcssion for the dissipation coefficient. For incompressible flow Truckenbrodt[15] has devised an approximate formula on the basis of the analysis of Rotta[16]. On the assumption that the shearing stress distribution is not altered in compressible flow, Walz modified the dissipation formula in the same way as the skin-friction formula. However, the shape of the shear stress distribution is somewhat fuller in compressible flow, and studies of the boundary layer on a flat plate suggested an increase in the ratio H_{32}/H^i_{32}. The following equation was therefore taken

$$c_D = 0{\cdot}012\left(\frac{\rho_\delta u_\delta \delta_2}{\mu_w}\right)^{-0\cdot168}\left(2\frac{\delta_2}{\delta^i_2}-1\right)\frac{H_{32}}{H^i_{32}}. \tag{6.4}$$

The multiplying factor was increased from 0·0112 (Ref. 14) to 0·012 in accord with the studies of Fernholz[17].

The calculations were programmed for an IBM 650 computer, starting from the point $\frac{x}{l} = 0{\cdot}1416$, the end of the conical nose, and assuming that viscosity is given by

$$\frac{\mu}{\mu_\infty} = \left(\frac{T}{T_\infty}\right)^{\frac{3}{4}}. \tag{6.5}$$

The initial values of δ_2 at the end of the conical nose were calculated in the following way. For supersonic flow with an attached shock wave (i.e. for $M_\infty \geqslant 1{\cdot}4$) the pressure on the cone is constant and since $R \propto x$ the momentum equation simplifies to

$$\frac{1}{x}\,\frac{d\left(x\frac{\delta_2}{l}\right)}{dx} = \frac{c_f}{2}. \tag{6.6}$$

For a turbulent boundary layer the skin friction was calculated from the simple power law

$$c_f = 0{\cdot}0256\left(\frac{u_\delta \delta_2}{\nu_\delta}\right)^{-\frac{1}{4}}\left(\frac{c_f}{c_{fi}}\right) \tag{6.7}$$

with the ratio of skin friction for compressible flow to that for incompressible flow estimated from Eckerts' intermediate temperature hypothesis. For laminar flow the Blasius formula gives

$$c_f = (0{\cdot}664)^2\frac{\nu_\delta}{u_\delta \delta_2} \tag{6.8}$$

for incompressible flow. Within the Mach number range under consideration this formula for incompressible flow can be used with little loss of accuracy. Using either equation (6.7) or (6.8) in (6.6) closed formulae can be obtained for δ_2 and c_f. The same formulae were used for subsonic flow although there is a strong favourable gradient with subsonic conditions.

Figs. 12a and b show the calculated values at $x = 0{\cdot}05$ and $x = 0{\cdot}1$ for a Reynolds number $Re_l = 10^7$.

For Mach numbers of 1·7 and greater the measured results at $x = 0{\cdot}05$ (Fig. 12a) are close to the calculated line for laminar flow* and for lower Mach numbers are somewhat lower than the estimate for turbulent flow. As noted earlier the transition trip was of inadequate size at $M_\infty > 1{\cdot}4$. At $x = 0{\cdot}1$ the measurements are close to the calculated turbulent values except for $M_\infty = 2{\cdot}8$ where the flow is still transitional. Fig. 13 shows the calculated values of momentum thickness at $x = 0{\cdot}142$. No measurements are available for comparison.

The parameter H_{32}, in conjunction with δ_2, is also needed to determine a starting value for δ_3. The calculations are not very sensitive to the initial value of δ_3 and so the simplifying assumption was made that H_{32} is constant along the conical forebody. Equations (6.1) and (6.2) then reduce to the simple form.

$$H_{32} = \frac{2\,c_D}{c_f}. \tag{6.9}$$

Substitution of equations (5.2) and (6.4) leads to

$$\left(\frac{\rho_\delta\, u_\delta\, \delta_2}{\mu_\delta}\right)^{0\cdot 1} = \frac{0{\cdot}246}{0{\cdot}024}\,\frac{H^i_{32}}{10^{0\cdot 678}\,H^i_{12}}\left(\frac{\mu_w}{\mu_\delta}\right)^{0\cdot 1} \tag{6.10}$$

from which H^i_{12} can be eliminated by equation (5.4). Use of equation (5.5) then enables H_{32} to be calculated. The values required were read from the chart shown in Fig. 14. The Reynolds number dependence invalidates the initial assumption but the variation of H_{32} is relatively small.

The calculations were made using two different assumptions for the initial conditions; firstly fully turbulent flow was taken over the conical nose and secondly the flow was assumed to be laminar with abrupt transition to turbulent flow at the end of the cone ($x = 0{\cdot}142$). The differences between the two sets of calculations for δ_2 and δ_3 are small at the lower Mach numbers but increase with increase of Mach number. The effect of the different assumptions on skin-friction coefficient is generally small.

The normal definitions for two-dimensional flow of the various boundary-layer parameters in the momentum and kinetic energy equations are valid only if the boundary-layer thickness is small compared with the body radius. The boundary-layer thickness is certainly not small compared with the radius particularly at the waist of the body. However, equations (6.1), (6.2) are still correct provided the appropriate definitions for $\delta_1, \delta_2, \delta_3$ and c_D are used. The definitions are as for two-dimensional flow with the factor $1+\frac{y}{R}$ introduced in the integrands. It is not known how this procedure affects the formula (6.4) for the dissipation coefficient but it is a reasonable assumption that $\left(1+\frac{y}{R}\right)\tau$ does not change greatly with R, so that the equation may approximately be valid. The skin-friction formula, equation (5.2), may also be expected to be approximately correct even when axisymmetric definitions are used for the boundary-layer parameters. The power law relationship equation (5.4) will also be slightly modified by the introduction of the factor $1+\frac{y}{R}$. The other short-coming of both the calculations and the experiment, the assumption of constant static pressure across the boundary layer, is likely to be increasingly inaccurate as the boundary layer becomes thicker with respect to the body radius in regions of high longitudinal curvature.

7. *Discussion of Results.*

7.1. *General.*

The main results of the experiment and comparisons with calculations are shown in Figs. 15 to 26 where schlieren photographs of the flow are also presented. As a check on the compatibility of the measured

*The razor blade calibration used is not necessarily valid in laminar flow.

values of skin-friction coefficient and momentum thickness an extra calculation was made in which the measured values of c_f and H_{12} were used in the momentum equation. This calculation took as a starting point the measured momentum thickness at $x = 0{\cdot}4$, except for $M_\infty = 2{\cdot}4$ where the measured value of δ_2, appears to be inconsistently low. A starting value of $\frac{\delta_2}{l} = 2{\cdot}3 \times 10^{-4}$ was taken instead of the measured value $1{\cdot}8 \times 10^{-4}$. (Why this low value was obtained is not clear. The profile has some appearance of being laminar but skin-friction measurements taken, along a different generator, at the same time as the profiles show no change from the original measurements and there seems no reason why an assymmetry round the body should occur for one particular Mach number.) The calculations are shown as the chain dotted line in Figs. 15, 18, 19, 20, 22, 24, 26. At $M_\infty = 0{\cdot}6$ (Fig. 15) the measured momentum thickness at the waist $x = 0{\cdot}7$ is higher than calculated but it is in good agreement at the end of the body, suggesting that the measurement of skin friction is low up to the waist and possibly high thereafter. At other Mach numbers the calculations and the experiments are in excellent agreement up to $x = 0{\cdot}7$ but the skin friction appears to be too large for $x > 0{\cdot}7$ leading to high values of momentum thickness in the calculations. It must be remarked that the technique for the measurement of skin friction, has not been completely established for the flows in which it has been used.

All the experimental results can be described in the same general way. Up to $x = 0{\cdot}4$ the boundary-layer thickness increases relatively slowly under the influence of a favourable pressure gradient and flow divergence. Between $x = 0{\cdot}4$ and $x = 0{\cdot}7$ the flow convergence and adverse pressure gradient lead to a rapid increase in thickness with a maximum thickness and minimum skin-friction coefficient near the waist, $x = 0{\cdot}7$. The flow divergence downstream of $x = 0{\cdot}7$ promotes a rapid thinning of the boundary layer and an increase in skin-friction coefficient. For $M_\infty = 1{\cdot}4$, $1{\cdot}7$ and $2{\cdot}0$ the shape parameter, H^i_{12}, has a maximum at $x = 0{\cdot}7$ but this feature is not shown at $M_\infty = 2{\cdot}4$ and $2{\cdot}8$. At $M_\infty = 0{\cdot}6$ the peak value of H^i_{12} occurs at least as far forward as $x = 0{\cdot}4$ where the adverse pressure gradient is strongest. In fact H^i_{12} appears to be correlated strongly with the pressure gradient.

There is good qualitative agreement generally between the calculations and the experiments but there are a number of features unexplained quantitatively. At $M_\infty = 0{\cdot}6$ (Fig. 15) the momentum and energy thicknesses calculated are in fair agreement with the measured values but their ratio, H_{32}, is larger than measured. In turn the calculated 'incompressible' shape parameter, H^i_{12}, which has a powerful influence on the skin-friction coefficient, is too small and the calculated skin friction too high. Nevertheless the general shape of the curves is faithfully reproduced. The schlieren photograph merely illustrates the thickening of the boundary layer in the body waist. No profile measurements were made at $M_\infty = 0{\cdot}8$ (Fig. 16) but the skin-friction comparison is similar to that at $M_\infty = 0{\cdot}6$.

At $M_\infty = 1{\cdot}4$, $2{\cdot}0$ and $2{\cdot}8$ (Figs. 17, 21, 25) measurements were made at a Reynolds number Re_l of approximately 5×10^6, when transition did not occur until near the body waist. These results are discussed later (Section 7.4).

For $M_\infty = 1{\cdot}4$, $1{\cdot}7$ and $2{\cdot}0$ and $Re_l \simeq 10^7$ and also for $M_\infty = 1{\cdot}4$, $2{\cdot}0$ and $Re_l \simeq 2 \times 10^7$ the results are fairly similar. The calculations tend to underestimate δ_2 and δ_3 but the ratio, H_{32}, is well calculated. Despite poor agreement for H^i_{12}, for which a strong peak in the body waist is predicted but not measured, the skin friction is in remarkable agreement up to the body waist ($x = 0{\cdot}7$) but the measured increase over the rear flare is underestimated.

At $M_\infty = 2{\cdot}4$ and $2{\cdot}8$ with $Re_l \simeq 10^7$ (Figs. 24 and 26) the experiments and calculations are in poor agreement. The calculations predict the same sort of behaviour as at lower Mach numbers, that is, sharp peaks in δ_2 and δ_3 at the waist with a low value of H_{32} and a peak in the value of H^i_{12}. In fact the peak in H^i_{12} is predicted to increase with increase of Mach number whereas the measurements show the opposite trend. The peak values of both δ_2 and δ_3 as measured at $M_\infty = 2{\cdot}8$ occur downstream of the body waist. The measured skin-friction coefficient is considerably greater than estimated.

This failure of the calculations may arise from inaccuracy in the assumed form for the dissipation coefficient. As can be seen in Figs. 24 and 26 the calculations are very sensitive to the value of H_{32} and a small increase in the dissipation coefficient with increasing Mach number could produce a radical change in the results. Some assessment of the applicability of the formula taken for the dissipation coefficient can be made by calculating a sort of mean value. Equation (6.2) can be integrated to give

$$\int_{x_1}^{x} \frac{c_D}{\delta_3/l}\,dx = ln\,(\delta_3\,\rho_\delta^{2-\gamma}\,u_\delta^3\,R)_x - ln\,(\delta_3\,\rho_\delta^{2-\gamma}\,u_\delta^3\,R)_{x_1}\,. \tag{7.1}$$

By taking $x_1 = 0{\cdot}4$ a 'mean' dissipation coefficient may be defined as

$$C_D = \frac{(\delta_3)_{0\cdot4}}{x-0{\cdot}4}\int_{0\cdot4}^{x}\frac{c_D}{\delta_3}\,dx\,. \tag{7.2}$$

Values of C_D obtained from the measurements and from the calculations are compared in Fig. 27.

Up to $M_\infty = 2$ the experimental points have a fairly similar trend in that initially C_D is overestimated but at $x = 0{\cdot}7$ the predicted C_D is too small. For $x > 0{\cdot}7$ the prediction is too large. The points thus roughly follow the trends of H^i_{12} (Figs. 15 to 22), and it is thus indicated that the expression for the dissipation coefficient should be dependent upon this shape parameter. At $M_\infty = 2{\cdot}4$ the high values of the experimental point can be partly attributed to the low values of δ_3 at $x = 0{\cdot}4$, and remarked upon previously. Nevertheless both for $M_\infty = 2{\cdot}4$ and $2{\cdot}8$ the change between $x = 0{\cdot}55$ and $x = 0{\cdot}7$ follows the trend of H^i_{12} (Figs. 24 and 26).

Some improvements in the details of the method of calculation could thus be made but the method used is essentially applicable only to two-dimensional flows with small streamwise curvature. In the experiment are included the effects of longitudinal and transverse curvature and of flow convergence and divergence. These effects may be expected to modify the basic structure of the boundary layers in ways of which no account is taken in the calculations. Some sonsideration of the effect of longitudinal curvature is given by one of the authors in Ref. 18.

7.2. *The Influence of Pressure Gradient and Streamline Convergence.*

The problem that the present work was intended to study was the combined influence of pressure gradient and streamline convergence on turbulent boundary-layer development. Though, as noted above, the method of calculation devised is not capable of taking into account fully the properties of the flow studied, some qualitative indication of the interaction of pressure gradient and streamline convergence can be obtained. Accordingly, further calculations have been made in which the surface pressure, p and the body radius, R have been taken as constant individually and together. The calculations start from $x = 0{\cdot}3$ which is near the maximum diameter of the body. Results are shown in Figs. 28, 29 and 30 for the momentum thickness, skin-friction coefficient and shape parameter H^i_{12}.

With both p and R constant the boundary layer is as on a flat plate with momentum thickness growing, and skin friction and shape parameter falling, with increasing x. (H^i_{12} increases between $x = 0{\cdot}3$ and $0{\cdot}4$ for supersonic speeds, presumably because of the slightly arbitrary choice of the starting values.) With the radius varying but p constant the boundary layer piles up in the body waist giving an increase in momentum thickness (Fig. 28) and a consequent small decrease in skin friction but the change in H^i_{12} is small. With p only varying the adverse pressure gradient up to the body waist causes an increase in momentum thickness over the flat plate values at $M_\infty = 0{\cdot}6$ and $1{\cdot}4$. At $M_\infty = 2{\cdot}8$ there is however a reduction because of the effect of the combined velocity and density gradient term in the momentum equation which changes sign at about $M = 2{\cdot}4$. The dominating influence of the pressure gradient is on the shape parameter (Fig. 30) which is increased over most of the body and markedly so at the waist for $M_\infty = 1{\cdot}4$ and $2{\cdot}8$. With both p and R varying the pressure gradient effects are amplified considerably. Thus though convergence and divergence of the flow alone produce almost solely geometric effects, appreciable changes in boundary-layer characteristics can be produced when convergence is combined with pressure gradient.

7.3. *Comment on Velocity Profiles.*

The shape parameters shown in Fig. 9b scatter considerably from the assumed power law line and it might be expected that the use of a two parameter family might give an improved correlation. The results of Ref. 8 show that flat plate velocity profiles in the Mach number range 0·2 to 2·8 correlate completely, both in a wall region and a wake region, at a given value of a Reynolds number $\frac{u_\delta \delta_2^i}{\nu_\delta}$ eliminating the scatter of Fig. 9a. It might be expected therefore that a similar correlation exists for boundary layers in pressure gradients with a family of lines with different values of the parameter $\frac{u_\delta \delta_2^i}{\nu_\delta}$. By varying the scale of a cosine wake term such a family has been constructed (Fig. 31). The dependence upon the Reynolds number is too small to explain the scatter of Fig. 9b and the only merit of the profiles is that the lines are rather steeper than a power law line (as are the experiments).

The failure of this approach is explained by plotting the experimental profiles in Clauser fashion (Figs. 32a to g). In these figures the 'law of the wall' lines are those of Ref. 8 but using freestream Mach number to determine the appropriate friction velocity. The feature that emerges from Fig. 32 is that the measured profiles are not all compatible with the wall law. This is so even at $M_\infty = 0{\cdot}6$ for $x = 0{\cdot}833$ and 0·983 and is thus not the fault of the compressibility factors used. The type of flattening of the profiles is similar to that found by Patel[19] in favourable pressure gradients in incompressible flow.

The implication is that, in flows with favourable gradients or strong streamline divergence, calculation methods, such as that developed in this report which depends implicitly on the assumption of an equilibrium type flow, may prove to be unsatisfactory.

To check whether any of the conclusions regarding the behaviour of the velocity profiles are influenced by the assumption of constant static pressure in their evaluation some reappraisal has been undertaken. The pressure distribution through the boundary layer has been calculated utilising, by means of an iterative procedure, equilibrium between normal pressure gradient and local centrifugal acceleration. The calculations are slightly inconsistent, for supersonic speeds, with the profiles previously evaluated in that the constant of integration for the static pressure was determined at the wall rather than at the boundary-layer edge. Velocity profiles calculated using this pressure distribution and the measured pitot pressure are shown for $M_\infty = 0{\cdot}6$ and 2·8 at $x = 0{\cdot}4$ and 0·7 in Fig. 33 (to be compared with Figs. 32a and g). The two positions taken have normal pressure gradients of opposite sign. Though appreciable changes of the profiles result it will be seen that there is no significant improvement in the relationship with the 'law of the wall' lines. A further comparison (Fig. 34) of the shape parameter, H_{12}^i, determined with and without the normal pressure gradient confirms also that in respect of this important parameter the results are little influenced by the neglect of the normal pressure gradient.

7.4. *Laminar Boundary-Layer Calculations.*

At Reynolds number $Re_l \simeq 5 \times 10^6$ at $M_\infty = 1{\cdot}4$, 2·0 and 2·8 (Figs. 17, 21 and 25) the boundary layer over the body apparently remains laminar up to the point at which the adverse pressure gradient becomes steep. This is about $x = 0{\cdot}5$, 0·55 and 0·65 at $M_\infty = 1{\cdot}4$, 2·0 and 2·8 respectively. The change in character of the boundary layer is shown by the jump in the skin-friction coefficient and can also be detected on the schlieren photographs. (Note that the skin friction is deduced from a razor blade calibration for turbulent flow and this cannot be accepted as accurate for a laminar flow.) It is therefore of interest to make laminar boundary-layer calculations.

Such calculations can be made using the basic equations (6.1), (6.2), provided that relations can be established for the various profile parameters. By making use of the Stewartson-Illingworth transformation and writing

$$dY = \frac{\rho}{\rho_\delta} dy \tag{7.3}$$

it follows that the momentum thickness

$$\delta_2 = \int_0^\infty \frac{u}{u_\delta}\left(1-\frac{u}{u_\delta}\right)dY \tag{7.4}$$

and energy thickness

$$\delta_3 = \int_0^\infty \frac{u}{u_\delta}\left\{1-\left(\frac{u}{u_\delta}\right)^2\right\} dY\,. \tag{7.5}$$

A transformed displacement thickness δ_1^+ can be defined as

$$\delta_1^+ = \int_0^\infty \left(1-\frac{u}{u_\delta}\right)dY\,. \tag{7.6}$$

For a Prandtl number of unity the total temperature through the boundary layer is constant so that, with $H_{12}^+ = \dfrac{\delta_1^+}{\delta_2}$,

$$H_{12} = \left(1+\frac{\gamma-1}{2}M_\delta^2\right)H_{12}^+ + \frac{\gamma-1}{2}M_\delta^2\,. \tag{7.7}$$

Taking a one parameter family of profiles, H_{12}^+ and H_{32} are uniquely related independently of M_δ. Furthermore if two functions ε^+ and D^+ are defined as follows

$$\left[\frac{\partial\left(\dfrac{u}{u_\delta}\right)}{\partial\left(\dfrac{Y}{\delta_2}\right)}\right]_w = \varepsilon^+(H_{32}) \tag{7.8}$$

and

$$\int_0^\infty \left[\frac{\partial\left(\dfrac{u}{u_\delta}\right)}{\partial\left(\dfrac{Y}{\delta_2}\right)}\right]^2 d\left(\frac{Y}{\delta_2}\right) = D^+(H_{32}) \tag{7.9}$$

and assuming that $\mu\rho =$ constant then the skin friction and dissipation coefficients can be expressed as

$$c_f = \frac{2\,\nu_\delta}{u_\delta\,\delta_2}\,\varepsilon^+(H_{32}) \tag{7.10}$$

$$c_D = \frac{2\,\nu_\delta}{u_\delta\,\delta_2}\,D^+(H_{32})\,. \tag{7.11}$$

Using Hartree type profiles Walz[20] has developed the following approximate formulae

$$H_{12}^{+} = 4{\cdot}038 - 3{\cdot}341\,(H_{32} - 1{\cdot}519)^{0{\cdot}2879} \tag{7.12}$$

$$\varepsilon^{+} = 1{\cdot}299\,(H_{32} - 1{\cdot}519)^{0{\cdot}6035} \tag{7.13}$$

$$D^{+} = 0{\cdot}1569 + 0{\cdot}1411\,(H_{32} - 1{\cdot}519) + 3{\cdot}810\,(H_{32} - 1{\cdot}519)^{2} - 11{\cdot}75\,(H_{32} - 1{\cdot}519)^{3}\,. \tag{7.14}$$

These formulae were used in equations (6.1), (6.2) with the starting point at $x = 0{\cdot}142$, using equation (6.8) for the skin friction and taking a flat plate value of $H_{32} = 1{\cdot}572$. The results agree qualitatively with the experimental values of skin friction (Figs. 17, 21, 25). Separation of the laminar boundary layer is predicted to occur close to the point at which transition to turbulence apparently occurs at $M_{\infty} = 1{\cdot}4$ and 2·0. No separation is predicted at $M_{\infty} = 2{\cdot}8$ though the measurements are similar to those at the lower Mach numbers but with transition slightly delayed.

Conclusions.

The measurements qualitatively confirm the findings for a delta wing[3] on the effects of combined adverse pressure gradient and streamline convergence in promoting low values of skin friction. Some guidance on these low values can be obtained in terms of local flow conditions by using the Ludwieg-Tillmann formula modified to take compressibility into account.

The calculation method developed, based on simultaneous integration of the momentum and kinetic energy equations, gives fair agreement with the experiments up to a Mach number of 2·0 but is less successful at higher Mach numbers. The main deficiencies of the method probably lie in the formula for the dissipation coefficient and in the single-parameter (power-low) representation of the velocity profiles; also no allowance is made, other than in the evaluation of the integral parameters and equations, for the effects of flow convergence or divergence or of surface curvatures both streamwise and transverse. Further work is needed to identify separately these effects, all of which are combined in the experiment.

The experiment could well be extended to higher Mach numbers and the measurement of temperature profiles through the boundary layers would add to its value.

LIST OF SYMBOLS

a	Defined by equation (5.8)
b	Defined by equation (5.5)
c_D	Local dissipation coefficient
C_D	'Mean' dissipation coefficient (equation (7.2))
c_f	Local skin-friction coefficient
c_{f_i}	Equivalent incompressible skin-friction coefficient
k	Defined by equation (5.2)
l	Body length (60 inches)
M	Mach number
R	Body radius (inches)
R_x	Radius of curvature in longitudinal direction
Re_l	Reynolds number based on free stream conditions and model length
Re_{δ_2}	Reynolds number based on local conditions outside boundary layer and momentum thickness
r	Temperature recovery factor
T	Temperature
u	Velocity
u_τ	Friction velocity
X	Distance along body axis from nose (inches)
x	$= \frac{X}{l}$
η	$= \frac{R}{l}$
y	Distance from body surface (inches)
Y	Defined by equation (7.3)
φ	Angular position round body
γ	Ratio of specific heats
μ	Viscosity
ν	Kinematic viscosity
ρ	Density
τ	Shearing stress

Boundary-layer parameters

δ	Total thickness
δ_1	$= \int_0^\delta \left(1+\frac{y}{R}\right)\left(1-\frac{\rho u}{\rho_\delta u_\delta}\right) dy$ displacement thickness

$\delta_2 \;=\; \int_0^\delta \left(1+\frac{y}{R}\right)\frac{\rho u}{\rho_\delta u_\delta}\left(1-\frac{u}{u_\delta}\right)dy$ momentum thickness

$\delta_3 \;=\; \int_0^\delta \left(1+\frac{y}{R}\right)\frac{\rho u}{\rho_\delta u_\delta}\left[1-\left(\frac{u}{u_\delta}\right)^2\right]dy$ kinetic energy thickness

$\delta_1^i \;=\; \int_0^\delta \left(1+\frac{y}{R}\right)\left(1-\frac{u}{u_\delta}\right)dy$

$\delta_2^i \;=\; \int_0^\delta \left(1+\frac{y}{R}\right)\frac{u}{u_\delta}\left(1-\frac{u}{u_\delta}\right)dy$

$\delta_3^i \;=\; \int_0^\delta \left(1+\frac{y}{R}\right)\frac{u}{u_\delta}\left[1-\left(\frac{u}{u_\delta}\right)^2\right]dy$

$H_{12} \;=\; \frac{\delta_1}{\delta_2}$

$H_{32} \;=\; \frac{\delta_3}{\delta_2}$

$H_{12}^i \;=\; \frac{\delta_1^i}{\delta_2^i}$

$H_{32}^i \;=\; \frac{\delta_3^i}{\delta_2^i}$

δ_1^+ Transformed laminar boundary-layer displacement thickness defined by equation (7.6)

$H_{12}^+ \;=\; \frac{\delta_1^+}{\delta_2}$

ε^+ Defined by equation (7.8)

D^+ Defined by equation (7.9)

Subscripts

∞ Refers to free stream

δ Refers to conditions at edge of boundary layer

w Refers to wall conditions

t Refers to transition point

Superscript

$*$ Refers to intermediate temperature conditions

REFERENCES

No.	*Author(s)*	*Title, etc.*
1	D. A. Spence	The growth of compressible turbulent boundary layers on isothermal and adiabatic walls. A.R.C. R. & M. 3191 (1959).
2	J. C. Cooke	Turbulent boundary layers on delta wings at zero lift. A.R.C. C.P. 696 (1963).
3	K. G. Winter and K. G. Smith	Measurements of skin friction on a cambered delta wing at supersonic speeds. A.R.C. R. & M. 3501 (1965).
4	K. G. Winter, K. G. Smith and J. C. Rotta	Turbulent boundary layer studies on a waisted body of revolution in subsonic and supersonic flow. AGARDograph 97, Pt. 2, pp. 933–961 (1965).
5	K. G. Winter, J. C. Rotta and K. G. Smith	Untersuchungen der turbulenten Grenzschicht an einem taillierten Drehkörper bei Unter- und Überschallströmung. Deutsche Luft-und Raumfart FB 65–52 (1965).
6	W. R. Sears (Ed.)	*High speed aerodynamics and jet propulsion.* Vol. VI General theory of high speed aerodynamics. Oxford University Press, pp. 452–457 (1955).
7	K. G. Smith, L. Gaudet and .. K. G. Winter	The use of surface pitot tubes as skin friction meters at supersonic speeds. A.R.C. R. & M. 3351 (1962).
8	K. G. Winter and L. Gaudet ..	Turbulent boundary layer studies at high Reynolds numbers, at Mach numbers between 0·2 and 2·8. R.A.E. Technical Report in preparation. (*See* also Paper 15 NASA SP-216, Dec. 1968).
9	G. J. Nothwang	An evaluation of four experimental methods for measuring mean properties of a supersonic turbulent boundary layer. NACA Report 1320 (1957).
10	J. Y. G. Evans	Transition fixing techniques and the interpretation of boundary layer conditions on slender wings in supersonic wind tunnels. R.A.E. Technical Note Aero 2946. (A.R.C. 25892) (1964).
11	E. R. G. Eckert	Survey on heat transfers at high speeds. WADC Technical Report 54–70 (1954).
12	H. Ludwieg and W. Tillmann	Untersuchungen über die Wandschubspannung in turbulenten Reibungsschichten. *Ing. Arch.* 17 pp. 288–299 (1949). English translation NACA TM 1285. (A.R.C. 14800) (1950).

No.	*Author(s)*	*Title, etc.*
13	A. Walz	Beitrag nur Näherungstheorie kompressibler turbulenter Granzschichten. DVL Report 84 (1959).
14	A. Walz	Beitrag zur Näherungstheorie kompressibler turbulenter Grenzschichten. 2 Teil: Berechnung der universellen Funktionen und Beispiele. DVL Report 136 (1960). English translation U.S. Library of C3ngress AID Report T–63–110 (1963).
15	E. Truckenbrodt	Ein Quadraturverfahren zur Berechnung der laminaren und turbulenten Reibungsschict bei ebener und rotationssymmetrischer Strömung. *Ing. Arch.* 20, pp. 211–228 (1952). English translation NACA TM 1379 (1955).
16	J. C. Rotta	Schubspannungsverteilung und Energiedissipation bei turbulenten Grenzschichten. *Ing. Arch.* 20, pp. 195–207 (1952).
17	H. Fernholz	Halbempirische Gesetze zur Berechnung turbulenter Grenzschichten nach der Methode der Integralbedingungen. *Ing. Arch.* 23, pp. 384–395 (1964).
18	J. C. Rotta	On the effect of streamwise wall curvature on compressible turbulent boundary layers. AVA Report 66A44 (1966).
19	V. C. Patel	Calibration of the Preston tube and limitations on its use in pressure gradients. *J. Fluid Mech.* Vol. 23, Part 1, pp. 185–208 (1965).
20	A. Walz	Beitrag zur Näherungstheorie kompressibler laminarer Grenzschichten mit Wärmeübergang. DVL Report 281 (1963).

TABLE 1

Pressure Distribution and Skin Friction.

x in	φ deg	$M_\infty = 0.597$ $Re_\ell = 9.85 \times 10^6$ C_p	M_δ	$10^3 c_f$	$M_\infty = 0.801$ $Re_\ell = 9.98 \times 10^6$ C_p	M_δ	$10^3 c_f$	$M_\infty = 1.390$ $Re_\ell = 5.04 \times 10^6$ C_p	M_δ	$10^3 c_f$	$M_\infty = 1.398$ $Re_\ell = 10.2 \times 10^6$ C_p	M_δ	$10^3 c_f$
3.0	0	0.311	0.493	3.92	0.371	0.631	3.66	0.413	1.050	2.52	0.417	1.053	3.88
3.0	90	0.310			0.369			0.407			0.406		
3.0	-180	0.314			0.374			0.409			0.402		
3.0	- 90	0.310			0.368			0.411			0.401		
6.0	0	0.202	0.530	3.70	0.262	0.681	3.70	0.427	1.040	1.91	0.433	1.042	3.79
12.0	0	-0.222	0.666	3.59	-0.218	0.900	3.87	0.153	1.251	0.68	0.151	1.260	1.01
15.0	0	-0.382	0.715	2.80	-0.458	1.012	3.37	-0.040	1.427	2.24	-0.042	1.438	3.56
18.0	0	-0.399	0.720	2.37	-0.499	1.032	2.72	-0.180	1.582	1.78	-0.181	1.593	3.17
21.0	0	-0.313	0.694	2.45	-0.349	0.960	2.37	-0.281	1.715	1.69	-0.281	1.727	3.37
21.0	90	-0.313			-0.348			-0.280			-0.284		
21.0	-180	-0.310			-0.346			-0.279			-0.275		
21.0	- 90	-0.313			-0.350			-0.279			-0.280		
24.0	0	-0.145	0.642	1.83	-0.133	0.861	1.62	-0.273			-0.302	1.759	2.72
27.0	0	-0.004	0.598	1.53	0.027	0.788	1.27	-0.256	1.679	0.65	-0.258	1.695	2.23
28.5	0	0.037	0.585	1.42	0.068	0.770	1.25	-0.248	1.669	0.71	-0.208	1.626	1.92
30.0	0	0.058	0.578	1.35	0.095	0.758	1.20	-0.204	1.611	0.74	-0.154	1.561	1.54
31.5	0	0.073	0.573	1.59	0.108	0.752	1.48	-0.116	1.508	1.97	-0.109	1.509	1.58
33.0	0	0.084	0.569	1.47	0.117	0.748	1.39	-0.062	1.450	2.99	-0.070	1.467	1.43
34.5	0	0.090	0.567	1.47	0.123	0.745	1.42	-0.021	1.409	2.90	-0.038	1.434	1.34
36.0	0	0.103	0.563	1.48	0.137	0.739	1.44	0.009	1.379	2.90	-0.010	1.406	1.31
37.5	0	0.115	0.559	1.31	0.149	0.733	1.35	0.034	1.356	2.58	0.016	1.381	1.16
40.0	0	0.158	0.545	1.31	0.197	0.711	1.19	0.091	1.304	2.24	0.093	1.310	1.00
42.0	0	0.183	0.537	1.43	0.221	0.700	1.38	0.196	1.215	1.73	0.166	1.247	0.83
42.0	90	0.181			0.218			0.191			0.166		
42.0	-180	0.182			0.222			0.198			0.168		
42.0	- 90	0.178			0.219			0.191			0.165		
44.0	0	0.168	0.542	1.40	0.208	0.707	1.29	0.249	1.173	1.75	0.200	1.219	0.91
45.5	0	0.138	0.552	1.62	0.178	0.720	1.53	0.228	1.182	2.02	0.198	1.221	1.14
47.0	0	0.118	0.558	1.72	0.150	0.733	1.74	0.208	1.206	2.24	0.188	1.229	1.33
48.5	0	0.103	0.563	1.76	0.133	0.740	1.79	0.191	1.219	2.46	0.178	1.237	1.56
50.0	0	0.092	0.567	1.85	0.128	0.743	1.84	0.188	1.222	2.50	0.176	1.238	1.71
51.5	0	0.086	0.569	1.79	0.124	0.745	1.70	0.186	1.223	2.30	0.178	1.237	1.70
53.0	0	0.074	0.573	2.12	0.116	0.748	2.02	0.197	1.215	2.63	0.188	1.229	1.97
54.5	0	0.058	0.578	2.10	0.097	0.757	2.06	0.197	1.215	2.63	0.190	1.227	2.05
56.0	0	0.037	0.585	2.10	0.077	0.766	2.09	0.218	1.197	2.44	0.207	1.213	2.00
57.5	0	-0.000	0.597	2.27	0.038	0.783	2.30	0.229	1.189	2.63	0.222	1.201	2.09
59.0	0	-0.083	0.623	2.47	-0.047	0.822	2.54	0.248	1.174	2.56	0.236	1.189	2.17
59.0	90	-0.074			-0.037			0.254			0.244		
59.0	-180	-0.080			-0.044			0.246			0.237		
59.0	- 90	-0.081			-0.045			0.253			0.237		

TABLE 1—*continued*

		$M_\infty = 1.404$, $Re_\ell = 19.97 \times 10^6$			$M_\infty = 1.700$, $Re_\ell = 10.08 \times 10^6$			$M_\infty = 1.996$, $Re_\ell = 4.98 \times 10^6$			$M_\infty = 2.000$, $Re_\ell = 9.96 \times 10^6$		
x in	φ deg	c_p	M_δ	$10^3\ c_f$	c_p	M_δ	$10^3\ c_f$	c_p	M_δ	$10^3\ c_f$	c_p	M_δ	$10^3\ c_f$
3.0	0	0.417	1.057	3.95	0.360	1.319	1.40	0.333	1.553	1.91	0.325	1.567	1.27
3.0	90	0.403			0.354			0.334			0.327		
3.0	−180	0.400			0.350			0.330			0.324		
3.0	− 90	0.408			0.350			0.329			0.323		
6.0	0	0.437	1.043	3.20	0.368	1.311	3.93	0.333	1.553	1.44	0.336	1.556	3.63
12.0	0	0.155	1.261	0.91	0.166	1.501	3.69	0.166	1.737	1.42	0.163	1.749	3.20
15.0	0	−0.040	1.442		0.000	1.696		0.029	1.933	1.46	0.022	1.954	2.54
18.0	0	−0.179	1.598	2.76	−0.115	1.870	2.58	−0.075	2.130	1.12	−0.080	2.154	2.10
21.0	0	−0.282	1.738	2.99	−0.201	2.036	2.75	−0.141	2.298	1.14	−0.150	2.341	2.19
21.0	90	−0.284			−0.199			−0.140			−0.149		
21.0	−180	−0.279			−0.198			−0.141			−0.149		
21.0	− 90	−0.277			−0.196			−0.140			−0.148		
24.0	0	−0.299	1.763	2.31	−0.223	2.086	2.34	−0.162	2.360	0.29	−0.173	2.416	1.88
27.0	0	−0.253	1.695	1.93	−0.196	2.025	1.96	−0.139	2.291	0.36	−0.160	2.372	1.73
28.5	0	−0.206	1.632	1.73	−0.168	1.966	1.90	−0.138			−0.140	2.310	1.69
30.0	0	−0.156	1.570	1.46	−0.134	1.903	1.60	−0.134			−0.116	2.244	1.50
31.5	0	−0.110	1.517	1.59	−0.104	1.852	1.67	−0.115			−0.094	2.187	1.47
33.0	0	−0.069	1.472	1.40	−0.074	1.803	1.47	−0.083	2.149	0.30	−0.070	2.134	1.44
34.5	0	−0.038	1.441	1.40	−0.050	1.767	1.38	−0.056	2.089	1.56	−0.051	2.093	1.34
36.0	0	−0.010	1.412	1.45	−0.029	1.737	1.38	−0.025	2.029	2.60	−0.033	2.054	1.33
37.5	0	0.016	1.386	1.26	−0.007	1.706	1.20	0.001	1.981	2.38	−0.015	2.021	1.16
40.0	0	0.089	1.318	1.13	0.046	1.637	1.07	0.038	1.917	2.49	0.024	1.951	1.11
42.0	0	0.174	1.245	0.86	0.123	1.547	0.83	0.118	1.799	2.24	0.095	1.840	0.85
42.0	90	0.171			0.122			0.106			0.092		
42.0	−180	0.174			0.125			0.112			0.100		
42.0	− 90	0.169			0.122			0.108			0.093		
44.0	0	0.211	1.215	0.90	0.169	1.498	0.92	0.181	1.718	2.20	0.147	1.770	0.94
45.5	0	0.205	1.219	1.17	0.172	1.495	1.18	0.181	1.719	2.51	0.154	1.761	1.23
47.0	0	0.191	1.231	1.40	0.163	1.504	1.46	0.173	1.728	2.45	0.150	1.765	1.53
48.5	0	0.180	1.241	1.54	0.156	1.512	1.75	0.163	1.740	2.60	0.145	1.772	1.82
50.0	0	0.181	1.239	1.65	0.156	1.512	1.93	0.157	1.748	2.64	0.144	1.773	1.98
51.5	0	0.182	1.239	1.56	0.154	1.513	1.94	0.153	1.753	2.44	0.142	1.776	1.96
53.0	0	0.194	1.229	1.83	0.164	1.504	2.23	0.157	1.748	2.75	0.148	1.767	2.26
54.5	0	0.194	1.229	1.87	0.162	1.505	2.38	0.160	1.744	2.69	0.150	1.766	2.35
56.0	0	0.210	1.216	1.83	0.178	1.489	2.27	0.174	1.727	2.44	0.165	1.746	2.17
57.5	0	0.224	1.204	1.90	0.190	1.476	2.38	0.184	1.715	2.59	0.175	1.734	2.33
59.0	0	0.239	1.192	1.95	0.202	1.464	2.43	0.194	1.702	2.58	0.185	1.721	2.37
59.0	90	0.249			0.211			0.199			0.188		
59.0	−180	0.240			0.204			0.191			0.181		
59.0	− 90	0.245			0.206			0.194			0.184		

TABLE 1—*continued*

x in	φ deg	$M_\infty = 2.002$, $Re_\ell = 16.85 \times 10^6$ C_p	M_δ	$10^3\ c_f$	$M_\infty = 2.401$, $Re_\ell = 10.03 \times 10^6$ C_p	M_δ	$10^3\ c_f$	$M_\infty = 2.793$, $Re_\ell = 5.03 \times 10^6$ C_p	M_δ	$10^3\ c_f$	$M_\infty = 2.799$, Re_ℓ 10.05×10^6 C_p	M_δ	$10^3\ c_f$
3.0	0	0.330	1.564	3.50	0.307	1.868	1.11	0.300	2.133	1.49	0.291	2.153	1.06
3.0	90	0.331			0.306			0.298			0.289		
3.0	-180	0.323			0.304			0.299			0.288		
3.0	- 90	0.322			0.302			0.294			0.286		
6.0	0	0.337	1.557	2.99	0.312	1.862	3.35	0.301	2.132	1.10	0.292	2.151	2.34
12.0	0	0.162	1.752	2.83	0.165	2.058	2.73	0.168	2.336	1.12	0.158	2.364	2.35
15.0	0	0.019	1.962	2.40	0.038	2.292	2.05	0.056	2.580	0.85	0.040	2.636	1.83
18.0	0	-0.081	2.162	2.01	-0.050	2.528	1.73	-0.028	2.859	0.93	-0.036	2.908	1.57
21.0	0	-0.153	2.354	2.17	-0.109	2.756	1.78	-0.048	2.950	1.06	-0.082	3.162	1.45
21.0	90	-0.152			-0.108			-0.049			-0.080		
21.0	-180	-0.150			-0.110			-0.046			-0.080		
21.0	- 90	-0.151			-0.106			-0.041			-0.078		
24.0	0	-0.176	2.430	1.82	-0.130	2.865	1.50	-0.074			-0.1[illegible]1	3.301	1.13
27.0	0	-0.163	2.385	1.60	-0.123	2.826	1.39	-0.065			-0.096	3.261	1.04
28.5	0	-0.142	2.321	1.58	-0.111	2.766	1.39	-0.068	3.050	0.35	-0.089	3.208	1.09
30.0	0	-0.118	2.252	1.35	-0.094	2.691	1.31	-0.066	3.043	0.45	-0.077	3.131	1.21
31.5	0	-0.096	2.196	1.42	-0.080	2.633	1.29	-0.068	3.051	0.87	-0.066	3.064	1.14
33.0	0	-0.074	2.143	1.35	-0.063	2.571	1.24	-0.066	3.039	0.41	-0.056	3.005	1.13
34.5	0	-0.053	2.099	1.27	-0.048	2.522	1.18	-0.061	3.011	0.31	-0.045	2.954	1.23
36.0	0	-0.035	2.061	1.26	-0.036	2.484	1.22	-0.050			-0.031	2.890	1.03
37.5	0	-0.017	2.026	1.11	-0.022	2.444	1.09	-0.037			-0.021	2.844	0.95
40.0	0	0.022	1.957	1.11	0.009	2.361	1.04	0.008	2.724	0.63	0.004	2.751	0.98
42.0	0	0.095	1.842	0.83	0.066	2.233	0.91	0.068	2.547	1.55	0.053	2.600	0.83
42.0	90	0.091			0.064			0.066			0.048		
42.0	-180	0.093			0.069			0.070			0.052		
42.0	- 90	0.090			0.064			0.069			0.050		
44.0	0	0.147	1.771	0.88	0.119	2.134	1.00	0.131	2.407	1.96	0.106	2.468	0.93
45.5	0	0.153	1.763	1.22	0.131	2.114	1.33	0.147	2.376	2.19	0.122	2.435	1.21
47.0	0	0.148	1.769	1.55	0.132	2.112	1.53	0.145	2.378	2.06	0.125	2.429	1.36
48.5	0	0.143	1.776	1.79	0.127	2.120	1.78	0.137	2.395	2.18	0.120	2.438	1.56
50.0	0	0.143	1.776	1.93	0.128	2.118	1.90	0.136	2.397	2.20	0.121	2.437	1.68
51.5	0	0.140	1.780	1.87	0.129	2.117	1.77	0.138	2.393	1.73	0.122	2.435	1.51
53.0	0	0.147	1.771	2.13	0.133	2.110	2.08	0.140	2.389	2.06	0.126	2.426	1.77
54.5	0	0.148	1.770	2.20	0.135	2.106	2.12	0.136	2.397	2.20	0.127	2.424	1.83
56.0	0	0.162	1.752	2.04	0.148	2.086	1.94	0.149	2.372	2.01	0.137	2.404	1.72
57.5	0	0.174	1.737	2.14	0.157	2.070	2.09	0.152	2.366	2.19	0.144	2.390	1.87
59.0	0	0.183	1.726	2.14	0.167	2.056	2.15	0.167	2.337	2.05	0.155	2.369	1.88
59.0	90	0.186			0.170			0.172			0.159		
59.0	-180	0.176			0.164			0.168			0.152		
59.0	- 90	0.181			0.167			0.166			0.156		

TABLE 2

Velocity Profiles.

Table 2a $M_\infty = 0.597$ $Re_\ell = 9.98 \times 10^6$

x = 0.4

y in	M	$\frac{u}{u_\delta}$ r = 0.89	$\frac{u}{u_\delta}$ r = 1
00.010	0.3251	0.5201	0.5217
00013	03276	05240	05256
00015	03303	05283	05299
00020	03441	05498	05514
00030	03624	05784	05800
00045	03847	06132	06148
00060	04091	06510	06525
00075	04321	06864	06879
00090	04553	07219	07233
00098	04728	07487	07500
00100	04744	07511	07525
00103	04762	07538	07552
00105	04771	07552	07565
00108	04830	07642	07656
00115	04882	07721	07734
00117	04969	07852	07865
00132	05146	08121	08132
00140	05215	08224	08235
00146	05355	08434	08444
00162	05535	08703	08712
00165	05498	08648	08657
00176	05707	08960	08967
00190	05883	09219	09225
00190	05786	09076	09082
00192	05845	09163	09169
00193	05890	09229	09235
00195	05902	09247	09253
00200	05959	09332	09337
00202	05937	09299	09304
00210	06050	09466	09470
00215	06019	09420	09424
00225	06150	09612	09615
00226	06145	09604	09607
00239	06253	09763	09765
00239	06223	09719	09721
00252	06291	09818	09819
00253	06344	09895	09896
00269	06380	09948	09948
00275	06385	09955	09955
00281	06404	09983	09983
00282	06410	09992	09992
00283	06404	09983	09983
00286	06401	09978	09978
00290	06410	09992	09992
00292	06410	09992	09992
00300	06410	09992	09992
00300	06408	09988	09988
00315	06421	10008	10008
00413	06418	10002	10002
00522	06421	10008	10008
00595	06418	10002	10002

x = 0.475

y in	M	$\frac{u}{u_\delta}$ r = 0.89	$\frac{u}{u_\delta}$ r = 1
00.010	0.2795	0.4702	0.4715
00013	02835	04774	04787
00018	02914	04914	04927
00043	03170	05367	05381
00058	03338	05665	05678
00074	03447	05854	05868
00090	03592	06107	06121
00104	03692	06281	06295
00105	03701	06297	06310
00107	03692	06281	06295
00112	03721	06333	06346
00120	03864	06579	06592
00122	03846	06548	06562
00138	03975	06770	06783
00148	04072	06938	06951
00152	04143	07059	07072
00168	04252	07245	07257
00174	04302	07331	07343
00184	04376	07457	07469
00199	04519	07698	07709
00200	04519	07698	07709
00203	04565	07777	07788
00206	04580	07801	07812
00207	03050	05157	05170
00211	04642	07906	07916
00215	04678	07967	07978
00221	04716	08031	08042
00236	04875	08297	08307
00240	04875	08297	08307
00252	04973	08461	08470
00266	05082	08644	08652
00267	05082	08644	08652
00282	05182	08809	08816
00293	05260	08940	08946
00298	05292	08992	08998
00300	05356	09097	09102
00303	05344	09077	09083
00308	05375	09128	09134
00314	05418	09200	09205
00317	05424	09210	09215
00333	05528	09381	09385
00340	05589	09480	09483
00348	05625	09539	09542
00363	05707	09673	09675
00365	05719	09693	09695
00379	05764	09767	09769
00390	05821	09860	09861
00394	05833	09879	09880
00400	05839	09888	09889
00403	05861	09924	09925
00408	05861	09924	09925
00408	05866	09933	09933
00418	05873	09943	09944
00434	05900	09988	09988
00435	05895	09979	09979
00449	059.00	09988	09988
00460	05900	09988	09988
00460	05900	09988	09988
00464	05905	09996	09996
00561	05905	09996	09996
00646	05912	10006	10006
00740	05912	10006	10006
00840	05917	10015	10015

x = 0.55

y in	M	$\frac{u}{u_\delta}$ r = 0.89	$\frac{u}{u_\delta}$ r = 1
00.010	0.2512	0.4505	0.4517
00013	02583	04631	04643
00015	02639	04730	04742
00018	02735	04900	04912
00020	02748	04922	04934
00025	02788	04993	05005
00035	02890	05174	05186
00051	03034	05427	05440
00065	03142	05616	05629
00081	03245	05797	05810
00097	03332	05950	05963
00105	03297	05888	05901
00108	03340	05964	05977
00110	03400	06069	06081
00112	03417	06099	06112
00113	03422	06107	06120
00115	03432	06124	06137
00120	03412	06090	06103
00131	03485	06218	06231
00140	03545	06322	06335
00147	03573	06371	06384
00162	03663	06528	06540
00170	03692	06579	06592
00177	03759	06695	06708
00193	03853	06858	06870
00196	03836	06828	06840
00207	03862	06873	06885
00209	03915	06965	06977
00209	03925	06983	06995
00211	03946	07019	07031
00215	03973	07066	07078
00216	03982	07081	07093
00222	03982	07081	07093
00232	04035	07173	07185
00237	04059	07215	07227
00248	04128	07333	07344
00263	04220	07491	07502
00265	04229	07508	07519
00278	04311	07649	07659
00292	04384	07774	07784
00295	04415	07827	07837
00304	04395	07793	07803
00307	04448	07883	07894
00310	04472	07924	07934
00310	04484	07945	07955
00312	04495	07964	07974
00315	04479	07936	07946
00320	04517	08001	08010
00330	04563	08079	08089
00338	04660	08246	08254
00346	04645	08219	08228
00362	04790	08467	08475
00367	04819	08515	08522
00377	04874	08609	08617
00392	04910	08669	08677
00394	04916	08680	08688
00401	04936	08713	08720
00404	04980	08788	08795
00406	04987	08799	08806
00408	05026	08866	08872
00408	04979	08786	08792
00411	05005	08831	08838
00416	05020	08855	08861
00427	05066	08934	08940
00437	05126	09035	09041
00442	05158	09089	09094
00457	05248	09240	09245
00465	05223	09198	09202
00466	05254	09250	09255
00473	05306	09337	09341
00489	05380	09460	09464
00492	05374	09451	09454
00505	05441	09563	09566
00533	05561	09763	09765
00559	05592	09814	09815
00562	05633	09882	09882
00588	05673	09949	09949
00622	05685	09969	09969
00660	05708	10006	10006
00716	05696	09985	09987
00726	05690	09978	09978
00726	05678	09958	09958
00757	05708	10006	10006
00855	05708	10006	10006
00921	05690	09978	09978
01012	05703	09998	09998
01115	05703	09998	09998

Table 2a (Contd)

x = 0.7				x = 0.833				x = 0.983			
y in	M	$\frac{u}{u_\delta}$ r = 0.89	$\frac{u}{u_\delta}$ r = 1	y in	M	$\frac{u}{u_\delta}$ r = 0.89	$\frac{u}{u_\delta}$ r = 1	y in	M	$\frac{u}{u_\delta}$ r = 0.89	$\frac{u}{u_\delta}$ r = 1
00.010	0.2271	0.4312	04322	00.010	0.3129	0.5631	0.5644	00.010	0.4084	0.6688	0.6702
00012	02282	04333	04343	00015	03204	05763	05776	00012	04088	06694	06709
00015	02315	04395	04406	00017	03172	05707	05720	00015	04152	06796	06811
00018	02341	04443	04454	00020	03232	05814	05827	00020	04223	06909	06923
00020	02373	04504	04515	00022	03289	05914	05927	00020	04275	06991	07005
00025	02436	04623	04634	00027	03348	06017	06030	00025	04389	07170	07184
00030	02454	04655	04666	00031	03415	06135	06148	00030	04508	07358	07372
00035	02498	04738	04749	00038	03480	06250	06263	00035	04541	07411	07424
00040	02528	04795	04806	00043	03544	06363	06376	00040	04592	07492	07505
00045	02545	04826	04837	00048	03605	06470	06482	00050	04713	07680	07693
00050	02587	04906	04917	00054	03637	06526	06539	00060	04791	07803	07816
00060	02632	04990	05001	00063	03707	06649	06661	00072	04890	07958	07970
00070	02674	05067	05079	00074	03747	06719	06731	00082	04927	08016	08027
00080	02729	05172	05183	00085	03826	06856	06869	00092	04972	08086	08097
00090	02757	05223	05235	00095	03845	06890	06902	00103	05038	08188	08199
00100	02775	05257	05269	00105	03873	06939	06951	00108	05105	08293	08304
00101	02846	05390	05402	00108	03941	07056	07068	00112	05125	08323	08333
00104	02841	05379	05391	00111	03913	07009	07021	00115	05125	08323	08333
00106	02867	05429	05440	00114	03918	07016	07028	00120	05102	08288	08299
00109	02849	05396	05407	00117	03928	07035	07046	00120	05144	08353	08363
00111	02849	05396	05407	00120	03937	07049	07061	00125	05129	08330	08341
00116	02902	05493	05505	00125	03947	07067	07079	00130	05150	08362	08372
00120	02876	05445	05456	00130	03984	07132	07144	00135	05186	08419	08428
00125	02902	05493	05505	00135	04013	07182	07194	00140	05182	08411	08421
00130	02916	05520	05532	00140	04003	07165	07176	00150	05216	08465	08474
00136	02902	05493	05505	00145	04039	07228	07240	00160	05238	08498	08508
00140	02978	05636	05648	00151	04021	07197	07208	00170	05258	08529	08538
00150	02978	05636	05648	00161	04058	07260	07271	00181	05299	08593	08602
00160	03028	05729	05740	00171	04112	07354	07365	00192	05313	08614	08623
00170	03028	05729	05740	00182	04147	07416	07427	00203	05333	08645	08654
00180	03090	05845	05857	00193	04130	07385	07396	00206	05336	08650	08658
00190	03104	05870	05881	00202	04200	07507	07518	00210	05355	08680	08688
00195	03096	05855	05867	00205	04192	07494	07505	00212	05354	08678	08686
00197	03128	05914	05926	00207	04167	07450	07461	00217	05366	08696	08704
00200	03104	05870	05881	00210	04175	07463	07474	00217	05378	08715	08723
00203	03149	05954	05965	00212	04185	07480	07491	00223	05385	08726	08734
00205	03136	05929	05941	00215	04181	07474	07484	00227	05399	08747	08755
00210	03172	05997	06009	00218	04206	07517	07528	00232	05378	08715	08723
00215	03159	05973	05985	00222	04216	07534	07545	00239	05387	08728	08737
00220	03206	06060	06072	00227	04225	07551	07562	00248	05433	08799	08807
00225	03196	06041	06052	00230	04250	07594	07605	00259	05454	08831	08839
00230	03206	06060	06072	00233	04225	07551	07562	00270	05440	08811	08819
00235	03219	06084	06095	00243	04284	07653	07664	00280	05512	08921	08928
00245	03275	06188	06199	00249	04294	07670	07680	00290	05519	08932	08939
00255	03320	06271	06282	00260	04318	07712	07722	00300	05525	08941	08948
00265	03332	06294	06305	00270	04352	07770	07780	00306	05584	09031	09038
00275	03364	06353	06364	00280	04369	07799	07809	00308	05591	09042	09049
00285	03386	05394	06405	00290	04393	07840	07850	00311	05584	09031	09038
00293	03477	06562	06573	00301	04426	07897	07907	00316	05594	09047	09053
00295	03453	06518	06529	00306	04460	07956	07966	00316	05594	09047	09053
00298	03432	06478	06490	00308	04469	07972	07982	00321	05600	09055	09062
00301	03482	06570	06581	00310	04476	07984	07994	00326	05612	09075	09081
00303	03482	06570	06581	00314	04469	07972	07982	00331	05620	09086	09092
00308	03482	06570	06581	00316	04456	07950	07960	00337	05628	09099	09106
00313	03503	06609	06620	00318	04456	07950	07960	00347	05672	09166	09171
00317	03535	06669	06680	00324	04491	08009	08019	00357	05666	09157	09163
00323	03556	06708	06719	00329	04514	08049	08058	00365	05691	09195	09201
00328	03556	06708	06719	00335	04521	08061	08071	00368	05690	09193	09199
00333	03565	06724	06736	00340	04537	08089	08098	00379	05709	09223	09228
00343	03597	06783	06794	00345	04546	08104	08113	00390	05734	09261	09266
00349	03579	06750	06761	00350	04593	08185	08194	00400	05778	09328	09333
00352	03617	06821	06832	00360	04600	08197	08206	00400	05764	09307	09312
00363	03647	06874	06885	00367	04605	08206	08215	00403	05790	09347	09351
00373	03675	06928	06939	00370	04631	08251	08260	00405	05783	09336	09341
00382	03735	07037	07047	00380	04654	08289	08298	00410	05805	09369	09374
00385	03741	07049	07059	00392	04662	08304	08313	00410	05793	09351	09355
00388	03728	07025	07035	00402	04718	08400	08408	00415	05805	09369	09374
00390	03719	07009	07019	00402	04700	08368	08377	00420	05805	09369	09374
00394	03735	07037	07047	00403	04725	08412	08420	00425	05811	09378	09382
00396	03735	07037	07047	00405	04733	08426	08434	00430	05813	09382	09386
00401	03765	07092	07103	00408	04718	08400	08408	00441	05831	09409	09413
00405	03784	07128	07138	00410	04713	08391	08400	00451	05855	09445	09449
00410	03793	07144	07154	00413	04728	08417	08426	00463	05874	09474	09478
00415	03804	07163	07174	00418	04745	08446	08454	00465	05886	09492	09496
00420	03842	07233	07243	00423	04767	08483	08491	00473	05898	09510	09514
00425	03861	07268	07278	00429	04760	08472	08480	00484	05932	09563	09566
00435	03861	07268	07278	00434	04775	08498	08505	00494	05934	09565	09568
00437	03900	07340	07350	00439	04803	08546	08553	00562	06017	09691	09693
00445	03896	07333	07343	00445	04812	08560	08567	00626	06115	09838	09839
00455	03906	07351	07362	00455	04833	08596	08604	00661	06149	09890	09890
00465	03980	07486	07496	00463	04867	08655	08662	00723	06181	09939	09939
00475	03998	07519	07529	00465	04871	08660	08668	00758	06187	09948	09948
00529	04159	07813	07823	00475	04885	08685	08692	00887	06213	09987	09987
00593	04319	08104	08112	00485	04927	08757	08763	00983	06213	09987	09987
00625	04480	08397	08405	00497	04964	08819	08825	01083	06196	09961	09961
00680	04596	08607	08613	00561	05089	09031	09037	01182	06218	09995	09995
00715	04724	08837	08842	00628	05268	09334	09338	01278	06213	09987	09987
00770	04833	09032	09037	00662	05361	09492	09495				
00833	05016	09361	09364	00722	05473	09680	09682				
00865	05118	09542	09544	00757	05512	09746	09748				
00917	05256	09788	09789	00819	05578	09857	09858				
00955	05269	09811	09812	00885	05626	09937	09937				
01006	05295	09857	09857	00920	05663	09998	09998				
01070	05329	09917	09918	01014	05657	09989	09989				
01101	05365	09980	09980	01141	05661	09995	09995				
01239	05352	09957	09958	01228	05661	09995	09995				
01330	05384	10015	10015	01325	05638	09957	09957				
01415	05377	10002	10002	01421	05663	09998	09998				
01523	05348	09950	09950	01513	05657	09989	09989				
01637	05373	09995	09995								
01770	05380	10007	10007								
01851	05380	10007	10007								

Table 2b $M_\infty = 1.398$ $Re_\ell = 10.08 \times 10^6$

x = 0.4

y in	M	$\frac{u}{u_\delta}$ r = 0.89	$\frac{u}{u_\delta}$ r = 1
00.010	0.8772	0.5808	0.5891
00013	08877	05869	05952
00015	09078	05985	06068
00017	09240	06078	06161
00020	09520	06237	06319
00025	09929	06466	06547
00030	10258	06647	06726
00045	11103	07099	07174
00060	11905	07511	07581
00075	12622	07866	'07930
00090	13274	08177	08235
00098	13838	08437	08489
00100	13873	08453	08504
00103	13961	08493	08543
00105	14014	08517	08567
00108	14118	08564	08612
00110	14031	08525	08574
00112	14309	08649	08695
00117	14444	08708	08753
00130	14729	08832	08874
00132	14893	08903	08942
00146	15390	09113	09146
00155	15516	09165	09197
00162	15764	09267	09295
00176	15948	09342	09367
00180	16068	09390	09413
00190	16629	09611	09627
00193	16645	09617	09632
00195	16702	09639	09653
00197	16615	09606	09621
00198	16731	09650	09664
00200	16789	09673	09686
00205	16845	09694	09707
00205	16687	09634	09648
00205	16687	09634	09648
00210	16974	09743	09754
00216	17017	09759	09769
00225	17185	09823	09830
00229	17129	09802	09810
00239	17380	09896	09900
00241	17353	09885	09890
00253	17533	09952	09954
00266	17587	09971	09973
00269	17628	09987	09987
00281	17615	09982	09982
00283	17628	09987	09987
00286	17628	09987	09987
00287	17670	10002	10002
00388	17670	10002	10002
00489	17737	10026	10025
00585	17777	10041	10039

x = 0.475

y in	M	$\frac{u}{u_\delta}$ r = 0.89	$\frac{u}{u_\delta}$ r = 1
00.010	0.7068	0.5036	0.5109
00013	07107	05061	05135
00015	07633	05402	05476
00018	07527	05334	05408
00033	08393	05882	05957
00049	08956	06229	06303
00065	09553	06588	06661
00081	10003	06852	06923
00096	10586	07187	07254
00104	10823	07320	07386
00107	10881	07353	07418
00109	10960	07397	07461
00112	11076	07461	07525
00112	11122	07486	07550
00127	11635	07765	07825
00143	12129	08028	08083
00143	12242	08087	08141
00158	12627	08286	08336
00169	12955	08452	08499
00174	13054	08502	08547
00190	13541	08742	08782
00195	13658	08799	08837
00203	13874	08903	08938
00205	13922	08925	08960
00206	13860	08896	08931
00203	13974	08950	08985
00211	14018	08971	09005
00221	14415	09157	09186
00226	14550	09220	09246
00236	14808	09338	09361
00242	14920	09388	09409
00248	15050	09446	09466
00257	15249	09535	09552
00262	15375	09591	09605
00273	15546	09665	09677
00274	15595	09686	09698
00288	15861	09801	09808
00288	15833	09789	09797
00300	16006	09863	09868
00300	16033	09874	09879
00303	16032	09873	09878
00304	16073	09891	09895
00305	16044	09879	09883
00308	16130	09915	09918
00314	16192	09941	09943
00323	16228	09956	09957
00335	16337	10001	10001
00338	16293	09983	09984
00340	16278	09977	09977
00354	16317	09993	09993
00360	16324	09996	09996
00464	16325	09996	09997
00558	16290	09982	09982
00660	16313	09991	09992

x = 0.55

y in	M	$\frac{u}{u_\delta}$ r = 0.89	$\frac{u}{u_\delta}$ r = 1
00.010	0.5293	0.4168	0.4225
00013	05338	04201	04259
00015	05515	04333	04392
00018	05602	04398	04457
00023	05848	04580	04641
00028	06040	04721	04783
00042	06479	05042	05104
00057	06854	05312	05375
00073	07165	05533	05597
00089	07540	05797	05861
00105	07779	05963	06026
00108	07857	06016	✓6080
00109	08002	06116	06180
00110	07936	06071	06134
00113	07986	06105	06169
00118	08036	06140	06203
00123	08185	06242	06305
00138	08519	06467	.06530
00140	08602	06523	06586
00154	08903	06724	06785
00167	09201	06919	06979
00170	09235	06942	07001
00185	09584	07168	07226
00206	10025	07449	07504
00207	10013	07441	07496
00209	10064	07473	07528
00211	10150	07527	07581
00215	10150	07527	07581
00220	10301	07622	07674
00225	10447	07712	07764
00237	10682	07856	07906
00240	10748	07897	07946
00255	11115	08118	08164
00263	11209	08174	08219
00270	11447	08315	08358
00286	11738	08486	08525
00304	12054	08668	08703
00307	12040	08660	08695
00307	12169	08733	08767
00310	12184	08742	08776
00312	12197	08749	08783
00317	12326	08822	08854
00322	12453	08894	08924
00338	12789	09080	09106
00338	12836	09106	09131
00353	13094	09246	09268
00365	13360	09389	09407
00369	13414	09418	09435
00385	13665	09550	09564
00401	13916	09681	09691
00404	13916	09681	09691
00406	13993	09721	09730
00406	13981	09715	09724
00408	13982	09715	09724
00414	14081	09766	09773
00418	14190	09822	09827
00430	14199	09827	09832
00435	14308	09882	09886
00437	14308	09882	09886
00450	14409	09933	09935
00463	14468	09963	09964
00465	14496	09976	09977
00480	14570	10014	10013
00502	14553	10005	10005
00524	14520	09989	09989
00626	14499	09978	09979
00723	14478	09967	09968
00820	14499	09978	09979

Table 2b (Contd)

x = 0.7

y in	M	$\frac{u}{u_\delta}$ r = 0.89	$\frac{u}{u_\delta}$ r = 1
00.010	0.4669	0.4049	0.4096
00012	04710	04083	04131
00015	04773	04136	04183
00018	04747	04114	04162
00020	04870	04217	04265
00025	04948	04281	04330
00035	05028	04347	04396
00045	05126	04428	04478
00055	05248	04529	04579
00080	05463	04705	04756
00101	05700	04899	04950
00104	05732	04925	04977
00105	05665	04870	04922
00106	05721	04915	04967
00109	05697	04896	04948
00111	05795	04976	05028
00116	05795	04976	05028
00125	05892	05054	05106
00136	05972	05119	05171
00146	06046	05178	05231
00170	06311	05390	05443
00195	06561	05589	05643
00195	06532	05566	05620
00197	06561	05589	05643
00200	06578	05603	05656
00203	06605	05624	05677
00205	06614	05631	05685
00210	06667	05672	05726
00220	06746	05735	05789
00230	06875	05836	05889
00240	07000	05934	05987
00265	07243	06122	06175
00290	07516	06332	06385
00293	07602	06399	06451
00295	07645	06431	06483
00298	07661	06443	06495
00301	07639	06427	06479
00303	07712	06482	06534
00308	07754	06514	06566
00317	07859	06594	06645
00328	07984	06687	06739
00338	08084	06763	06814
00353	08163	06822	06873
00363	08374	06979	07028
00385	08610	07153	07201
00387	08667	07195	07243
00388	08664	07192	07240
00390	08676	07202	07250
00394	08695	07216	07263
00396	08700	07219	07267
00401	08753	07258	07305
00410	08909	07371	07417
00420	09009	07443	07489
00430	09127	07528	07573
00441	09223	07597	07642
00455	09380	07709	07753
00479	09684	07923	07964
00534	10242	08310	08346
00598	10915	08763	08791
00630	11365	09058	09080
00685	11885	09391	09406
00720	12277	09636	09645
00775	12587	09826	09830
00839	12780	09943	09944
00870	12860	09991	09991
00922	12866	09995	09995
00960	12879	10003	10003
01106	12876	10001	10001
01193	12866	09995	09995

x = 0.833

y in	M	$\frac{u}{u_\delta}$ r = 0.89	$\frac{u}{u_\delta}$ r = 1
00.010	0.6508	0.5661	0.5712
00012	06662	05785	05837
00015	06811	05905	05956
00017	06909	05983	06034
00017	06861	05945	05996
00020	06932	06002	06053
00025	07090	06127	06178
00030	07249	06253	06304
00035	07316	06306	06357
00045	07468	06425	06476
00055	07595	06524	06574
00065	07740	06637	06687
00076	07899	06760	06809
00086	07959	06806	06854
00097	08036	06865	06914
00108	08136	06942	06990
00108	08150	06952	07000
00109	08175	06971	07019
00111	08229	07013	07060
00114	08211	06999	07046
00114	08211	06999	07046
00114	08193	06985	07033
00117	08229	07013	07060
00122	08279	07050	07097
00127	08314	07077	07124
00132	08352	07106	07152
00143	08441	07173	07219
00153	08529	07239	07285
00163	08598	07291	07337
00173	08649	07329	07374
00184	08733	07392	07437
00195	08800	07442	07486
00205	08871	07494	07538
00205	08882	07503	07546
00207	08871	07494	07538
00210	08888	07507	07551
00212	08936	07543	07586
00215	08920	07531	07574
00220	08969	07567	07610
00225	09027	07610	07652
00230	09058	07633	07675
00241	09121	07679	07721
00252	09184	07725	07766
00261	09275	07791	07832
00272	09365	07857	07896
00282	09439	07910	07949
00293	09540	07983	08022
00303	09611	08035	08072
00306	09644	08058	08096
00308	09701	08099	08136
00310	09714	08108	08145
00314	09729	08119	08156
00316	09757	08139	08175
00321	09784	08158	08194
00326	09847	08203	08239
00331	09902	08242	08277
00342	09969	08289	08323
00352	10035	08336	08369
00362	10087	08373	08406
00370	10139	08409	08442
00374	10204	08454	08486
00383	10304	08524	08555
00394	10354	08559	08590
00402	10421	08605	08635
00403	10433	08614	08643
00405	10457	08630	08659
00405	10441	08619	08648
00408	10506	08664	08693
00410	10506	08664	08693
00415	10555	08698	08726
00420	10599	08728	08755
00426	10622	08744	08771
00436	10718	08809	08835
00447	10799	08865	08890
00457	10868	08912	08936
00466	10949	08967	08990
00468	10961	08974	08997
00478	11051	09035	09057
00489	11118	09080	09101
00499	11185	09125	09145
00563	11668	09443	09456
00630	12045	09687	09694
00665	12234	09806	09811
00724	12389	09904	09907
00760	12447	09940	09942
00820	12504	09976	09977
00887	12533	09994	09994
00921	12542	10000	10000
01016	12542	10000	10000
01176	12542	10000	10000
01270	12542	10000	10000

x = 0.983

y in	M	$\frac{u}{u_\delta}$ r = 0.89	$\frac{u}{u_\delta}$ r = 1
00.010	0.7148	0.6330	0.6378
00012	07235	06401	06448
00015	07361	06502	06550
00017	07438	06565	06612
00020	07559	06662	06709
00025	07717	06788	06834
00030	07944	06967	07013
00030	07944	06967	07013
00035	08055	07055	07100
00045	08372	07302	07345
00056	08572	07457	07499
00066	08734	07581	07621
00077	08907	07713	07752
00087	08998	07782	07820
00098	09119	07872	07910
00098	09148	07894	07932
00108	09253	07973	08010
00108	09192	07927	07965
00112	09253	07973	08010
00115	09295	08005	08041
00116	09293	08003	08039
00120	09307	08013	08049
00125	09336	08035	08071
00130	09364	08056	08091
00130	09420	08098	08133
00135	09420	08098	08133
00145	09545	08190	08224
00155	09572	08210	08243
00166	09667	08280	08312
00176	09733	08328	08360
00187	09786	08367	08398
00198	09838	08405	08436
00198	09838	08405	08436
00206	09866	08425	08456
00208	09889	08442	08472
00210	09878	08434	08465
00212	09891	08443	08474
00215	09927	08470	08500
00217	09940	08479	08509
00223	09952	08488	08518
00227	10003	08525	08554
00227	10003	08525	08554
00232	10017	08534	08564
00243	10091	08588	08617
00253	10152	08632	08660
00264	10176	08650	08677
00274	10250	08702	08729
00285	10333	08762	08787
00296	10369	08787	08812
00296	10369	08787	08812
00306	10452	08847	08871
00306	10416	08821	08845
00308	10452	08847	08871
00311	10452	08847	08871
00314	10462	08853	08877
00316	10462	08853	08877
00321	10486	08870	08894
00326	10532	08903	08926
00326	10543	08911	08934
00331	10555	08919	08942
00342	10646	08983	09005
00353	10668	08999	09020
00363	10735	09045	09066
00370	10760	09063	09083
00370	10734	09045	09065
00373	10792	09085	09105
00384	10868	09138	09157
00395	10901	09161	09180
00395	10901	09161	09180
00400	10902	09162	09180
00403	10892	09155	09173
00405	10934	09184	09202
00408	10923	09176	09194
00408	10933	09184	09202
00410	10933	09184	09202
00415	10966	09206	09224
00420	10999	09229	09246
00420	10999	09229	09246
00425	11010	09236	09253
00436	11084	09287	09303
00447	11137	09324	09339
00457	11169	09346	09361
00468	11232	09389	09402
00470	11223	09383	09397
00470	11219	09380	09394
00478	11305	09438	09451
00489	11325	09452	09465
00489	11305	09438	09451
00500	11356	09473	09486
00567	11640	09665	09673
00567	11607	09642	09651
00632	11804	09774	09779
00667	11895	09834	09838
00667	11891	09831	09836
00728	12006	09907	09909
00763	12066	09947	09948
00763	12053	09938	09940
00827	12101	09969	09970
00892	12129	09988	09988
00931	12139	09994	09994
01024	12158	10006	10008
01187	12148	10000	10000
01283	12148	10000	10000

Table 2c $M_\infty = 1.404$ $Re_\ell = 19.34 \times 10^6$

$x = 0.4$

y in	M	$\frac{u}{u_\delta}$ r = 0.89	$\frac{u}{u_\delta}$ r = 1
00.010	0.9116	0.5985	0.6068
00013	09396	06144	06227
00016	09490	06198	06280
00017	09704	06317	06400
00022	10165	06572	06653
00028	10502	06754	06834
00042	11387	07220	07295
00058	12223	07642	07710
00073	12958	07998	08060
00088	13607	08301	08357
00098	14364	08641	08688
00100	14497	08700	08745
00103	14515	08708	08753
00103	13345	08180	08238
00105	14619	08752	08796
00110	14839	08847	08889
00115	14994	08914	08953
00123	14922	08883	08923
00130	15467	09112	09145
00144	15877	09279	09307
00159	16309	09451	09473
00173	16425	09497	09517
00174	16699	09603	09619
00190	17141	09771	09780
00193	17197	09791	09800
00195	17227	09802	09811
00198	17254	09813	09820
00202	17340	09845	09851
00207	17469	09892	09897
00209	17319	09837	09843
00222	17636	09953	09955
00222	17392	09864	09869
00236	17704	09977	09978
00237	17577	09932	09935
00251	17744	09992	09992
00259	17740	09991	09991
00266	17772	10002	10002
00369	17798	10012	10011
00462	17813	10017	10016
00530	17837	10026	10025
00592	17936	10061	10058

$x = 0.475$

y in	M	$\frac{u}{u_\delta}$ r = 0.89	$\frac{u}{u_\delta}$ r = 1
00.010	0.7468	0.5268	0.5344
00013	07693	05413	05488
00015	07873	05526	05602
00018	08007	05611	05687
00033	08792	06097	06173
00049	09452	06494	06568
00065	10038	06837	06909
00081	10653	07188	07256
00096	11295	07542	07606
00104	11413	07606	07669
00107	11545	07677	07739
00109	11638	07728	07788
00112	11726	07774	07834
00112	11874	07853	07911
00127	12154	08000	08056
00143	12812	08337	08386
00143	12975	08419	08466
00158	13369	08613	08657
00169	13798	08821	08859
00174	13930	08883	08920
00190	14452	09127	09157
00195	14623	09205	09233
00203	14781	09277	09302
00205	14943	09350	09373
00206	14835	09301	09326
00208	14929	09344	09367
00211	15008	09379	09401
00221	15245	09484	09503
00226	15385	09546	09562
00236	15637	09655	09668
00242	15726	09693	09704
00248	15810	09729	09739
00257	15995	09807	09814
00262	16100	09851	09857
00273	16259	09918	09921
00288	16384	09969	09970
00288	16364	09961	09962
00300	16426	09987	09987
00303	16425	09986	09987
00304	16436	09991	09991
00305	16448	09996	09996
00308	16446	09995	09995
00314	16454	09998	09998
00412	16454	09998	09998
00500	16484	10010	10010
00607	16430	09988	09988

$x = 0.55$

y in	M	$\frac{u}{u_\delta}$ r = 0.89	$\frac{u}{u_\delta}$ r = 1
00.010	0.6009	0.4663	0.4725
00013	05970	04635	04697
00015	06061	04701	04763
00018	06252	04840	04902
00023	06328	04895	04958
00023	06403	04949	05012
00039	06953	05341	05406
00054	07326	05604	05668
00070	07648	05827	05892
00085	07943	06030	06094
00105	08449	06371	06435
00108	08472	06387	06451
00109	08397	06337	06401
00110	08502	06407	06470
00113	08596	06470	06533
00118	08621	06486	06549
00118	08666	06516	06579
00130	09016	06747	06808
00134	09111	06808	06870
00149	09479	07047	07106
00165	09806	07254	07312
00181	10060	07414	07470
00204	10633	07767	07819
00207	10830	07886	07936
00210	10862	07906	07955
00212	10911	07935	07984
00215	11004	07991	08039
00220	11050	08018	08066
00220	11095	08045	08092
00227	11271	08149	08195
00229	11421	08237	08281
00236	11540	08307	08350
00251	11935	08534	08573
00267	12273	08725	08760
00282	12624	08921	08951
00304	13105	09182	09206
00306	13051	09153	09177
00307	13116	09188	09212
00309	13153	09207	09231
00312	13250	09259	09281
00317	13310	09292	09313
00317	13347	09311	09331
00326	13641	09466	09482
00328	13639	09465	09481
00330	13582	09435	09452
00333	13725	09509	09524
00348	14058	09680	09690
00364	14259	09782	09789
00380	14424	09865	09869
00383	14370	09838	09843
00401	14626	09965	09966
00403	14586	09945	09947
00404	14623	09963	09965
00406	14623	09963	09965
00409	14645	09974	09975
00414	14655	09979	09980
00414	14655	09979	09980
00425	14674	09989	09989
00427	14686	09995	09995
00427	14686	09995	09995
00430	14698	10001	10001
00526	14696	10000	10000
00625	14674	09989	09989
00726	14664	09984	09984

Table 2o (Contd)

x = 0.7

y in	M	$\frac{u}{u_\delta}$ r = 0.89	$\frac{u}{u_\delta}$ r = 1
00.010	0.4919	0.4252	0.4301
00012	05040	04353	04402
00015	05081	04387	04436
00015	05074	04381	04430
00017	05198	04483	04533
00020	05237	04515	04566
00025	05312	04577	04627
00030	05385	04636	04687
00035	05485	04718	04769
00044	05591	04805	04856
00055	05701	04894	04946
00064	05768	04948	05000
00074	05836	05004	05056
00089	05965	05107	05160
00101	06151	05257	05310
00103	06151	05257	05310
00104	06085	05204	05257
00106	06183	05282	05336
00106	06178	05278	05331
00108	06215	05308	05361
00111	06246	05333	05386
00116	06274	05355	05408
00121	06333	05402	05455
00126	06386	05444	05498
00136	06473	05514	05567
00146	06564	05585	05639
00156	06674	05672	05726
00166	06756	05737	05790
00181	06889	05841	05894
00195	07045	05962	06016
00195	07040	05959	06012
00197	07069	05981	06034
00200	07069	05981	06034
00200	07069	05981	06034
00202	07116	06018	06071
00205	07121	06021	06075
00210	07170	06060	06113
00215	07244	06117	06170
00220	07292	06154	06207
00230	07407	06243	06296
00241	07524	06332	06385
00249	07597	06388	06440
00260	07709	06473	06525
00275	07862	06589	06640
00290	07987	06683	06734
00293	08175	06824	06874
00295	08196	06839	06890
00298	08255	06883	06933
00298	08196	06839	06890
00300	08233	06866	06917
00303	08234	06868	06918
00308	08354	06956	07006
00313	08432	07015	07064
00318	08432	07015	07064
00328	08562	07110	07159
00338	08674	07192	07241
00348	08769	07261	07309
00353	08638	07166	07214
00358	08840	07313	07360
00373	08999	07428	07474
00385	09187	07563	07608
00387	09202	07574	07619
00390	09202	07574	07619
00390	09218	07586	07630
00392	09265	07619	07663
00395	09299	07643	07687
00400	09316	07655	07699
00405	09382	07702	07745
00409	09447	07748	07791
00420	09570	07835	07877
00430	09709	07933	07973
00440	09786	07986	08026
00442	09708	07932	07972
00449	09860	08038	08077
00465	10048	08168	08206
00479	10187	08263	08300
00534	10758	08649	08679
00598	11438	09095	09117
00633	11891	09384	09400
00684	12355	09673	09682
00721	12634	09844	09848
00776	12808	09949	09950
00838	12867	09985	09985
00874	12897	10003	10003
00960	12897	10003	10003
01011	12887	09996	09997
01107	12887	09996	09997

x = 0.833

y in	M	$\frac{u}{u_\delta}$ r = 0.89	$\frac{u}{u_\delta}$ r = 1
00.010	0.7242	0.6184	0.6235
00013	07350	06275	06327
00015	07443	06348	06399
00018	07532	06417	06468
00020	07600	06469	06520
00026	07727	06567	06618
00031	07814	06634	06684
00036	08042	06808	06857
00036	08005	06780	06829
00041	08087	06842	06891
00052	08183	06914	06963
00062	08357	07045	07093
00073	08394	07073	07121
00082	08470	07130	07177
00092	08562	07199	07246
00105	08617	07239	07286
00108	08690	07293	07340
00111	08744	07333	07379
00113	08744	07333	07379
00116	08744	07333	07379
00118	08760	07345	07391
00124	08795	07371	07417
00129	08830	07397	07442
00134	08918	07461	07506
00134	08903	07450	07495
00139	08903	07450	07495
00150	08985	07510	07554
00160	09051	07559	07603
00170	09134	07619	07662
00178	09232	07690	07732
00189	09264	07713	07755
00202	09375	07793	07834
00205	09392	07805	07847
00208	09439	07839	07880
00210	09439	07839	07880
00213	09454	07850	07890
00215	09439	07839	07880
00221	09469	07860	07901
00226	09579	07939	07979
00231	09596	07951	07991
00231	09564	07928	07968
00236	09593	07949	07989
00247	09682	08012	08051
00257	09740	08053	08091
00268	09797	08094	08131
00277	09912	08175	08211
00288	09983	08224	08260
00300	10080	08292	08327
00306	10192	08370	08403
00309	10192	08370	08403
00311	10192	08370	08403
00314	10219	08388	08422
00316	10219	08388	08422
00322	10273	08426	08459
00327	10301	08445	08478
00332	10344	08474	08507
00332	10354	08481	08514
00337	10393	08509	08540
00348	10495	08578	08609
00358	10557	08621	08650
00369	10620	08664	08693
00370	10620	08664	08693
00378	10721	08732	08760
00388	10783	08774	08801
00401	10893	08848	08874
00402	10896	08849	08875
00405	10920	08866	08891
00407	10943	08882	08907
00410	10968	08898	08923
00412	10968	08898	08923
00418	11088	08978	09001
00423	11066	08963	08987
00428	11104	08988	09012
00428	11114	08995	09018
00433	11125	09003	09026
00444	11240	09079	09100
00454	11307	09122	09143
00464	11387	09175	09194
00466	11398	09183	09202
00473	11467	09227	09246
00483	11534	09271	09288
00497	11634	09336	09352
00564	12066	09612	09622
00629	12367	09801	09807
00664	12509	09889	09892
00724	12620	09957	09959
00759	12659	09982	09982
00821	12689	10000	10000
00887	12689	10000	10000
00921	12699	10006	10006
01017	12689	10000	10000
01176	12689	10000	10000
01271	12689	10000	10000

x = 0.983

y in	M	$\frac{u}{u_\delta}$ r = 0.89	$\frac{u}{u_\delta}$ r = 1
00010	0.7402	0.6551	0.6599
00013	07509	06638	06684
00015	07732	06816	06862
00018	07808	06877	06923
00020	07902	06951	06997
00023	07976	07010	07055
00026	08142	07140	07185
00031	08230	07209	07253
00041	08573	07476	07517
00046	08706	07578	07618
00046	08707	07579	07619
00051	08801	07651	07691
00057	08902	07728	07767
00067	08978	07786	07824
00077	09101	07879	07916
00087	09252	07992	08028
00098	09312	08037	08072
00108	09412	08112	08147
00108	09413	08113	08147
00111	09386	08092	08127
00113	09429	08125	08159
00116	09455	08144	08178
00118	09455	08144	08178
00121	09483	08164	08198
00124	09497	08175	08209
00129	09580	08236	08269
00134	09606	08256	08289
00134	09606	08256	08289
00139	09608	08257	08290
00145	09664	08298	08330
00145	09685	08314	08346
00150	09696	08321	08354
00155	09753	08364	08395
00166	09818	08411	08442
00177	09870	08449	08479
00187	09949	08507	08536
00197	09988	08535	08564
00206	10016	08556	08584
00208	10053	08582	08610
00209	10016	08556	08584
00211	10029	08564	08593
00214	10030	08565	08594
00216	10077	08600	08628
00219	10077	08600	08628
00222	10101	08617	08645
00227	10152	08653	08681
00232	10188	08680	08707
00237	10174	08670	08697
00243	10201	08689	08716
00243	10207	08693	08720
00248	10244	08720	08746
00253	10295	08756	08782
00263	10330	08781	08807
00274	10425	08849	08873
00284	10438	08858	08882
00295	10498	08901	08924
00306	10548	08936	08959
00306	10545	08934	08956
00309	10548	08936	08959
00311	10583	08961	08983
00314	10571	08953	08975
00316	10592	08968	08990
00319	10627	08992	09013
00322	10649	09007	09029
00327	10649	09007	09029
00332	10694	09039	09060
00343	10751	09079	09099
00343	10745	09075	09095
00348	10757	09084	09103
00353	10794	09109	09128
00364	10858	09154	09173
00370	10890	09176	09195
00373	10890	09176	09195
00383	10947	09216	09233
00394	11003	09255	09271
00400	10996	09250	09267
00403	11008	09258	09274
00405	11040	09280	09296
00405	11058	09293	09309
00408	11040	09280	09296
00411	11059	09293	09309
00413	11070	09301	09317
00416	11080	09308	09323
00421	11090	09315	09330
00426	11133	09344	09359
00432	11143	09351	09366
00432	11143	09351	09366
00437	11177	09374	09388
00437	11203	09392	09406
00442	11214	09400	09413
00447	11226	09408	09422
00458	11319	09472	09484
00468	11339	09485	09497
00469	11328	09478	09490
00478	11382	09514	09526
00489	11435	09550	09561
00500	11465	09571	09581
00568	11693	09724	09731
00633	11864	09838	09842
00667	11934	09884	09887
00728	12013	09936	09938
00763	12042	09955	09956
00828	12091	09987	09988
00988	12111	10001	10001
01088	12101	09994	09994
01187	12101	09994	09994
01284	12101	09994	09994

Table 2d $M_{\infty} = 1.700$ $Re_{\ell} = 10.00 \times 10^{6}$

x = 0.4

y in	M	$\frac{u}{u_\delta}$ r = 0.89	$\frac{u}{u_\delta}$ r = 1
00.010	0.9728	0.5746	0.5847
00013	09859	05812	05913
00015	09991	05878	05979
00017	10242	06003	06104
00020	10562	06160	06260
00022	10756	06253	06353
00025	11091	06414	06512
00028	11281	06504	06602
00030	11598	06651	06748
00037	11947	06811	06907
00048	12657	07128	07220
00057	13251	07385	07472
00073	14040	07712	07794
00088	14786	08010	08084
00098	15607	08322	08389
00100	15678	08349	08414
00103	15678	08349	08414
00105	15775	08385	08449
00108	15874	08421	08484
00108	15725	08366	08431
00110	15945	08447	08510
00112	16039	08481	08542
00115	16140	08518	08578
00117	16278	08567	08626
00125	16475	08637	08694
00128	16496	08645	08701
00135	16866	08774	08826
00145	17194	08886	08934
00148	17186	08883	08931
00160	17758	09074	09115
00168	17932	09130	09169
00174	18201	09217	09253
00188	18507	09313	09345
00190	18876	09427	09454
00193	18915	09439	09466
00194	18807	09406	09434
00195	18954	09451	09477
00198	18993	09463	09489
00200	19060	09483	09508
00202	19099	09495	09519
00205	19196	09524	09547
00207	19242	09538	09560
00210	19339	09567	09588
00212	19159	09513	09536
00215	19335	09566	09587
00217	19523	09621	09640
00225	19720	09679	09695
00235	19735	09683	09698
00236	19870	09722	09736
00237	19735	09683	09698
00250	20213	09820	09829
00254	20128	09796	09806
00266	20476	09893	09898
00273	20457	09888	09893
00281	20659	09943	09946
00283	20659	09943	09946
00285	20657	09943	09946
00286	20659	09943	09946
00288	20694	09953	09955
00290	20723	09961	09963
00293	20723	09961	09963
00295	20728	09962	09964
00298	20747	09967	09969
00298	20676	09948	09950
00300	20766	09972	09974
00305	20782	09977	09978
00307	20760	09971	09972
00310	20771	09974	09975
00316	20820	09987	09988
00322	20801	09982	09983
00325	20818	09986	09987
00326	20820	09987	09988
00341	20830	09990	09990
00344	20836	09991	09992
00355	20855	09996	09997
00363	20872	10001	10001
00466	20914	10012	10012
00568	20996	10034	10033
00661	21091	10060	10057
00731	21108	10064	10061

x = 0.55

y in	M	$\frac{u}{u_\delta}$ r = 0.89	$\frac{u}{u_\delta}$ r = 1
00.010	0.7222	0.4794	0.4877
00013	07285	04832	04915
00013	07330	04859	04943
00018	07436	04923	05007
00023	07632	05041	05126
00028	07834	05162	05246
00028	07882	05190	05275
00033	08051	05290	05375
00038	08251	05408	05493
00042	08405	05497	05583
00048	08593	05606	05692
00053	08720	05679	05765
00057	08884	05773	05859
00063	11678	07269	07346
00073	09319	06019	06104
00083	0'9571	06159	06244
00094	09867	06321	06406
00104	10147	06473	06557
00105	10304	06557,	06641
00108	10314	06563	06646
00108	10319	06566	06649
00113	10384	06601	06683
00118	10471	06647	06729
00120	10494	06659	06741
00120	10494	06659	06741
00123	10567	06698	06780
00123	10569	06699	06781
00128	10697	06766	06848
00133	10846	06844	06925
00138	10920	06883	06963
00143	11065	06958	07037
00150	11195	07025	12056
00154	11345	07101	07180
00159	11499	07180	07257
00170	11797	07329	07404
00172	11797	07329	07404
00180	12057	07458	07531
00191	12330	07590	07662
00200	12614	07727	07796
00207	12964	07893	07959
00209	12970	07896	07961
00209	12981	07901	07967
00215	13051	07933	07998
00216	12970	07896	07961
00216	12970	07896	07961
00220	13115	07963	08028
00225	13243	08023	08086
00225	13243	08023	08086
00225	13104	07958	08023
00230	13395	08093	08154
00235	13526	08152	08213
00240	13617	08193	08253
00245	13745	08251	08309
00250	13878	08311	08368
00255	14027	08377	08432
00260	14145	08429	08483
00268	14290	08493	08545
00270	14480	08575	08625
00277	14376	08530	08581
00281	14734	08684	08731
00293	14984	08789	08833
00302	15325	08931	08970
00304	15432	08974	09013
00304	14963	08780	08825
00307	15447	08980	09019
00307	15451	08982	09020
00312	15528	09014	09051
00317	15582	09036	09072
00317	15612	09048	09084
00317	15581	09035	09071
00322	15691	09080	09115
00322	15702	09084	09119
00322	15533	09015	09053
00327	15842	09140	09173
00330	15549	09022	09059
00330	15581	09035	09071
00333	15965	09189	09220
00338	16042	09219	09250
00344	16154	09263	09292
00349	16320	09328	09355
00356	16229	09292	09320
00358	16514	09403	09427
00369	16909	09552	09571
00370	16749	09492	09513
00373	16677	09465	09486
00380	17010	09590	09607
00383	16764	09498	09518
00383	16764	09498	09518
00390	17225	09669	09683
00399	17266	09685	09698
00400	17506	09772	09782
00401	17541	09784	09794
00404	15462	08987	09025
00404	17551	09788	09797
00408	17649	09823	09831
00414	17625	09815	09823
00417	17645	09822	09829
00417	17617	09812	09820
00418	17692	09839	09846
00418	17701	09842	09849
00422	17687	09837	09844
00424	17771	09867	09872
00425	17576	09797	09806
00425	17604	09807	09815
00430	17852	09896	09900
00435	17894	09910	09914
00440	18032	09959	09961
00445	18032	09959	09961
00450	18059	09968	09970
00451	17934	09924	09928
00455	18123	09991	09991
00465	18164	10005	10005
00564	18150	10000	10000
00668	18137	09995	09996
00773	18110	09986	09987
00895	18106	09985	09985
00989	18065	09970	09972

Table 2d (Contd)

x = 0.7

y in	M	u/u_δ r = 0.89	u/u_δ r = 1
00.010	0.5813	0.4263	0.4329
00012	05905	04327	04394
00015	05996	04389	04456
00018	06130	04481	04549
00020	06171	04509	04577
00028	06344	04627	04696
00035	06426	04683	04752
00043	06544	04763	04833
00057	06780	04922	04993
00072	07001	05070	05141
00087	07180	05188	05260
00101	07418	05346	05418
00104	07418	05346	05418
00105	07418	05346	05418
00106	07484	05389	05461
00109	07484	05389	05461
00111	07515	05409	05482
00119	07646	05495	05567
00126	07676	05514	05587
00134	07801	05595	05668
00148	08012	05731	05804
00163	08188	05844	05917
00178	08385	05969	06041
00195	08599	06104	06176
00195	08651	06136	06209
00197	08651	06136	06209
00200	08678	06153	06226
00203	08730	06186	06258
00205	08730	06186	06258
00212	08881	06280	06352
00220	08931	06310	06382
00228	09079	06402	06473
00243	09267	06517	06588
00258	09473	06642	06712
00272	09693	05774	06843
00290	09924	06912	06980
00293	10065	06995	07062
00295	10106	07020	07087
00298	10146	07043	07110
00301	10185	07066	07132
00303	10204	07077	07143
00310	10339	07156	07222
00317	10417	07201	07266
00326	10529	07266	07330
00340	10766	07401	07464
00353	10856	07452	07515
00355	10979	07522	07584
00370	11202	07647	07707
00385	11436	07777	07835
00387	11468	07795	07852
00388	11468	07795	07852
00390	11516	07821	07878
00394	11550	07840	07897
00396	11598	07866	07922
00403	11695	07919	07975
00410	11806	07979	08034
00418	11931	08047	08100
00433	12160	08170	08221
00441	12282	08234	08284
00448	12371	08281	08330
00462	12605	08404	08450
00479	12891	08551	08594
00534	13668	08941	08974
00598	14557	09366	09388
00630	15086	09610	09623
00685	15596	09837	09843
00720	15832	09941	09943
00775	15954	09994	09994
00841	15954	09994	09994
00960	15932	09984	09985
01075	15865	09955	09957
01156	15854	09950	09952
01243	15809	09931	09933
01335	15809	09931	09933
01420	15764	09911	09914

x = 0.833

y in	M	u/u_δ r = 0.89	u/u_δ r = 1
00.010	0.7795	0.5763	0.5832
00015	08010	05906	05974
00017	08252	06066	06134
00022	08405	06165	06233
00027	08598	06291	06359
00035	08865	06463	06530
00048	09142	06638	06704
00060	09350	06769	06835
00081	09667	06966	07030
00108	09967	07151	07213
00108	09929	07127	07190
00111	09978	07157	07219
00114	10040	07195	07257
00120	10095	07229	07290
00125	10131	07251	07312
00132	10229	07310	07370
00145	10342	07377	07437
00159	10443	07438	07497
00179	10654	07563	07620
00205	11755	08196	08244
00205	10965	07745	07800
00210	10930	07725	07780
00212	10998	07764	07819
00218	11015	07775	07829
00222	11066	07804	07858
00230	11147	07851	07904
00243	11309	07944	07996
00255	11432	08014	08065
00276	11644	08134	08183
00303	11978	08320	08365
00306	11982	08322	08367
00310	12036	08352	08397
00314	12087	08380	08425
00318	12118	08398	08441
00324	12192	08438	08481
00331	12279	08486	08528
00345	12424	08564	08605
00357	12549	08632	08670
00370	12649	08686	08723
00376	12798	08765	08801
00402	13044	08894	08927
00405	13086	08916	08948
00405	13095	08921	08953
00408	13126	08937	08969
00413	13181	08965	08996
00418	13224	08988	09018
00426	13319	09037	09066
00439	13464	09112	09139
00452	13589	09175	09201
00466	13755	09259	09282
00473	13796	09280	09303
00499	14098	09430	09449
00563	14612	09681	09692
00630	14983	09857	09862
00665	15132	09927	09929
00724	15238	09976	09977
0.0760	15270	09991	09991
00820	15291	10001	10001
00921	15291	10001	10001
01016	15291	10001	10001
01176	15280	09996	09996
01270	15270	09991	09991

x = 0.983

y in	M	u/u_δ r = 0.89	u/u_δ r = 1
00.010	0.8605	0.6397	0.6462
00012	08736	06483	06548
00015	08996	06652	06716
00017	09125	06735	06798
00020	09318	06858	06921
00025	09586	07028	07089
00030	09875	07209	07269
00035	09985	07278	07337
00045	10380	07520	07576
00056	10633	07673	07727
00066	10816	07782	07835
00077	11025	07906	07957
00092	11227	08025	08074
00108	11473	08167	08214
00108	11397	08124	08171
00112	11449	08153	08200
00115	11481	08172	08218
00116	11544	08208	08254
00120	11567	08221	08267
00125	11621	08252	08297
00130	11702	08299	08343
00135	11706	08301	08345
00145	11807	08358	08401
00155	11913	08418	08460
00166	11991	08462	08503
00176	12070	08507	08547
00192	12224	08592	08631
00206	11242	08033	08082
00209	12351	08662	08699
00210	12266	08615	08653
00212	12297	08633	08671
00215	12379	08678	08714
00215	12358	08666	08703
00217	12381	08679	08716
00223	12434	08708	08744
00227	12480	08733	08769
00232	12505	08747	08782
00243	12600	08799	08833
00253	12648	08825	08859
00264	12795	08904	08936
00274	12819	08918	08949
00290	12915	08969	08999
00306	13040	09036	09064
00306	13010	09020	09048
00308	13018	09024	09053
00311	13050	09041	09069
00314	13122	09079	09106
00314	13088	09061	09089
00316	13109	09073	09100
00321	13159	09099	09126
00326	13178	09109	09135
00331	13225	09134	09160
00342	13290	09168	09193
00353	13358	09204	09228
00363	13428	09240	09263
00370	13451	09252	09275
00373	13495	09275	09297
00390	13608	09334	09354
00400	13672	09366	09386
00403	13653	09356	09376
00405	13686	09373	09393
00408	13729	09395	09414
00408	13707	09384	09404
00408	13698	09379	09399
00410	13727	09394	09413
00415	13772	09418	09436
00420	13791	09427	09445
00425	13813	09438	09456
00436	13874	09470	09486
00447	13940	09503	09519
00457	14006	09536	09551
00468	14092	09580	09593
00470	14070	09569	09583
00484	14135	09601	09614
00500	14220	09644	09655
00567	14516	09790	09797
00632	14717	09888	09892
00667	14784	09921	09923
00728	14880	09967	09968
00763	14926	09989	09989
00827	14940	09996	09996
00892	14966	10008	10008
00988	14946	09999	09999
01087	14943	09997	09997
01187	14943	09997	09997
01283	14943	09997	09997

Table 2e $M_\infty = 2.000$ $Re_\ell = 9.88 \times 10^6$

x = 0.4

y in		$\frac{u}{u_\delta}$ r = 0.89	$\frac{u}{u_\delta}$ r = 1
00.010	1.0038	0.5465	0.5582
00013	10419	05639	05756
00015	10723	05776	05894
00017	11177	05977	06094
00020	11557	06142	06258
00022	12071	06360	06475
00025	12365	06482	06596
00030	12787	06653	06766
00035	13256	06840	06951
00045	14119	07172	07277
00055	14704	07387	07489
00065	15373	07626	07722
00075	15945	07822	07913
00085	16600	08039	08124
00095	17049	08183	08264
00098	17246	08245	08324
00100	17315	08266	08345
00103	17414	08297	08375
00105	17478	08317	08394
00105	17482	08318	08395
00108	17610	08357	08433
00110	17804	08416	08490
00112	17996	08474	08546
00115	17937	08456	08529
00117	18127	08513	08583
00122	18390	08590	08658
00125	18473	08614	08681
00132	18822	08715	08777
00135	18813	08712	08775
00141	19171	08812	08871
00152	19624	08937	08991
00162	20153	09077	09125
00171	20452	09155	09199
00182	20758	09233	09273
00190	21076	09312	09349
00192	21113	09321	09357
00193	21102	09318	09355
00195	21182	09338	09374
00198	21291	09364	09399
00200	21346	09378	09411
00202	21426	09397	09430
00202	21382	09367	09420
00205	21557	09429	09460
00210	21669	09455	09485
00212	21729	09470	09499
00215	21861	09501	09528
00221	22017	09537	09563
00225	22121	09561	09586
00234	22370	09618	09640
00243	22657	09683	09701
00253	22941	09746	09761
00263	23133	09788	09800
00274	23280	09819	09830
00281	23459	09858	09866
00282	23499	09866	09874
00283	23509	09868	09876
00286	23531	09873	09880
00288	23604	09888	09895
00290	23629	09894	09900
00292	23621	09892	09898
00293	23654	09899	09905
00295	23750	09919	09924
00300	23758	09921	09925
00302	23765	09922	09927
00304	23815	09932	09936
00312	23886	09947	09950
00315	23933	09957	09959
00324	23997	09970	09972
00333	24053	09981	09983
00343	24077	09986	09987
00352	24099	09991	09991
00363	24099	09991	09991
00372	24148	10001	10001
00475	24219	10015	10014
0,0550'	24345	10041	10038
00698	24453	10062	10059
00781	24547	10081	10076
00867	24618	10095	10089

x = 0.475

y in	M	$\frac{u}{u_\delta}$ r = 0.89	$\frac{u}{u_\delta}$ r = 1
00.010	0.9265	0.5190	0.5302
00013	09508	05307	05420
00015	09816	05454	05567
00018	10166	05619	05732
00020	10501	05774	05888
00022	10660	05847	05960
00027	11018	06009	06122
00033	11311	06139	06252
00043	11964	06423	06534
00053	12482	06642	06751
00065	12979	06846	06953
00081	13706	07136	07238
00096	14295	07362	07461
00104	14847	07567	07662
00107	14904	07588	07682
00109	14971	07613	07706
00112	15143	07675	07767
00112	15028	07633	07726
00114	15209	07698	07790
00117	15309	07734	07825
00122	15477	07794	07883
00126	15663	07859	07947
00127	15673	07862	07950
00138	16152	08027	08110
00148	16555	08163	08242
00158	16980	08302	08377
00174	17614	08503	08571
00190	18180	08676	08738
00203	18858	08875	08930
00205	18808	08861	08916
00206	18875	08880	08934
00208	18957	08904	08957
00211	19143	08957	09008
00212	19195	08971	09022
00216	19273	08993	09043
00220	19338	09011	09060
00221	19405	09030	09078
00226	19560	09073	09119
00236	19936	09176	09218
00247	20313	09276	09313
00257	20608	09353	09387
00273	21106	09480	09507
00288	21508	09579	09602
00300	21857	09663	09682
00303	21895	09673	09690
00304	21926	09680	09697
00305	21940	09683	09701
00308	22032	09705	09721'
00310	22100	09721	09736
00312	22147	09732	09747
00317	22238	09753	09767
00319	22266	09760	09773
00323	22350	09779	09792
00333	22587	09834	09843
00342	22766	09875	09882
00354	22943	09914	09919
00369	23129	09956	09958
00385	23239	09980	09981
00388	23152	09961	09963
00400	23348	10003	10003
00400	23304	09994	09994
00403	23299	09993	09993
00405	23341	10002	10002
00408	23319	09997	09997
00410	23319	09997	09997
00413	23319	09997	09997
00414	23304	09994	09994
00418	23299	09993	09993
00423	23319	09997	09997
00434	23355	10005	10005
00443	23310	09995	09996
00454	23332	10000	10000
00469	23326	09999	09999
00500	23326	09999	09999
00644	23239	09980	09981
00734	23194	09970	09972
00826	23152	09961	09963
00920	23152	09961	09963
01019	23129	09956	09958

x = 0.55

y in	M	$\frac{u}{u_\delta}$ r = 0.89	$\frac{u}{u_\delta}$ r = 1
00.010	0.8104	0.4812	0.4913
00013	08239	04883	04984
00015	08382	04959	05061
00018	08558	05051	05153
00020	08779	05166	05269
00023	09051	05306	05410
00028	09259	05411	05516
00033	09597	05582	05686
00038	09822	05694	05798
00042	10034	05798	05903
00053	10342	05948	06052
00063	10704	06121	06225
00079	11117	06316	06419
00094	11597	06536	06638
00105	12122	06772	06871
00108	12261	06833	06932
00109	12054	06742	06841
00110	12338	06867	06965
00113	12371	06882	06980
00115	12371	06882	06980
00118	12434	06909	07007
00123	12562	06965	07062
00125	12519	06946	07043
00128	12688	07019	07115
00133	12832	07081	07176
00138	12974	07141	07235
00150	13252	07258	07351
00159	13601	07402	07492
00175	14046	07582	07669
00191	14517	07768	07851
00206	14950	07935	08013
00207	15230	08040	08116
00209	15419	08110	08185
00211	15453	08123	08197
00215	15427	08113	08187
00216	15501	08140	08214
00220	15550	08158	08231
00222	15440	08118	08192
00225	15675	08204	08276
00230	15821	08257	08327
00235	15906	08287	08357
00240	16062	08343	08411
00250	16304	08429	08494
00260	16675	08558	08619
00276	17149	08718	08774
00293	17594	08865	08915
00304	18105	09028	09073
00307	18265	09078	09121
00307	17992	08992	09038
00310	18328	09098	09139
00312	18349	09104	09146
00315	18349	09104	09146
00317	18411	09124	09164
00322	18535	09162	09201
00322	18501	09151	09191
00327	18685	09207	09245
00333	18758	09230	09266
00338	18887	09269	09303
00349	19119	09338	09369
00358	19396	09419	09447
00375	19840	09546	09569
00388	19939	09574	09595
00390	20226	09654	09671
00401	20746	09795	09806
00404	20759	09799	09809
00406	20778	09804	09814
00406	20573	09749	09762
00408	20797	09809	09819
00411	20887	09833	09842
00414	20887	09833	09842
00418	20923	09842	09851
00421	20917	09841	09849
00424	21018	09868	09874
00430	21118	09894	09899
00435	21140	09900	09905
00445	21259	09930	09934
00455	21418	09971	09973
00470	21508	09994	09995
00483	21531	10000	10000
00584	21513	09996	09996
00682	21531	10000	10000
00779	21426	09973	09975
00915	21343	09952	09955
01041	21356	09955	09958
01200	21246	09927	09931
01297	21227	09922	09926

Table 2e (Contd)

x = 0.7

y in	M	u/u_δ r = 0.89	u/u_δ r = 1
00.010	0.7231	0.4639	0.4726
00012	07279	04667	04754
00015	07476	04782	04871
00020	07617	04864	04953
00030	07934	05046	05137
00045	08233	05216	05307
00065	08630	05439	05531
00085	08926	05603	05695
00101	09276	05794	05886
00104	09276	05794	05886
00105	09276	05794	05886
00106	09344	05831	05923
00111	09411	05867	05959
00120	09574	05954	06046
00136	09794	06071	06163
00155	10121	06243	06334
00175	10433	06405	06495
00195	10781	06582	06671
00195	10781	06582	06671
00197	10781	06582	06671
00200	10886	06635	06724
00205	10938	06661	06749
00215	11115	06750	06837
00230	11384	06883	06969
00250	11716	07045	07129
00270	12081	07220	07302
00290	12454	07395	07474
00293	12644	07483	07561
00295	12644	07483	07561
00298	12728	07522	07599
00303	12790	07550	07627
00313	13018	07653	07728
00328	13279	07770	07843
00349	13630	07925	07995
00353	13689	07951	08020
00367	14011	08090	08156
00385	14397	08253	08315
00387	14433	08269	08330
00388	14416	08261	08323
00390	14470	08284	08345
00396	14559	08321	08381
00405	14772	08409	08467
00420	14999	08501	08557
00440	15427	08672	08723
00441	15443	08679	08729
00460	15758	08802	08849
00479	16163	08957	08998
00534	17138	09315	09344
00598	18200	09682	09696
00630	18673	09838	09846
00685	19081	09969	09971
00720	19161	09995	09995
00775	19148	09991	09991
00870	19134	09986	09987
00960	19014	09948	09950
01010	18968	09933	09936
01106	18941	09925	09928
01193	18846	09894	09899

x = 0.833

y in	M	u/u_δ r = 0.89	u/u_δ r = 1
00.010	0.8869	0.5786	0.5871
00012	09198	05973	06058
00015	09328	06046	06131
00017	09577	06185	06269
00020	09710	06258	06343
00025	10090	06466	06549
00030	10307	06584	06666
00035	10517	06696	06777
00040	10651	06767	06848
00050	10958	06928	07008
00060	11191	07049	07127
00076	11478	07195	07272
00091	11695	07305	07380
00108	11914	07415	07488
00108	11888	07401	07475
00109	11989	07452	07525
00111	11965	07440	07513
00114	12003	07459	07531
00117	12039	07476	07549
00122	12115	07514	07586
00127	12170	07541	07612
00132	12263	07586	07657
00137	12300	07604	07675
00149	12447	07675	07745
00159	12571	07735	07803
00173	12766	07828	07895
00190	12939	07910	07975
00205	13149	08009	08072
00205	13162	08015	08078
00207	13183	08025	08087
00210	13178	08022	08085
00212	13212	08038	08100
00215	13228	08045	08108
00220	13329	08092	08154
00225	13379	08115	08176
00230	13477	08160	08220
00235	13510	08175	08235
00246	13657	08242	08300
00255	13832	08321	08377
00272	14022	08406	08460
00288	14194	08482	08534
00303	14454	08596	08645
00306	14504	08617	08666
00308	14565	08643	08691
00310	14560	08641	08689
00314	14591	08654	08702
00316	14635	08674	08720
00321	14724	08711	08757
00326	14770	08731	08776
00331	14857	08768	08813
00336	14946	08806	08849
00347	15076	08860	08902
00357	15235	08926	08966
00370	15348	08973	09011
00374	15447	09014	09051
00389	15644	09094	09128
00402	15799	09157	09189
00403	15827	09168	09200
00405	15864	09182	09214
00405	15864	09182	09214
00408	15864	09182	09214
00410	15932	09210	09240
00415	16014	09242	09272
00420	16082	09269	09298
00426	16136	09290	09318
00431	16229	09327	09353
00441	16363	09379	09404
00452	16481	09425	09448
00466	16625	09480	09501
00468	16664	09495	09515
00484	16833	09559	09577
00499	17011	09626	09641
00563	17549	09824	09831
00630	17853	09933	09936
00665	17962	09971	09972
00724	18034	09997	09997
00760	18046	10001	10001
00887	18038	09998	09998
00981	18038	09998	09998
01075	18038	09998	09998
01176	18038	09998	09998
01270	18038	09998	09998

x = 0.983

y in	M	u/u_δ r = 0.89	u/u_δ r = 1
00.010	0.9722	0.6387	0.6468
00012	09935	06507	06587
00015	10231	06670	06749
00017	10383	06754	06832
00020	10711	06931	07008
00022	10853	07007	07083
00025	11000	07085	07160
00028	11244	07214	07288
00030	11377	07283	07356
00033	11470	07332	07403
00035	11579	07388	07459
00040	11837	07520	07589
00045	12083	07644	07711
00050	12237	07722	07788
00056	12388	07796	07861
00060	12527	07865	07928
00072	12782	07989	08050
00087	13105	08144	08202
00108	13438	08301	08356
00108	13397	08282	08337
00112	13468	08315	08370
00115	13499	08330	08383
00116	13513	08336	08390
00120	13553	08355	08408
00122	13599	08376	08429
00123	13618	08385	08438
00127	13718	08431	08483
00130	13702	08424	08475
00132	13762	08451	08502
00135	13746	08444	08495
00140	13840	08487	08537
00145	13913	08521	08570
00150	13943	08534	08583
00155	14305	08697	08742
00160	14064	08589	08636
00170	14187	08644	08691
00187	14348	08716	08761
00206	14512	08789	08831
00208	14516	08791	08833
00210	14527	08795	08837
00212	14553	08807	08849
00215	14553	08807	08849
00217	14577	08817	08859
00220	14618	08835	08876
00223	14618	08835	08876
00225	14657	08853	08893
00227	14657	08853	08893
00230	14700	08871	08911
00232	14727	08883	08923
00239	14768	08901	08940
00243	14827	08926	08965
00248	14895	08956	08993
00253	14906	08961	08998
00259	14962	08985	09021
00270	15058	09025	09061
00285	15207	09089	09122
00306	15388	09165	09196
00306	15379	09161	09192
00308	15427	09182	09212
00311	15464	09197	09227
00314	15438	09186	09216
00316	15473	09201	09230
00319	15486	09206	09236
00321	15499	09211	09241
00325	15562	09238	09266
00326	15549	09233	09261
00329	15588	09248	09277
00331	15600	09254	09281
00337	15652	09275	09302
00342	15695	09293	09319
00347	15720	09303	09329
00353	15797	09334	09360
00357	15822	09345	09370
00368	15899	09376	09400
00370	15916	09383	09407
00384	16041	09434	09455
00400	16150	09478	09498
00403	16162	09482	09502
00405	16161	09482	09502
00408	16198	09497	09516
00408	16190	09493	09513
00410	16219	09505	09524
00413	16244	09515	09534
00415	16255	09520	09538
00418	16302	09538	09556
00420	16291	09534	09552
00423	16315	09543	09561
00425	16327	09548	09566
00430	16376	09568	09585
00436	16405	09579	09595
00441	16441	09593	09609
00447	16490	09612	09628
00451	16501	09617	09632
00463	16600	09656	09669
00470	16628	09666	09680
00478	16688	09690	09702
00500	16795	09731	09742
00567	17102	09848	09855
00632	17286	09918	09921
00667	17356	09944	09946
00728	17436	09974	09975
00763	17458	09982	09983
00827	17493	09995	09995
00931	17504	09999	09999
01024	17504	09999	09999
01187	17470	09986	09987
01283	17458	09982	09983

Table 2f $M_{\infty} = 2.401$ $Re_{\ell} = 9.92 \times 10^{6}$

x = 0.4

y in	M	$\frac{u}{u_\delta}$ r = 0.89	$\frac{u}{u_\delta}$ r = 1
00.010	0.9932	0.5004	0.5138
00013	11145	05510	05646
00015	11263	05558	05694
00017	11587	05687	05824
00022	12178	05918	06054
00028	12974	06217	06352
00032	14140	06634	06765
00043	15902	07214	07336
00052	18174	07879	07984
00065	20977	08582	08660
00078	23424	09102	09156
00090	25096	09414	09451
00098	26048	09577	09604
00100	26486	09649	09672
00100	26044	09576	09604
00103	26537	09657	09680
00105	26744	09690	09711
00110	26858	09709	09728
00113	26767	09694	09714
00115	27216	09765	09780
00120	27430	09798	09811
00125	27310	09779	09794
00130	27564	09818	09830
00140	27745	09845	09856
00152	27895	09868	09876
00165	27969	09879	09887
00176	28026	09887	09895
00187	28096	09897	09904
00190	28235	09917	09923
00193	28248	09919	09925
00195	28231	09917	09922
00198	28291	09926	09931
00200	28179	09909	09915
00202	28274	09923	09928
00207	28352	09934	09939
00212	28429	09945	09949
00212	28308	09928	09933
00222	28494	09955	09958
00232	28537	09961	09963
00243	28554	09963	09966
00256	28626	09974	09975
00269	28678	09981	09982
00278	28682	09981	09983
00281	28754	09992	09992
00283	28767	09993	09994
00286	28746	09990	09991
00288	28720	09987	09988
00290	28763	09993	09993
00293	28793	09997	09997
00298	28805	09999	09999
00302	28818	10001	10001
00405	29008	10027	10025
00541	29273	10063	10059
00628	29398	10080	10075
00719	29589	10106	10099
00842	29819	10137	10127
00920	29946	10153	10142
00999	30190	10185	10172
01081	30312	10200	10186
01167	30436	10216	10201

x = 0.55

y in	M	$\frac{u}{u_\delta}$ r = 0.89	$\frac{u}{u_\delta}$ r = 1
00.010	1.1387	0.5844	05971
00013	11933	06069	06194
00015	12365	06242	06367
00018	12571	06323	06448
00020	12905	06453	06577
00023	12983	06484	06606
00025	13475	06670	06791
00028	13636	06730	06850
00030	13910	06831	06950
00042	14642	07093	07207
00056	15383	07347	07457
00068	15948	07534	07640
00094	17110	07899	07995
00105	17802	08105	08195
00107	17668	08066	08157
00108	17926	08141	08230
00110	17995	08161	08249
00113	18068	08182	08263
00115	18154	08206	08293
00118	18208	08222	08308
00120	18419	08281	08365
00123	18538	08315	08397
00125	18671	08351	08433
00138	19143	08480	08556
00153	19645	08612	08684
00165	20207	08756	08822
00191	21183	08993	09048
00203	21750	09125	09174
00207	22029	09188	09234
00209	22129	09210	09255
00211	22239	09235	09278
00215	22239	09235	09278
00216	22309	09250	09293
00220	22356	09260	09303
00222	22582	09309	09349
00225	22574	09308	09348
00227	22682	09331	09370
00240	23068	09413	09447
00252	23429	09488	09518
00266	23798	09562	09589
00293	24424	09685	09704
00304	24818	09760	09775
00305	24772	09751	09767
00307	24811	09759	09773
00310	24860	09768	09782
00312	24860	09768	09782
00315	24919	09779	09793
00317	24968	09788	09801
00320	25024	09798	09811
00322	25111	09815	09826
00325	25111	09815	09826
00338	25312	09851	09860
00351	25456	09877	09885
00370	25603	09904	09910
00377	25749	09930	09934
00390	25843	09946	09950
00401	25985	09971	09973
00403	25925	09961	09963
00404	25975	099[illegible]	09971
00406	25975	09969	09971
00408	25975	09969	09971
00411	25985	09971	09973
00414	25985	09971	09973
00416	26038	09980	09982
00418	26029	09979	09980
00422	26076	09987	09988
00433	26026	09978	09980
00435	26079	09987	09988
00447	26126	09995	09996
00465	26129	09996	09996
00473	26129	09996	09996
00487	26129	09996	09996
00500	26160	10001	10001
00664	26026	09978	09980
00727	25975	09969	09971
00827	25928	09961	09964
00923	25881	09953	09956
01023	25834	09945	09948

x = 0.7

y in	M	$\frac{u}{u_\delta}$ r = 0.89	$\frac{u}{u_\delta}$ r = 1
00.010	1.0178	0.5599	0.5713
00012	10370	05688	05803
00015	10632	05807	05922
00025	11388	06145	06259
00035	12003	06411	06523
00047	12580	06652	06762
00060	12983	06817	06925
00101	14320	07338	07438
00104	14386	07363	07462
00106	14440	07383	07482
00116	14623	07451	07549
00125	14912	07557	07652
00139	15203	07661	07754
00150	15530	07777	07867
00195	16549	08123	08204
00197	16542	08121	08202
00200	16608	08143	08224
00210	16815	08211	08289
00220	17055	08288	08364
00234	17313	08370	08443
00245	17589	08456	08527
00293	18678	08783	08841
00295	18713	08793	08851
00298	18771	08810	08867
00308	18951	08861	08917
00309	18818	08823	08880
00317	19120	08909	08963
00330	19473	09008	09057
00343	19676	09064	09111
00385	20618	09313	09349
00388	20612	09312	09348
00390	20699	09334	09369
00398	20856	09374	09407
00401	20862	09375	09408
00410	21012	09413	09444
00423	21295	09484	09511
00435	21557	09548	09572
00490	22493	09768	09781
00554	23028	09888	09894
00587	23391	09967	09969
00640	23488	09988	09989
00676	23529	09997	09997
00795	23384	09966	09968
00880	23349	09958	09961
00969	23171	09920	09924
01064	23101	09904	09910
01151	22992	09880	09887

x = 0.833

y in	M	$\frac{u}{u_\delta}$ r = 0.89	$\frac{u}{u_\delta}$ r = 1
00010	1.0931	0.6241	0.6344
00012	11106	06323	06426
00015	11336	06430	06532
00017	11722	06607	06707
00022	12656	07020	07115
00027	13179	07242	07335
00027	13129	07221	07314
00031	13568	07404	07494
00043	14177	07650	07735
00054	14714	07860	07941
00063	15109	08011	08088
00074	15448	08137	08211
00085	15682	08223	08294
00097	15873	08293	08362
00108	16219	08416	08481
00109	16219	08416	08481
00110	16101	08374	08441
00111	16219	08416	08481
00114	16255	08429	08494
00120	16335	08457	08521
00121	16233	08421	08486
00125	16408	08482	08546
00125	16396	08478	08542
00130	16487	08510	08573
00132	16417	08486	08549
00140	16587	08545	08606
00151	16723	08591	08651
00161	16836	08630	08689
00171	16962	08673	08730
00182	17050	08703	08759
00195	17174	08744	08799
00205	17220	08760	08814
00207	17289	08782	08836
00208	17296	08785	08838
00210	17289	08782	08836
00212	17289	08782	08836
00218	17330	08796	08849
00219	17400	08819	08871
00222	17400	08819	08871
00222	17396	08818	08870
00227	17515	08857	08908
00230	17522	08859	08910
00239	17567	08874	08924
00249	17703	08918	08967
00260	17805	08951	08998
00270	17946	08996	09042
00280	18047	09028	09072
00293	18147	09060	09103
00306	18296	09106	09148
00306	18296	09106	09148
00308	18296	09106	09148
00310	18296	09106	09148
00314	18328	09116	09157
00316	18377	09132	09172
00318	18398	09138	09178
00324	18462	09158	09197
00324	18454	09155	09195
00327	18524	09177	09215
00329	18518	09175	09214
00340	18615	09205	09242
00350	18775	09254	09289
00360	18919	09297	09330
00367	18887	09288	09321
00380	19115	09355	09386
00394	19287	09406	09435
00402	19278	09404	09433
00403	19309	09413	09441
00405	19309	09413	09441
00407	19396	09438	09465
00408	19370	09431	09458
00413	19406	09441	09468
00417	19519	09474	09500
00418	19467	09459	09485
00418	19513	09472	09498
00423	19589	09494	09519
00428	19641	09509	09533
00434	19635	09507	09532
00445	19789	09551	09573
00455	19909	09585	09606
00463	19999	09611	09630
00465	20005	09612	09632
00475	20125	09646	09663
00489	20228	09674	09691
00501	20347	09707	09722
00513	20420	09727	09741
00523	20524	09756	09768
00561	20808	09832	09841
00630	21094	09908	09913
00662	21207	09937	09941
00724	21319	09966	09968
00757	21362	09977	09978
00820	21418	09992	09992
00921	21418	09992	09992
01016	21404	09988	09989
01174	21376	09981	09982
01269	21349	09974	09975

x = 0.983

y in	M	$\frac{u}{u_\delta}$ r = 0.89	$\frac{u}{u_\delta}$ r = 1
00010	1.1448	0.6566	0.6664
00012	11603	06638	06735
00015	11992	06816	06912
00017	12516	07049	07142
00020	12723	07140	07232
00022	13080	07294	07384
00025	13319	07396	07483
00028	13616	07520	07606
00033	13968	07665	07747
00038	14310	07803	07882
00043	14612	07923	08000
00043	14655	07939	08016
00050	15176	08140	08212
00064	15686	08332	08398
00075	16077	08475	08537
00090	16578	08653	08709
00105	16965	08787	08839
00108	17147	08849	08899
00112	17196	08865	08915
00115	17202	08868	08917
00116	17283	08895	08943
00120	17300	08900	08948
00122	17380	08927	08974
00125	17397	08933	08980
00127	17460	08954	09000
00132	17539	08980	09025
00138	17635	09012	09055
00143	17688	09029	09072
00143	17730	09043	09085
00150	17861	09086	09127
00164	18048	09146	09185
00173	18171	09185	09222
00190	18360	09245	09280
00205	18497	09288	09321
00206	18540	09301	09334
00210	18525	09297	09329
00212	18570	09311	09343
00215	18619	09326	09357
00217	18619	09326	09357
00220	18650	09335	09366
00223	18679	09344	09375
00225	18695	09349	09380
00230	18724	09358	09388
00236	18769	09372	09402
00241	18784	09377	09406
00241	18844	09395	09424
00248	18923	09419	09447
00262	19027	09451	09477
00273	19115	09477	09502
00288	19246	09516	09540
00304	19323	09539	09561
00306	19363	09551	09573
00308	19378	09555	09577
00311	19421	09568	09589
00316	19425	09569	09590
00319	19425	09569	09590
00319	19468	09582	09602
00321	19453	09578	09598
00325	19483	09586	09606
00329	19511	09595	09614
00335	19553	09607	09626
00340	19526	09599	09618
00340	19600	09621	09639
00347	19676	09643	09660
00360	19774	09671	09687
00370	19816	09683	09699
00370	19812	09682	09698
00386	19915	09712	09726
00400	19944	09720	09734
00402	19991	09733	09747
00403	19986	09732	09745
00405	20013	09740	09752
00408	20002	09736	09750
00410	20002	09736	09750
00413	20017	09741	09753
00415	20044	09748	09761
00418	20058	09752	09765
00423	20086	09760	09772
00429	20115	09768	09780
00433	20115	09768	09780
00433	20160	09781	09792
00441	20207	09794	09805
00455	20260	09809	09819
00465	20289	09817	09826
00470	20339	09831	09840
00481	20384	09844	09852
00498	20418	09853	09861
00567	20662	09920	09924
00630	20795	09956	09959
00667	20849	09971	09972
00725	20901	09985	09986
00763	20929	09993	09993
00825	20927	09992	09992
00887	20945	09997	09997
00983	20931	09993	09993
01083	20891	09982	09983
01182	20877	09979	09980
01278	20837	09968	09969

Table 2g $M_\infty = 2.799$ $Re_\ell = 10.10 \times 10^6$

x = 0.4

y in	M	$\frac{u}{u_\delta}$ r = 0.89	$\frac{u}{u_\delta}$ r = 1
00.010	1.1790	0.5468	0.5620
00013	12365	05679	05831
00015	12790	05831	05982
00017	13425	06051	06202
00022	14584	06435	06582
00028	15135	06608	06754
00037	16506	07017	07156
00048	17931	07408	07538
00057	19536	07809	07928
00073	22044	08362	08459
00088	24281	08786	08863
00098	26057	09083	09144
00100	26428	09141	09198
00103	26620	09170	09226
00105	27045	09234	09286
00105	26811	09199	09253
00110	27833	09348	09393
00115	28128	09389	09432
00123	28573	09450	09489
00125	28986	09505	09540
00135	29501	09572	09602
00138	29722	09600	09629
00145	30200	09659	09684
00153	30424	09686	09709
00160	30702	09719	09740
00174	31188	09776	09792
00190	31351	09794	09810
00192	31606	09823	09836
00193	31467	09808	09822
00195	31537	09815	09829
00198	31698	09833	09846
00202	31812	09846	09858
00207	31881	09854	09865
00210	31987	09865	09875
00217	32071	09874	09884
00224	32176	09886	09894
00226	32169	09885	09894
00236	32432	09913	09920
00240	32454	09916	09922
00250	32618	09933	09938
00266	32804	09952	09956
00281	33061	09979	09981
00282	33017	09975	09976
00283	33039	09977	09979
00286	33135	09987	09988
00288	33120	09985	09986
00293	33193	09993	09993
00298	33193	09993	09993
00300	33201	09993	09994
00307	33193	09993	09993
00315	33201	09993	09994
00316	33171	09990	09991
00326	33266	10000	10000
00329	33288	10002	10002
00341	33354	10009	10008
00433	33629	10036	10033
00510	33830	10056	10052
00631	34222	10094	10087
00710	34484	10119	10110
00862	35007	10167	10154
00940	35180	10183	10169
01019	35359	10199	10184
01186	35869	10244	10225

x = 0.55

y in	M	$\frac{u}{u_\delta}$ r = 0.89	$\frac{u}{u_\delta}$ r = 1
00.010	1.2604	0.5944	0.6086
00013	12831	06027	06169
00015	13584	06295	06435
00018	13889	06400	06540
00020	14186	06501	06640
00023	14761	06692	06828
00028	15203	06835	06969
00038	16079	07107	07236
00048	16711	07295	07420
00063	17685	07570	07689
00079	18455	07777	07890
00094	19463	08034	08138
00105	19713	08095	08197
00107	20284	08231	08328
00108	20300	08235	08332
00110	20476	08276	08371
00113	20580	08300	08394
00115	20777	08345	08437
00118	20972	08389	08479
00123	21372	08478	08564
00133	21810	08572	08655
00143	22180	08650	08729
00159	23184	08852	08922
00175	23773	08965	09029
00191	24220	09048	09107
00203	24967	09181	09233
00207	24314	09065	09123
00209	24980	09183	09235
00211	25130	09209	09260
00215	25207	09223	09272
00216	25368	09250	09298
00220	25451	09264	09312
00225	25863	09333	09376
00235	26069	09367	09408
00245	26459	09429	09467
00260	26843	09489	09523
00276	27429	09579	09607
00293	27817	09636	09661
00304	27841	09639	09664
00305	28108	09678	09700
00307	28183	09689	09710
00310	28258	09699	09720
00312	28327	09709	09729
00315	28401	09719	09739
00317	28555	09741	09759
00322	28612	09749	09766
00335	28815	09777	09792
00344	29023	09805	09819
00358	29379	09853	09863
00370	29406	09856	09866
00375	29643	09887	09895
00390	29867	09916	09922
00401	30078	09943	09947
00403	30067	09942	09946
00404	30137	09951	09954
00406	30137	09951	09954
00408	30137	09951	09954
00411	30207	09959	09962
00414	30218	09961	09964
00418	30271	09968	09970
00430	30325	09974	09976
00440	30395	09983	09984
00455	30464	09991	09992
00465	30427	09987	09988
00470	30522	09999	09999
00487	30538	10001	10001
00500	30602	10008	10008
00633	30427	09987	09988
00727	30357	09978	09980
00827	30293	09970	09972
00923	30293	09970	09972
01023	30223	09961	09964

Table 2g (Contd)

x = 0.7

y in	M	$\frac{u}{u_\delta}$ r = 0.89	$\frac{u}{u_\delta}$ r = 1
00.010	1.3326	0.6461	0.6589
00012	13621	06569	06696
00015	14009	06708	06834
00020	14751	06966	07088
00035	16044	07390	07504
00050	16845	07637	07745
00065	17536	07841	07943
00080	18113	08005	08102
00092	18610	08141	08234
00101	19039	08256	08344
00104	19110	08276	08363
00105	19028	08253	08342
00106	19176	08292	08379
00111	19311	08327	08413
00125	19846	08463	08544
00140	20366	08592	08667
00155	20937	08728	08798
00170	21479	08852	08917
00183	21783	08921	08982
00195	22092	08989	09046
00195	22373	09049	09104
00197	22148	09001	09058
00200	22327	09039	09095
00205	22327	09039	09095
00220	22844	09148	09198
00235	23183	09218	09265
00250	23677	09317	09358
00265	23957	09372	09410
00278	24221	09422	09458
00290	24486	09472	09505
00293	24601	09494	09525
00295	24601	09494	09525
00298	24656	09504	09535
00303	24706	09513	09543
00317	24971	09562	09589
00333	25178	09599	09624
00349	25478	09652	09674
00353	25552	09665	09686
00363	25843	09716	09734
00375	25884	09723	09740
00385	25992	09741	09758
00387	26036	09749	09765
00388	25944	09733	09750
00390	26044	09750	09766
00396	25992	09741	09758
00410	26291	09792	09805
00425	26441	09816	09828
00440	26531	09831	09842
00441	26602	09843	09853
00455	26734	09865	09873
00468	26773	09871	09879
00479	26870	09887	09894
00534	27209	09941	09944
00598	27369	09966	09968
00630	27589	10000	10000
00720	27494	09985	09986
00839	27282	09952	09955
00922	27186	09937	09941
01010	27090	09922	09927
01193	26948	09899	09906

x = 0.833

y in	M	$\frac{u}{u_\delta}$ r = 0.89	$\frac{u}{u_\delta}$ r = 1
00.010	1.3350	0.6794	0.6907
00012	14048	07058	07168
00015	14248	07132	07241
00017	15000	07403	07507
00020	15245	07489	07590
00025	16001	07746	07841
00030	16372	07868	07960
00035	16729	07983	08072
00045	17343	08175	08258
00055	17863	08332	08410
00071	18562	08536	08607
00086	19012	08662	08728
00108	19573	08815	08875
00108	19451	08782	08844
00109	19614	08826	08885
00111	19583	08817	08878
00114	19703	08850	08908
00117	19714	08852	08911
00122	19751	08862	08920
00127	19877	08896	08952
00132	19962	08918	08974
00143	20140	08964	09018
00153	20301	09005	09057
00169	20591	09079	09128
00184	20754	09120	09167
00205	21028	09187	09231
00205	20996	09180	09224
00207	21028	09187	09231
00210	20990	09178	09222
00212	21070	09198	09241
00215	21159	09219	09261
00220	21239	09239	09280
00225	21233	09237	09278
00230	21312	09256	09296
00241	21400	09277	09317
00252	21588	09322	09359
00266	21784	09368	09403
00282	21938	09404	09437
00303	22243	09473	09503
00306	22276	09481	09510
00308	22276	09481	09510
00310	22276	09481	09510
00314	22276	09481	09510
00316	22361	09500	09528
00321	22400	09509	09536
00326	22466	09523	09550
00331	22541	09540	09566
00342	22624	09559	09584
00352	22728	09581	09605
00368	22949	09630	09651
00370	22914	09622	09644
00383	23060	09654	09674
00402	23241	09692	09710
00403	23165	09676	09695
00405	23203	09684	09702
00405	23244	09693	09711
00408	23275	09700	09717
00410	23247	09693	09711
00415	23319	09709	09726
00420	23278	09700	09718
00426	23313	09708	09725
00436	23500	09747	09762
00447	23531	09753	09768
00462	23708	09790	09802
00466	23708	09790	09802
00478	23779	09805	09816
00499	23920	09834	09843
00563	24236	09897	09903
00630	24512	09952	09955
00668	24580	09965	09967
00724	24681	09985	09986
00760	24681	09985	09986
00880	24749	09998	09998
00921	24749	09998	09998
01016	24749	09998	09998
01270	24681	09985	09986

x = 0.983

y in	M	$\frac{u}{u_\delta}$ r = 0.89	$\frac{u}{u_\delta}$ r = 1
00.010	1.3477	0.6908	0.7018
00012	13769	07021	07129
00015	14343	07236	07341
00017	14616	07336	07439
00022	15359	07600	07698
00025	15717	07724	07819
00030	16115	07858	07949
00030	16115	07858	07949
00035	16456	07971	08,059
00045	17157	08195	08277
00060	17921	08429	08503
00077	18685	08653	08718
00092	19234	08807	08866
00108	19872	08979	09032
00108	19755	08948	09002
00112	19913	08990	09042
00115	19991	09011	09062
00116	20028	09021	09071
00122	20147	09052	09101
00125	20224	09072	09120
00130	20302	09092	09139
00130	20302	09092	09139
00135	20378	09112	09158
00145	20571	09161	09205
00160	20798	09218	09260
00176	21090	09291	09329
00192	21317	09346	09382
00206	21489	09388	09421
00208	21536	09399	09432
00210	21498	09390	09423
00212	21571	09407	09440
00215	21536	09399	09432
00220	21608	09416	09448
00223	21680	09433	09464
00227	21715	09441	09472
00232	21790	09459	09489
00243	21895	09484	09512
00259	22038	09517	09544
00274	22215	09558	09583
00290	22392	09598	09621
00305	22450	09611	09633
00306	22522	09628	09649
00308	22459	09613	09635
00311	22528	09629	09650
00314	22564	09637	09657
00319	22633	09652	09672
00321	22666	09660	09679
00326	22672	09661	09680
00326	22638	09654	09673
00326	22702	09668	09686
00331	22702	09668	09686
00342	22803	09690	09708
00357	22907	09713	09729
00370	23002	09734	09749
00373	23010	09735	09751
00390	23111	09757	09771
00400	23070	09748	09763
00403	23111	09757	09771
00405	23143	09764	09778
00408	23178	09772	09785
00408	23205	09778	09790
00413	23245	09786	09799
00415	23245	09786	09799
00420	23285	09795	09807
00420	23280	09794	09806
00425	23280	09794	09806
00436	23379	09815	09826
00451	23414	09822	09833
00468	23512	09843	09852
00470	23507	09842	09851
00484	23546	09850	09859
00500	23673	09877	09884
00567	23870	09918	09923
00632	24037	09952	09955
00667	24096	09964	09966
00728	24169	09979	09980
00763	24195	09984	09985
00827	24264	09998	09998
00931	24264	09998	09998
01024	24264	09998	09998
01.187	24200	09985	09986
01283	24135	09972	09974

TABLE 3

Integral Properties of the Boundary Layers.

(a) r = 0.89

x	δ_1 in	δ_2 in	δ_3 in	δ_1^i in	δ_2^i in	δ_3^i in	H_{12}	H_{32}	H_{12}^i	H_{32}^i	$\frac{u_\delta}{\nu_\delta}$ $\times 10^5$/in	M_δ
$M_\infty = 0.597$ $Re_\ell = 9.98 \times 10^6$												
0.4	0.0635	0.0363	0.0624	0.0590	0.0375	0.0645	1.751	1.720	1.571	1.718	1.752	0.642
0.475	0.1095	0.0630	0.1064	0.1030	0.0649	0.1096	1.739	1.690	1.587	1.689	1.644	0.586
0.55	0.1572	0.0939	0.1597	0.1480	0.0965	0.1641	1.675	1.701	1.533	1.700	1.612	0.570
0.7	0.3059	0.1858	0.3157	0.2897	0.1906	0.3235	1.646	1.699	1.520	1.697	1.472	0.538
0.833	0.1683	0.1142	0.2037	0.1566	0.1166	0.2080	1.473	1.784	1.343	1.783	1.543	0.566
0.983	0.0859	0.0609	0.1130	0.0781	0.0620	0.1149	1.411	1.856	1.261	1.855	1.662	0.622
$M_\infty = 1.398$ $Re_\ell = 10.08 \times 10^6$												
0.4	0.0654	0.0234	0.0417	0.0422	0.0282	0.0500	2.799	1.784	1.499	1.775	1.516	1.766
0.475	0.0970	0.0362	0.0628	0.0671	0.0437	0.0755	2.681	1.737	1.535	1.727	1.592	1.633
0.55	0.1581	0.0618	0.1043	0.1189	0.0736	0.1234	2.559	1.687	1.616	1.678	1.647	1.454
0.7	0.3244	0.1359	0.2263	0.2576	0.1573	0.2607	2.388	1.665	1.638	1.658	1.702	1.288
0.833	0.1837	0.0916	0.1629	0.1381	0.1014	0.1799	2.006	1.779	1.362	1.775	1.706	1.254
0.983	0.1233	0.0665	0.1224	0.0912	0.0714	0.1313	1.855	1.842	1.276	1.839	1.695	1.215
$M_\infty = 1.404$ $Re_\ell = 19.34 \times 10^6$												
0.4	0.0584	0.0207	0.0370	0.0376	0.0249	0.0443	2.824	1.789	1.509	1.779	2.922	1.777
0.475	0.0840	0.0312	0.0544	0.0578	0.0377	0.0654	2.692	1.744	1.533	1.735	3.051	1.646
0.55	0.1356	0.0534	0.0906	0.1008	0.0635	0.1073	2.542	1.698	1.587	1.689	3.219	1.470
0.7	0.2866	0.1234	0.2077	0.2252	0.1421	0.2382	2.322	1.683	1.584	1.676	3.219	1.289
0.833	0.1594	0.0806	0.1450	0.1179	0.0887	0.1593	1.979	1.799	1.329	1.796	3.218	1.269
0.983	0.1112	0.0605	0.1120	0.0820	0.0647	0.1197	1.839	1.851	1.267	1.849	3.303	1.211

TABLE 3(a)—*continued*

x	δ_1 in	δ_2 in	δ_3 in	δ_1^i in	δ_2^i in	δ_3^i in	H_{12}	H_{32}	H_{12}^i	H_{32}^i	$\frac{u_\delta}{\nu_\delta}$ $\times 10^5$/in	M_δ
$M_\infty = 1.700$ $Re_\ell = 10.00 \times 10^6$												
0.4	0.0800	0.0244	0.0438	0.0461	0.0312	0.0556	3.273	1.792	1.474	1.779	1.419	2.087
0.55	0.1594	0.0538	0.0925	0.1051	0.0684	0.1168	2.963	1.720	1.537	1.708	1.592	1.815
0.7	0.2901	0.1070	0.1807	0.2081	0.1315	0.2206	2.712	1.689	1.583	1.678	1.712	1.597
0.833	0.1763	0.0764	0.1365	0.1195	0.0881	0.1570	2.309	1.788	1.356	1.782	1.712	1.529
0.983	0.1172	0.0545	0.1009	0.0770	0.0603	0.1114	2.149	1.851	1.276	1.847	1.768	1.495
$M_\infty = 2.000$ $Re_\ell = 9.88 \times 10^6$												
0.4	0.0916	0.0238	0.0429	0.0471	0.0322	0.0575	3.851	1.802	1.462	1.785	1.311	2.414
0.475	0.1232	0.0329	0.0583	0.0668	0.0453	0.0795	3.746	1.770	1.473	1.754	1.363	2.333
0.55	0.1678	0.0482	0.0839	0.0986	0.0656	0.1131	3.481	1.739	1.504	1.724	1.487	2.153
0.7	0.2736	0.0878	0.1505	0.1751	0.1149	0.1954	3.117	1.714	1.524	1.701	1.693	1.918
0.833	0.1689	0.0636	0.1148	0.1023	0.0764	0.1372	2.654	1.804	1.340	1.796	1.778	1.804
0.983	0.1180	0.0478	0.0888	0.0695	0.0544	0.1008	2.469	1.858	1.277	1.853	1.816	1.751
$M_\infty = 2.401$ $Re_\ell = 9.92 \times 10^6$												
0.4	0.0582	0.0110	0.0194	0.0296	0.0172	0.0297	5.312	1.768	1.723	1.731	1.266	2.881
0.55	0.1170	0.0281	0.0510	0.0549	0.0392	0.0705	4.165	1.815	1.403	1.800	1.453	2.615
0.7	0.1903	0.0527	0.0950	0.0965	0.0707	0.1264	3.608	1.802	1.365	1.788	1.631	2.354
0.833	0.1447	0.0475	0.0885	0.0722	0.0569	0.1058	3.048	1.865	1.267	1.858	1.813	2.145
0.983	0.0959	0.0322	0.0606	0.0485	0.0375	0.0704	2.977	1.883	1.292	1.874	1.849	2.096
$M_\infty = 2.799$ $Re_\ell = 10.10 \times 10^6$												
0.4	0.0796	0.0129	0.0233	0.0337	0.0214	0.0379	6.167	1.804	1.576	1.770	1.216	3.3[illegible]7
0.55	0.1323	0.0259	0.0474	0.0537	0.0387	0.0701	5.112	1.830	1.387	1.810	1.411	3.053
0.7	0.1410	0.0329	0.0611	0.0581	0.0443	0.0816	4.285	1.858	1.313	1.844	1.608	2.759
0.833	0.1199	0.0333	0.0631	0.0510	0.0404	0.0763	3.599	1.895	1.262	1.885	1.866	2.476
0.983	0.0998	0.0283	0.0536	0.0436	0.0339	0.0639	3.531	1.896	1.286	1.886	1.922	2.427

TABLE 3—*continued*

(b) r = 1

x	δ_1 in	δ_2 in	δ_3 in	δ_1^i in	δ_2^i in	δ_3^i in	H_{12}	H_{32}	H_{12}^i	H_{32}^i	$\frac{u_\delta}{\nu_\delta}$ $\times 10^5$/in	M_δ
$M_\infty = 0.597$ $Re_\ell = 9.98 \times 10^6$												
0.4	0.0638	0.0360	0.0620	0.0587	0.0374	0.0643	1.771	1.721	1.569	1.719	1.752	0.642
0.475	0.1099	0.0626	0.1059	0.1026	0.0647	0.1094	1.756	1.692	1.585	1.690	1.644	0.586
0.55	0.1578	0.0933	0.1588	0.1474	0.0963	0.1638	1.691	1.702	1.531	1.701	1.612	0.570
0.7	0.3069	0.1849	0.3143	0.2887	0.1902	0.3229	1.660	1.700	1.518	1.698	1.472	0.538
0.833	0.1689	0.1135	0.2026	0.1559	0.1162	0.2073	1.488	1.785	1.341	1.784	1.543	0.566
0.983	0.0863	0.0604	0.1122	0.0777	0.0616	0.1144	1.429	1.856	1.260	1.865	1.662	0.622
$M_\infty = 1.398$ $Re_\ell = 10.08 \times 10^6$												
0.4	0.0663	0.0225	0.0403	0.0412	0.0276	0.0491	2.948	1.789	1.493	1.779	1.516	1.766
0.475	0.0982	0.0350	0.0609	0.0657	0.0430	0.0745	2.808	1.742	1.526	1.732	1.592	1.633
0.55	0.1599	0.0601	0.1017	0.1168	0.0728	0.1224	2.661	1.692	1.606	1.682	1.647	1.454
0.7	0.3275	0.1328	0.2217	0.2541	0.1560	0.2591	2.467	1.670	1.628	1.661	1.702	1.288
0.833	0.1858	0.0894	0.1594	0.1357	0.1000	0.1778	2.078	1.783	1.357	1.778	1.706	1.254
0.983	0.1263	0.0656	0.1208	0.0907	0.0710	0.1306	1.926	1.842	1.276	1.839	1.695	1.215
$M_\infty = 1.404$ $Re_\ell = 19.34 \times 10^6$												
0.4	0.0591	0.0199	0.0356	0.0366	0.0243	0.0434	2.977	1.794	1.505	1.784	2.922	1.777
0.475	0.0851	0.0301	0.0527	0.0565	0.0370	0.0645	2.822	1.749	1.525	1.740	3.051	1.646
0.55	0.1371	0.0518	0.0882	0.0989	0.0627	0.1062	2.645	1.703	1.578	1.693	3.219	1.470
0.7	0.2895	0.1205	0.2034	0.2219	0.1409	0.2365	2.401	1.687	1.575	1.679	3.219	1.289
0.833	0.1611	0.0782	0.1409	0.1157	0.0870	0.1564	2.059	1.802	1.329	1.797	3.218	1.269
0.983	0.1126	0.0591	0.1095	0.0805	0.0637	0.1179	1.906	1.854	1.264	1.851	3.303	1.211

TABLE 3(b)—*continued*

x	δ_1 in	δ_2 in	δ_3 in	δ_1^i in	δ_2^i in	δ_3^i in	H_{12}	H_{32}	H_{12}^i	H_{32}^i	$\frac{u_\delta}{\nu_\delta}$ $\times 10^5$/in	M_δ
	$M_\infty = 1.700$ $Re_\ell = 10.00 \times 10^6$											
0.4	0.0811	0.0233	0.0419	0.0446	0.0304	0.0543	3.480	1.799	1.468	1.784	1.419	2.087
0.55	0.1535	0.0487	0.0833	0.0986	0.0643	0.1097	3.152	1.711	1.534	1.707	1.592	1.815
0.7	0.2935	0.1036	0.1755	0.2040	0.1299	0.2185	2.832	1.694	1.570	1.682	1.712	1.597
0.833	0.1779	0.0737	0.1322	0.1161	0.0861	0.1539	2.414	1.793	1.348	1.787	1.712	1.529
0.983	0.1197	0.0531	0.0984	0.0757	0.0594	0.1098	2.254	1.853	1.275	1.849	1.768	1.495
	$M_\infty = 2.000$ $Re_\ell = 9.88 \times 10^6$											
0.4	0.0929	0.0225	0.0407	0.0454	0.0312	0.0559	4.125	1.809	1.454	1.791	1.311	2.414
0.475	0.1249	0.0312	0.0555	0.0645	0.0441	0.0777	4.002	1.778	1.462	1.761	1.363	2.333
0.55	0.1701	0.0460	0.0803	0.0956	0.0641	0.1110	3.698	1.747	1.491	1.731	1.487	2.153
0.7	0.2772	0.0843	0.1451	0.1705	0.1129	0.1927	3.289	1.721	1.510	1.707	1.698	1.918
0.833	0.1714	0.0612	0.1106	0.0993	0.0746	0.1343	2.802	1.809	1.332	1.801	1.778	1.804
0.983	0.1197	0.0459	0.0855	0.0673	0.0528	0.0981	2.610	1.863	1.274	1.857	1.816	1.751
	$M_\infty = 2.401$ $Re_\ell = 9.92 \times 10^6$											
0.4	0.0589	0.0103	0.0183	0.0285	0.0166	0.0289	5.723	1.776	1.714	1.739	1.266	2.881
0.55	0.1257	0.0283	0.0520	0.0546	0.0397	0.0720	4.435	1.836	1.375	1.815	1.453	2.615
0.7	0.1930	0.0500	0.0904	0.0928	0.0685	0.1229	3.862	1.809	1.355	1.795	1.631	2.354
0.833	0.1476	0.0453	0.0846	0.0697	0.0551	0.1026	3.261	1.870	1.264	1.861	1.813	2.145
0.983	0.0974	0.0306	0.0578	0.0467	0.0361	0.0679	3.181	1.887	1.290	1.878	1.849	2.096
	$M_\infty = 2.799$ $Re_\ell = 10.10 \times 10^6$											
0.4	0.0805	0.0120	0.0218	0.0323	0.0206	0.0365	6.696	1.813	1.568	1.777	1.216	3.327
0.55	0.1340	0.0242	0.0445	0.0512	0.0371	0.0674	5.543	1.838	1.379	1.818	1.411	3.053
0.7	0.1430	0.0309	0.0575	0.0554	0.0423	0.0783	4.633	1.865	1.308	1.850	1.608	2.759
0.833	0.1219	0.0314	0.0597	0.0487	0.0386	0.0730	3.879	1.898	1.261	1.889	1.866	2.476
0.983	0.1014	0.0267	0.0507	0.0417	0.0324	0.0612	3.803	1.901	1.286	1.890	1.922	2.427

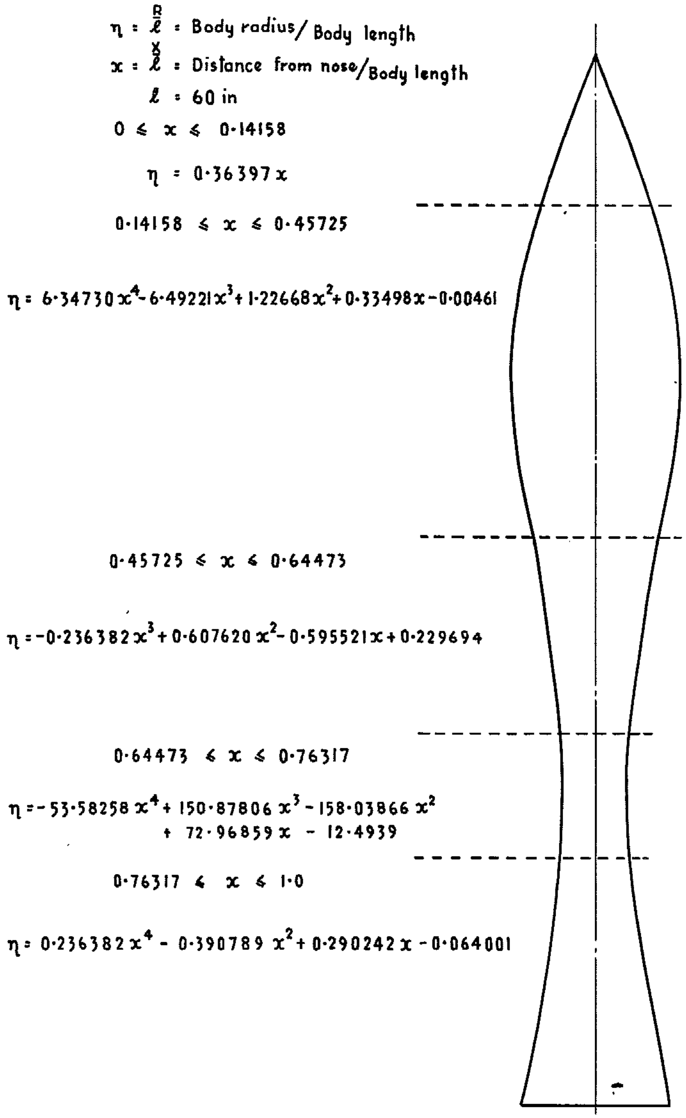

FIG. 1. Geometry of body.

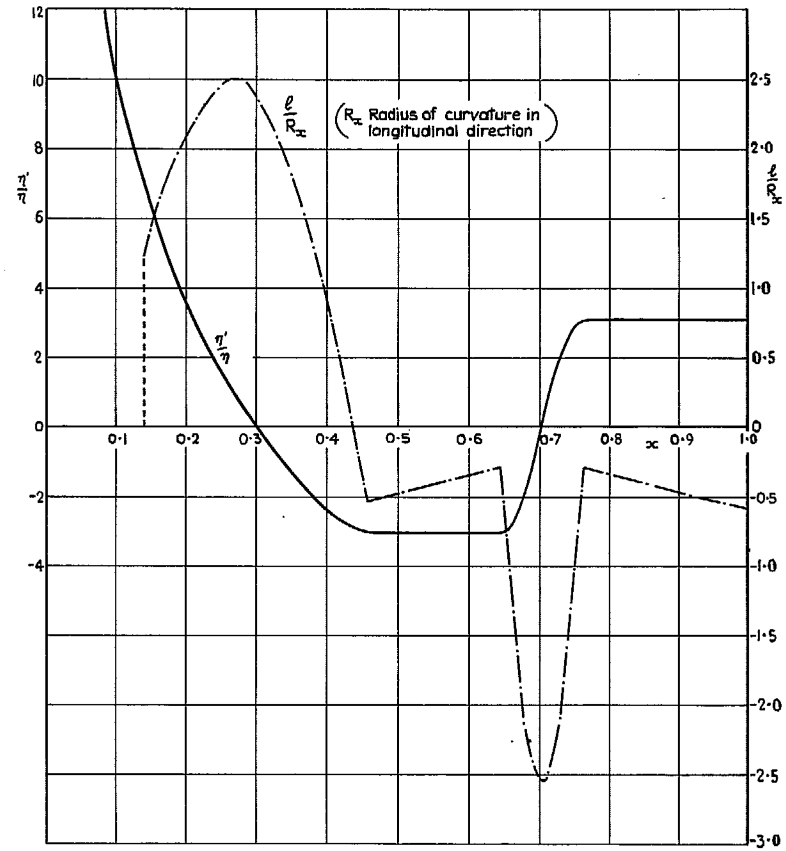

FIG. 2. Divergence parameter and longitudinal curvature.

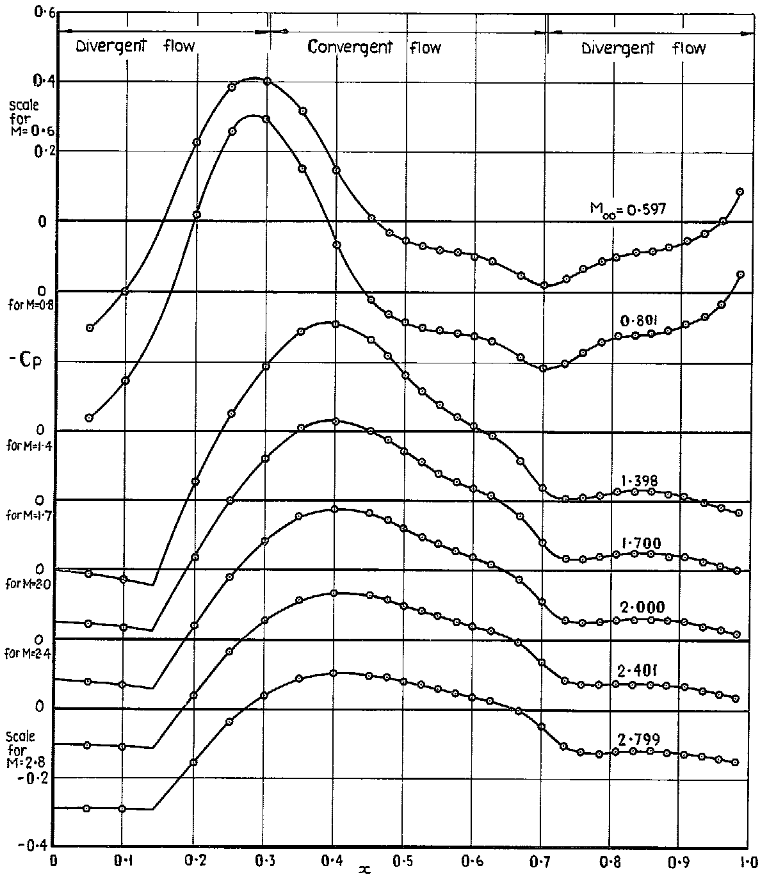

FIG. 3. Pressure distribution $Re_l \simeq 10^7$.

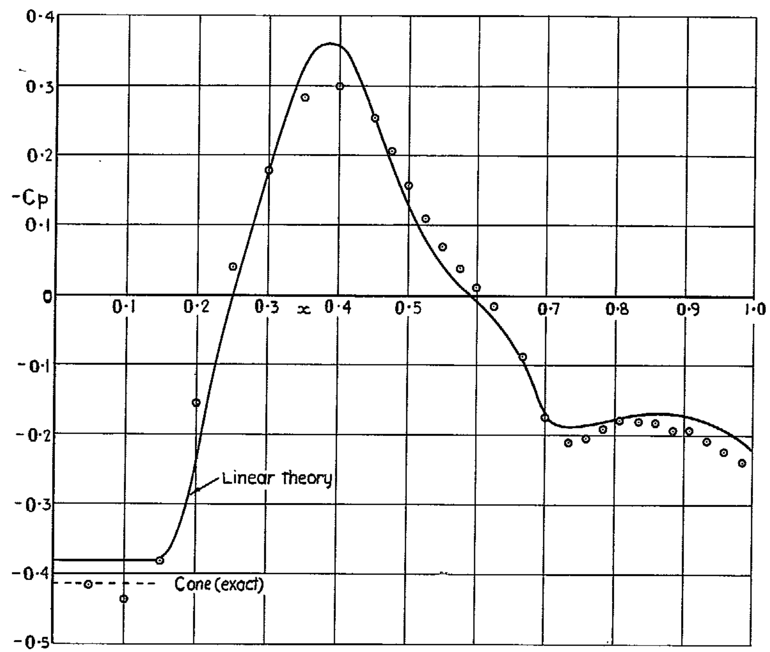

FIG. 4. Comparison of predicted (inviscid) and measured pressure distribution $M = 1{\cdot}404$ $Re_l = 19{\cdot}97 \times 10^6$.

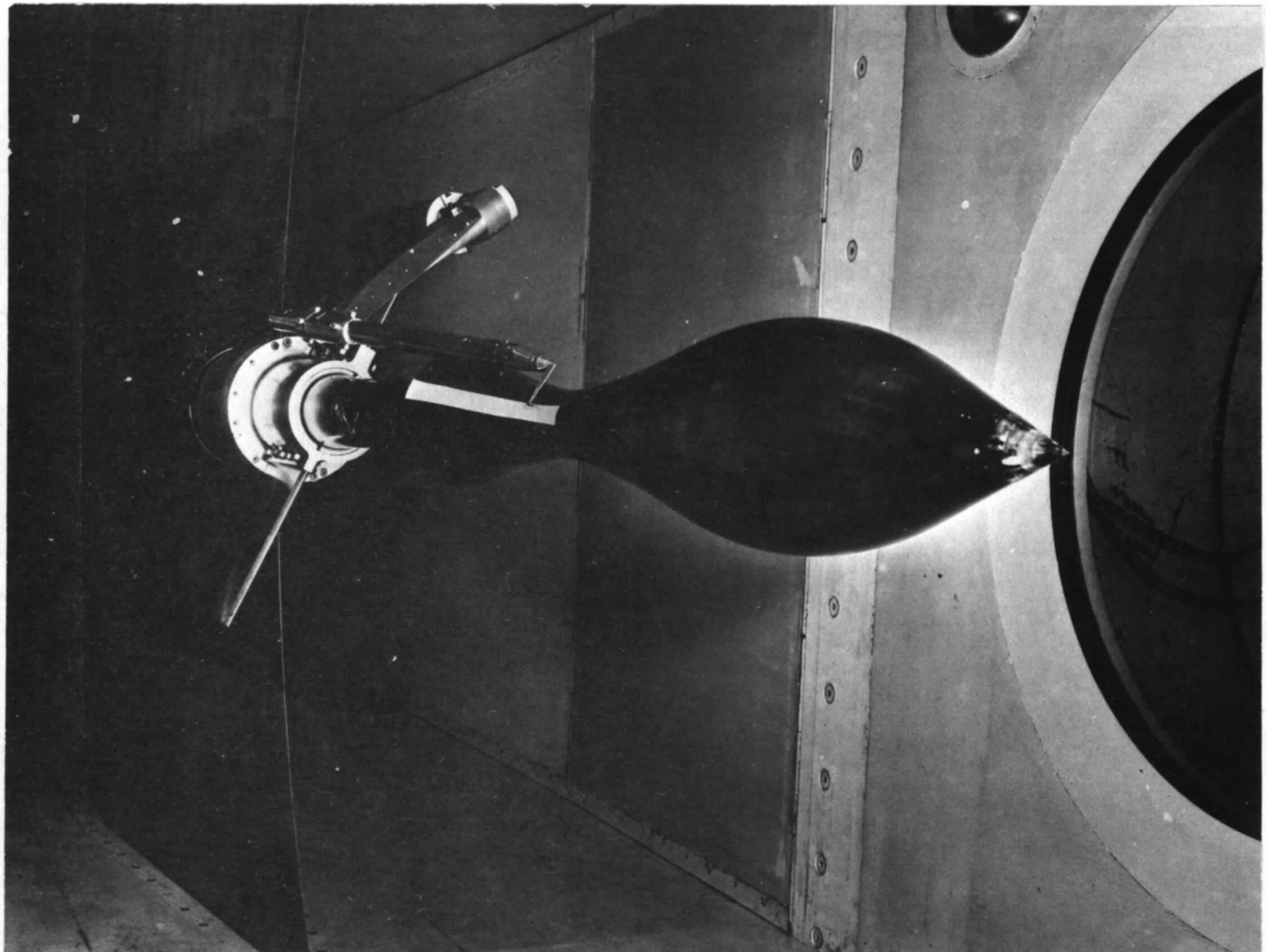

FIG. 5a. Model with boundary-layer survey equipment.

FIG. 5b. Detail of model with rake.

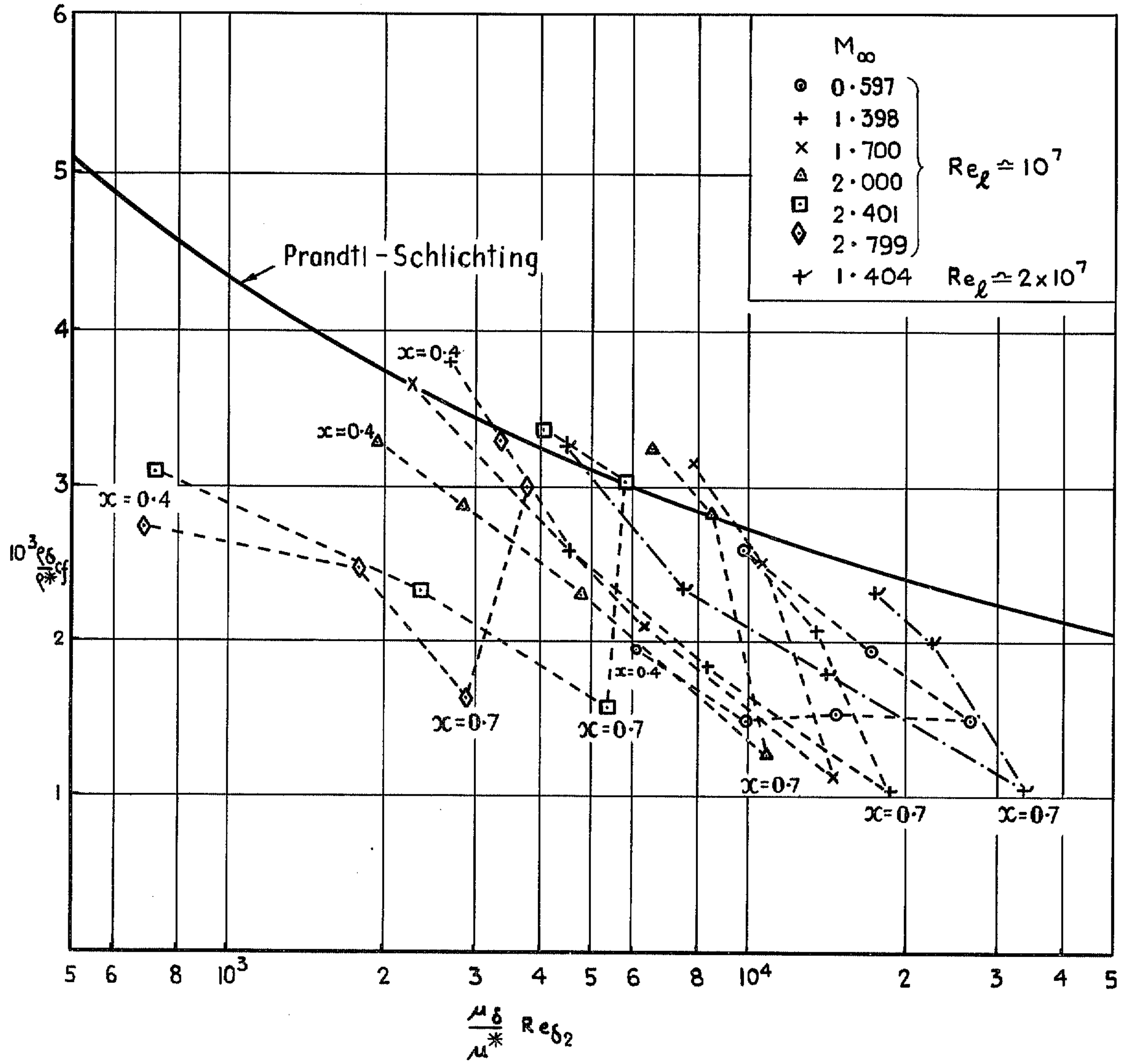

FIG. 6. Local skin friction as a function of momentum thickness Reynolds number in intermediate temperature form.

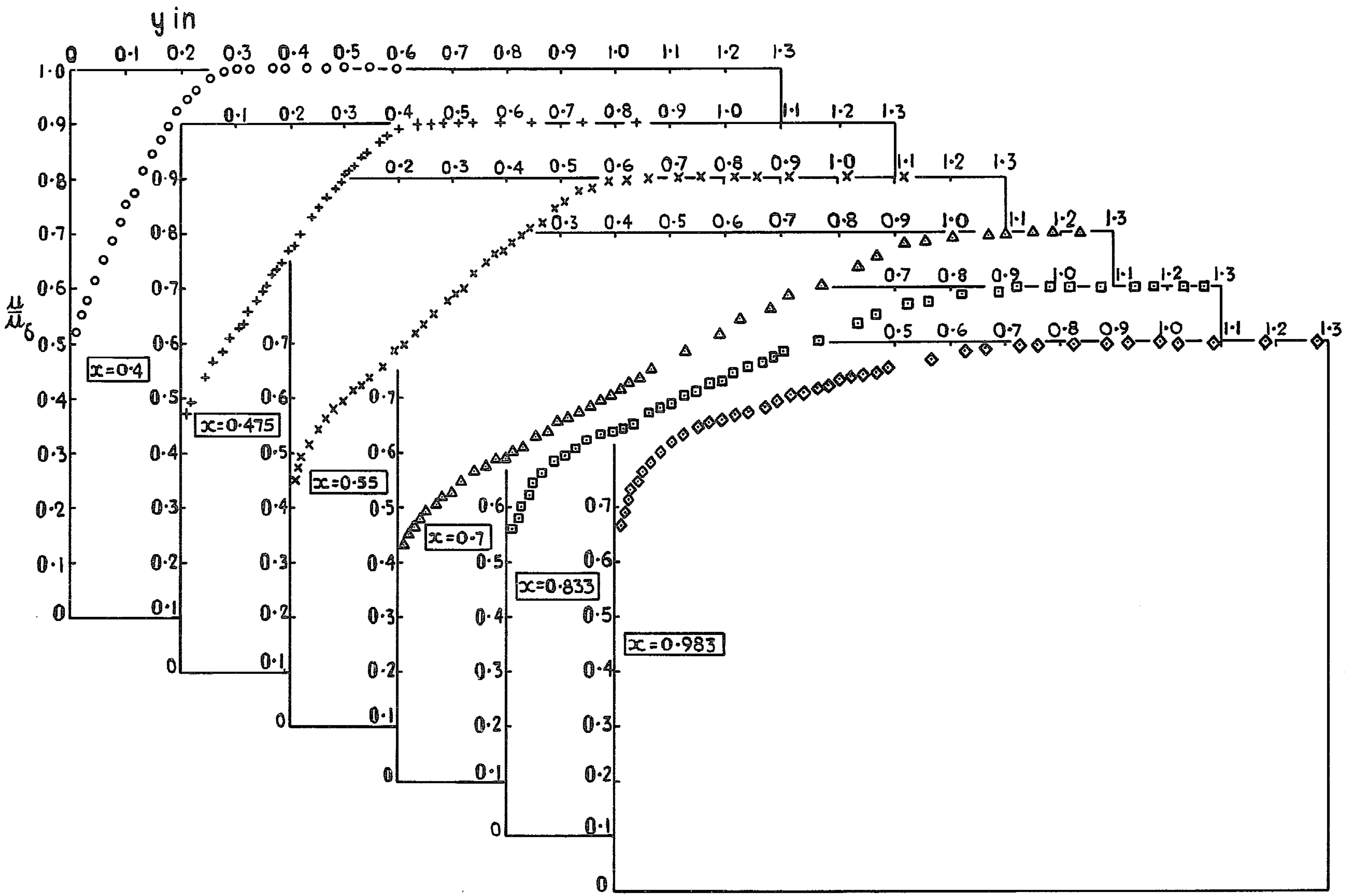

FIG. 7a. Velocity profiles $M_{\infty} = 0{\cdot}597$ $Re_l = 9{\cdot}98 \times 10^6$.

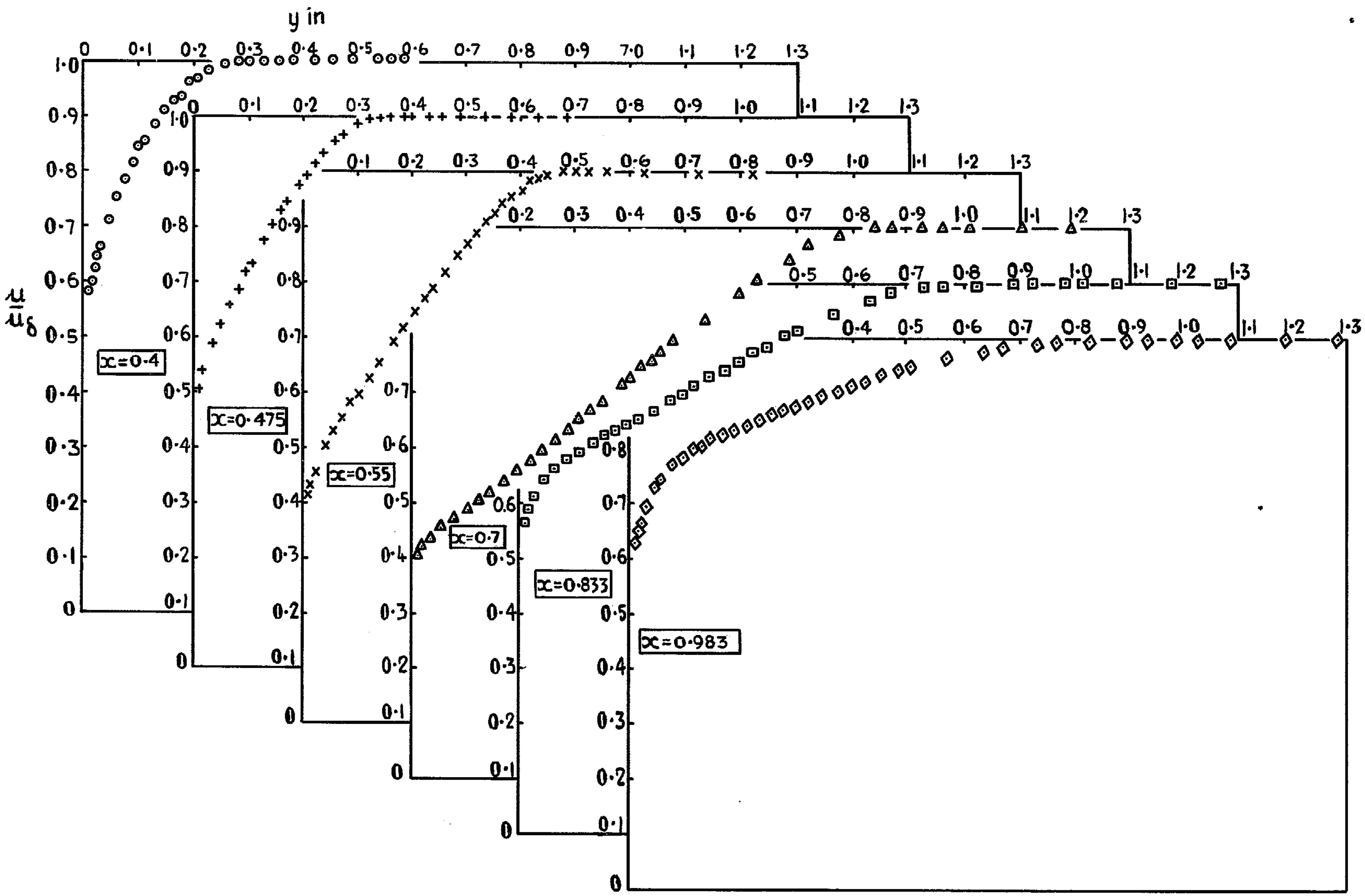

FIG. 7b. Velocity profiles $M_{\infty} = 1{\cdot}398$ $Re_l = 10{\cdot}1 \times 10^6$.

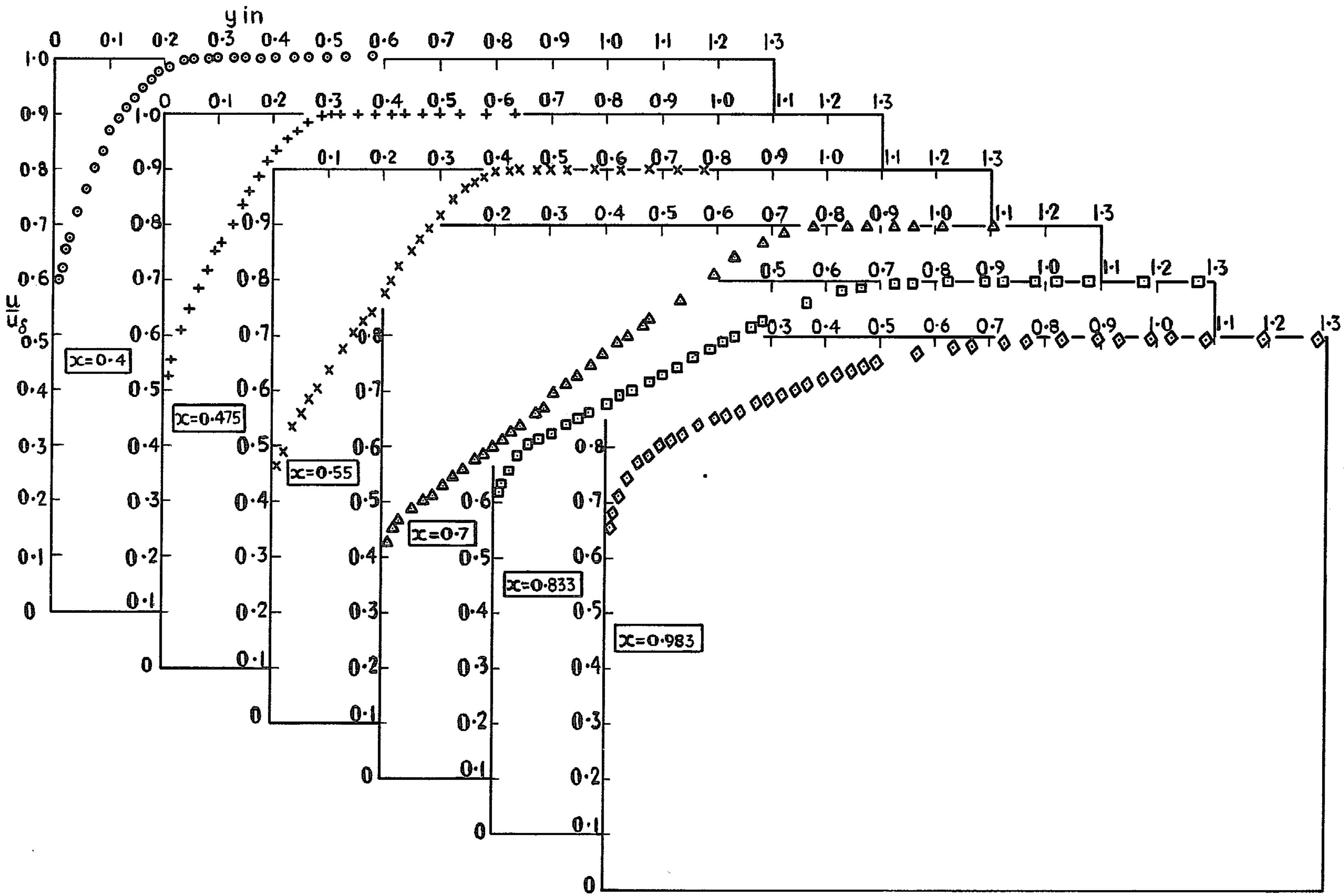

FIG. 7c. Velocity profiles $M_\infty = 1{\cdot}404$ $Re_l = 19{\cdot}34 \times 10^6$.

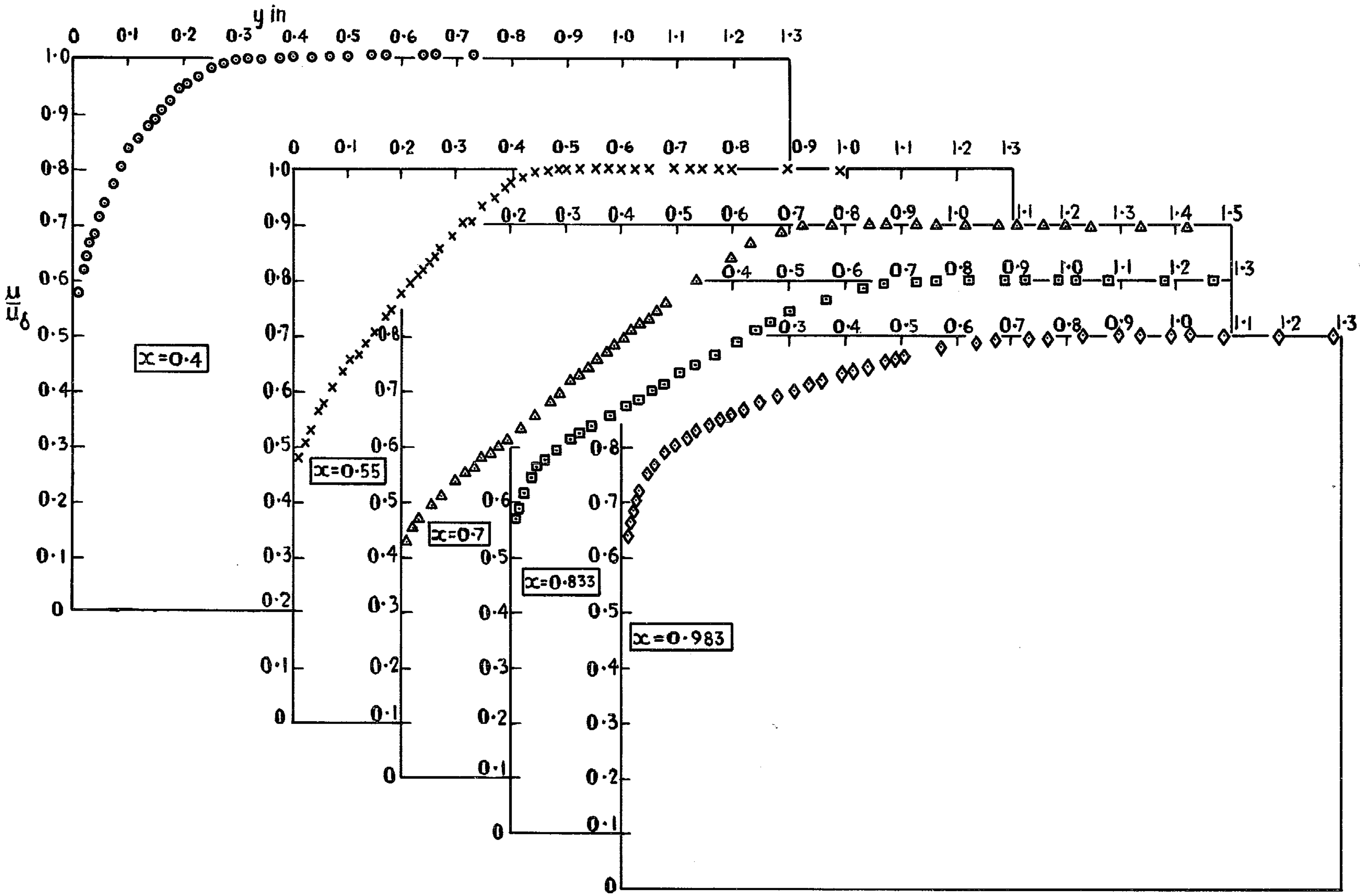

FIG. 7d. Velocity profiles $M_\infty = 1{\cdot}700$ $Re_l = 10{\cdot}00 \times 10^6$.

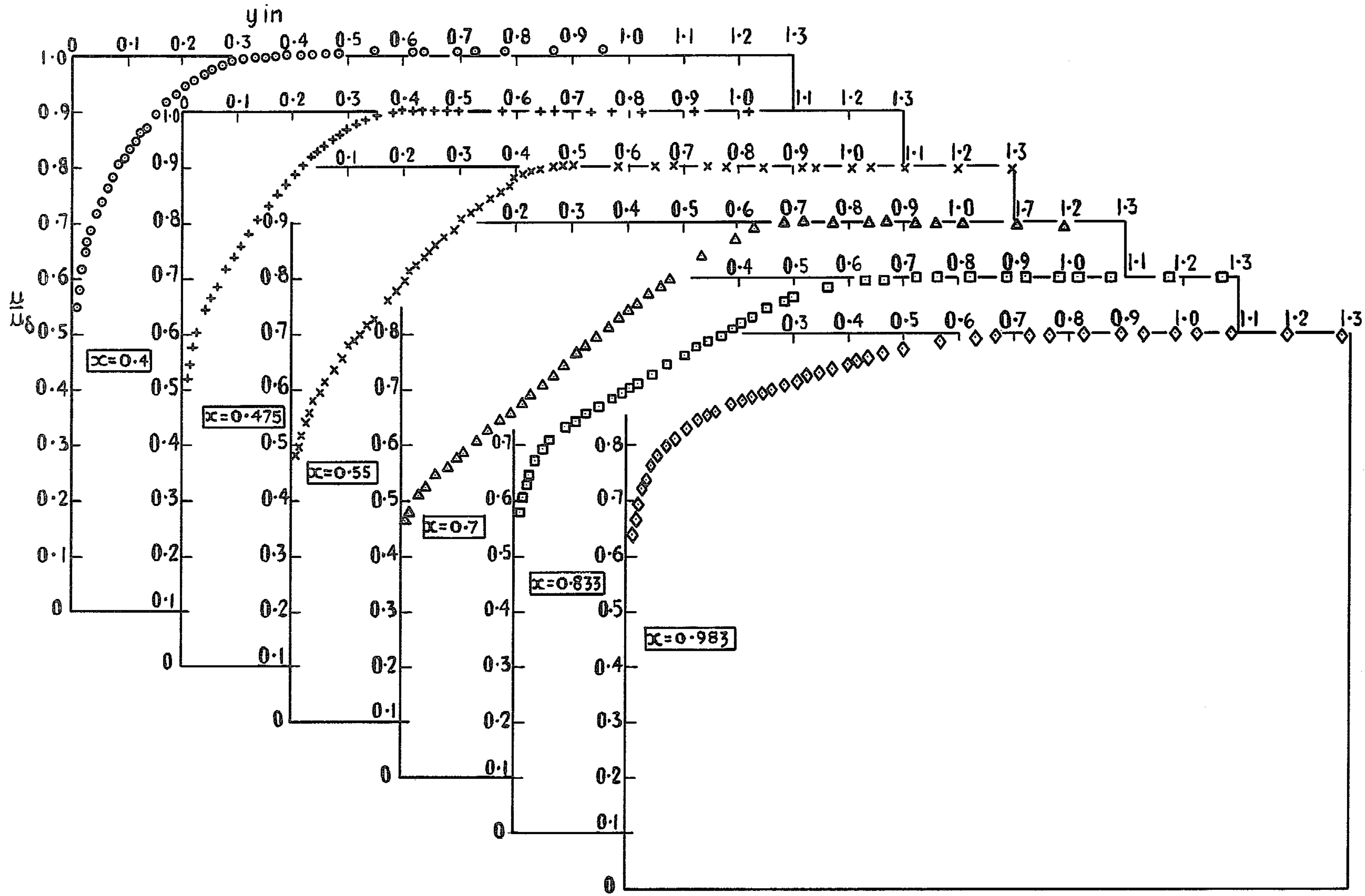

FIG. 7e. Velocity profiles $M_\infty = 2{\cdot}001$ $Re_l = 9{\cdot}88 \times 10^6$.

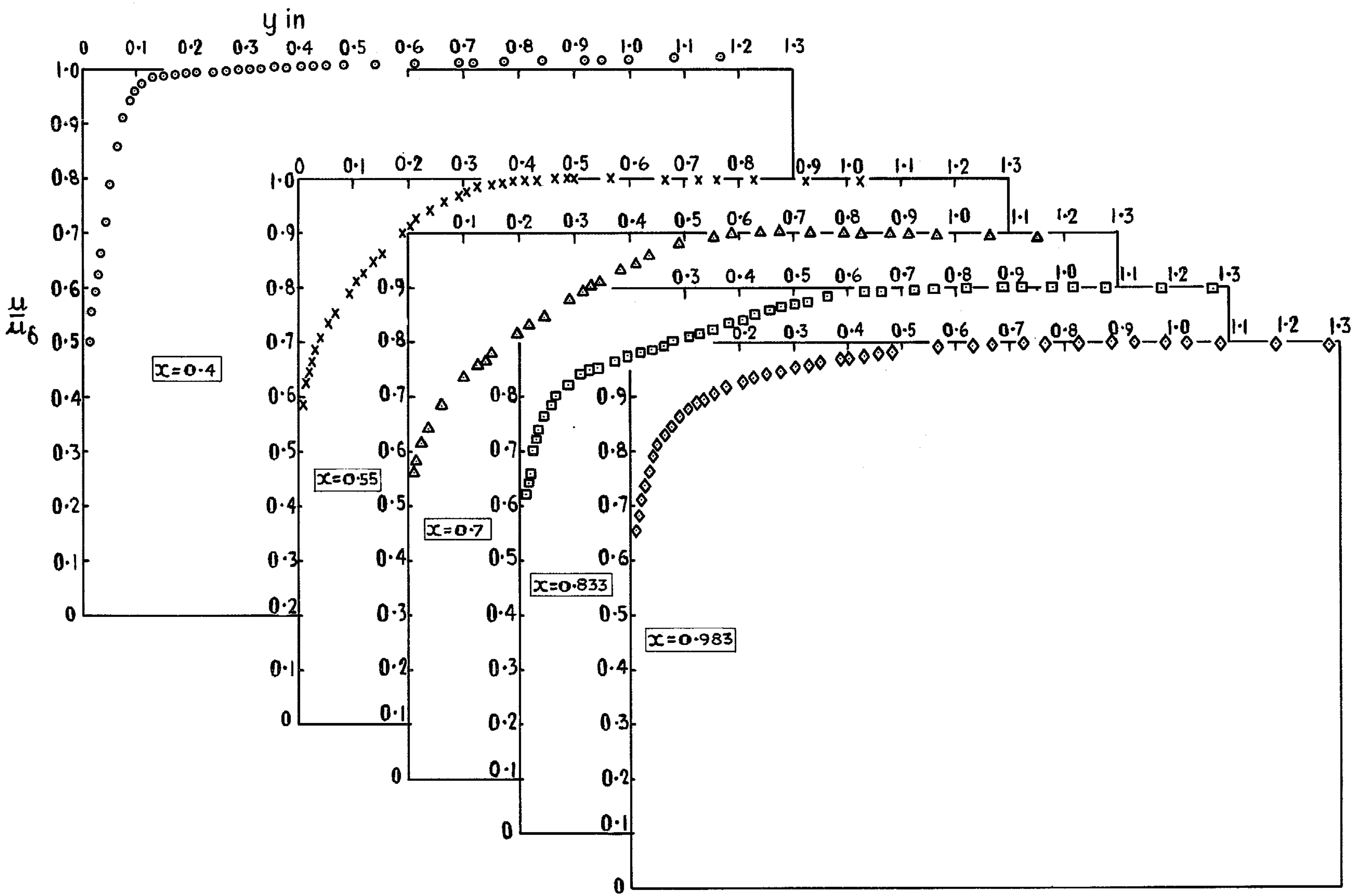

FIG. 7f. Velocity profiles $M_{\infty} = 2{\cdot}401$ $Re_l = 9{\cdot}92 \times 10^6$.

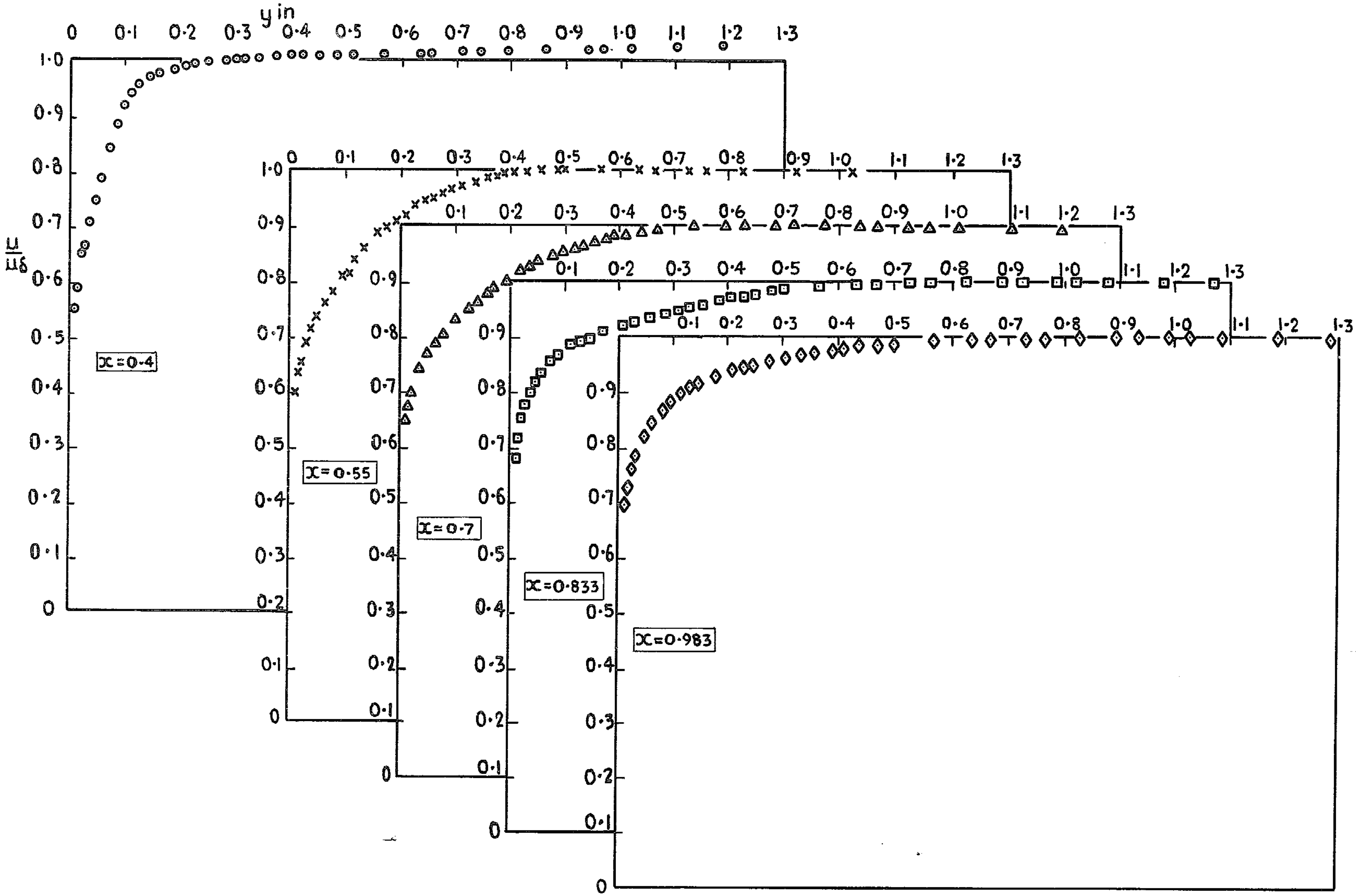

FIG. 7g. Velocity profiles $M_x = 2{\cdot}798$ $Re_l = 10{\cdot}10 \times 10^6$.

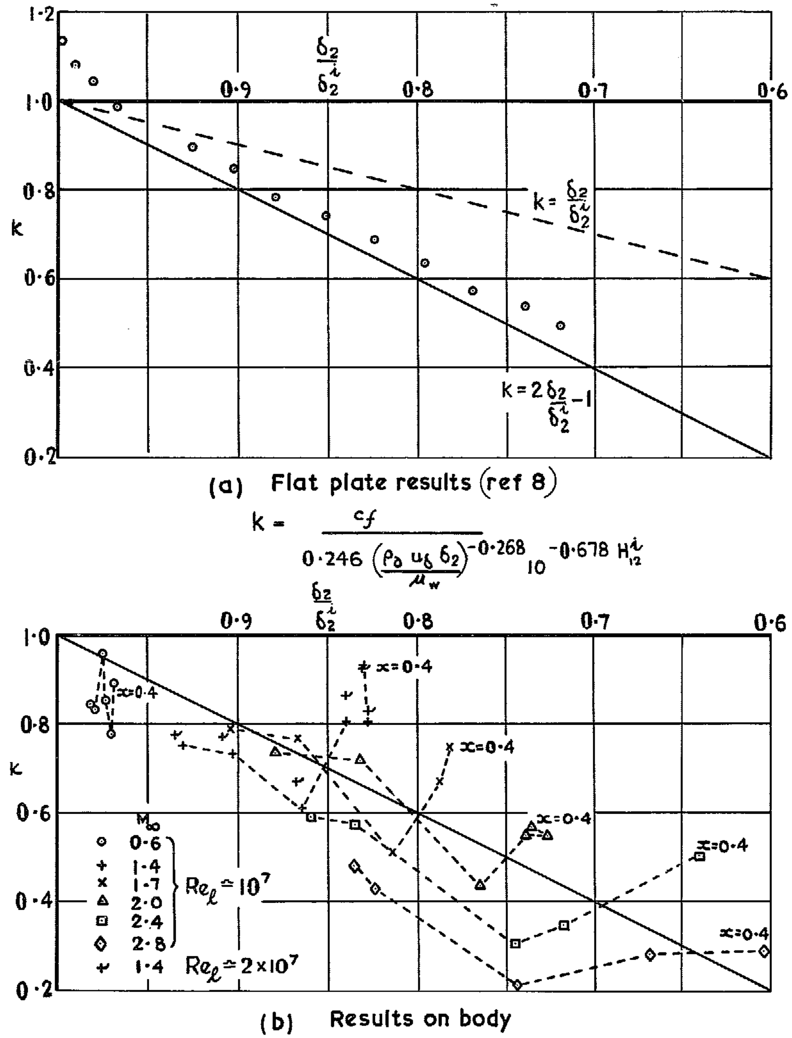

FIG. 8 a & b. Compressibility correction to Ludwieg-Tillman formula.

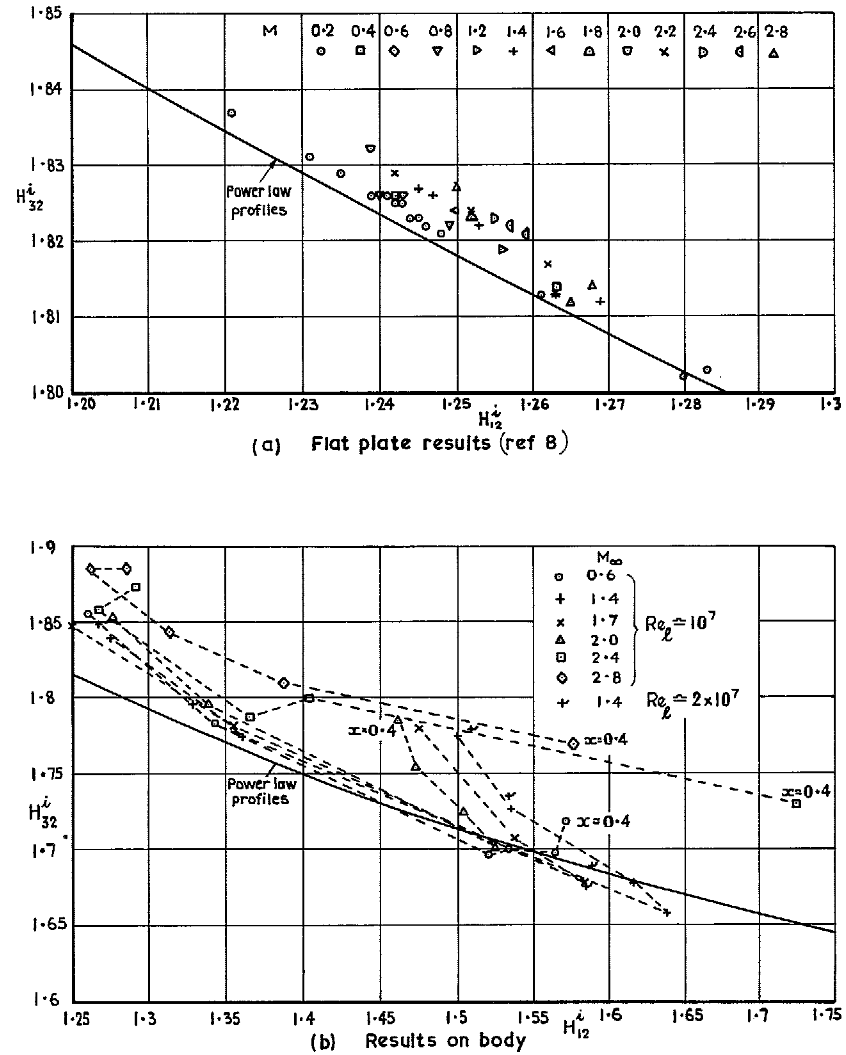

FIG. 9 a & b. Relationship between 'incompressible' shape parameters.

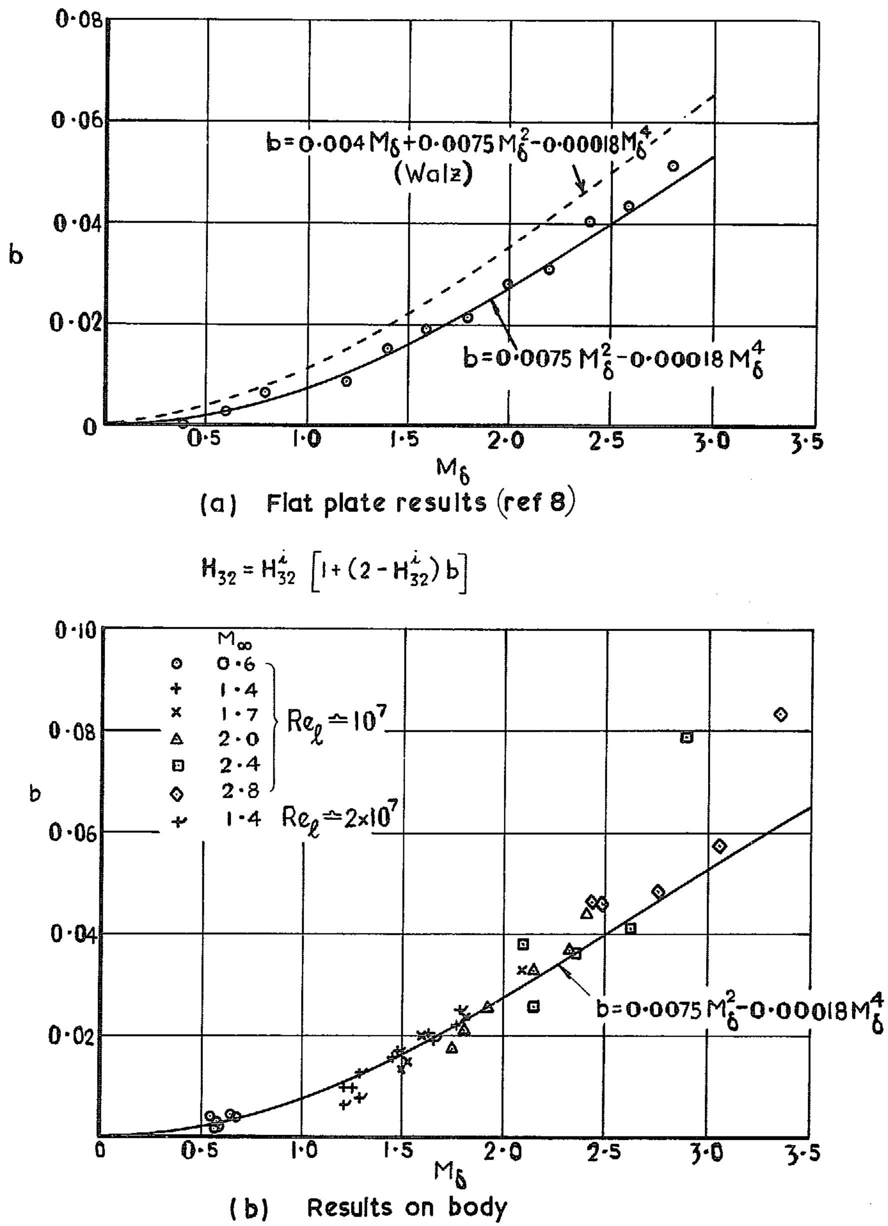

FIG. 10 a & b. Relationship between H_{32} and H^i_{32}.

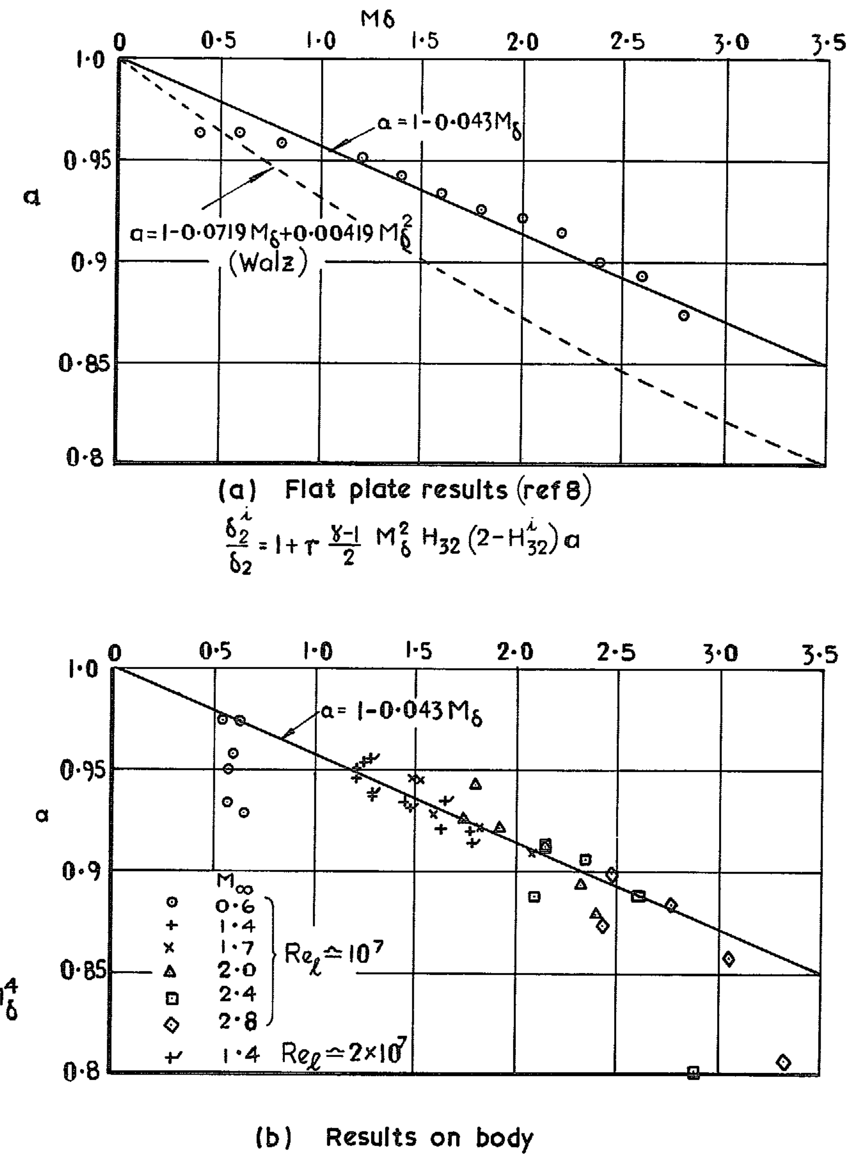

FIG. 11 a & b. Determination of $\frac{\delta_2^i}{\delta_2}$.

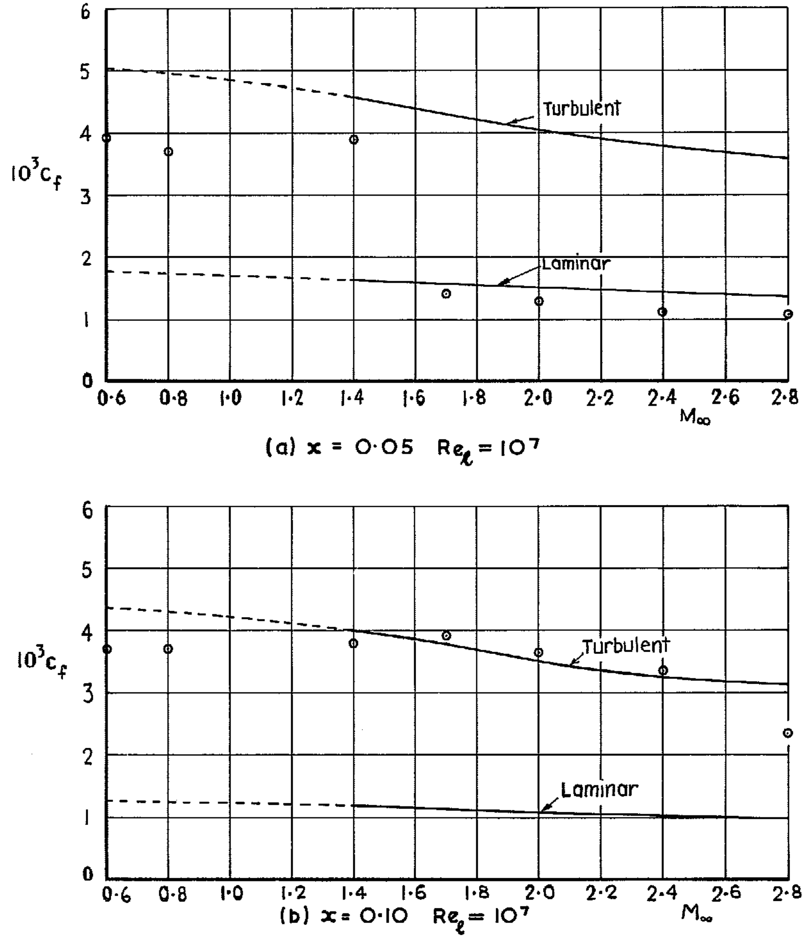

FIG. 12 a & b. Skin friction on conical nose.

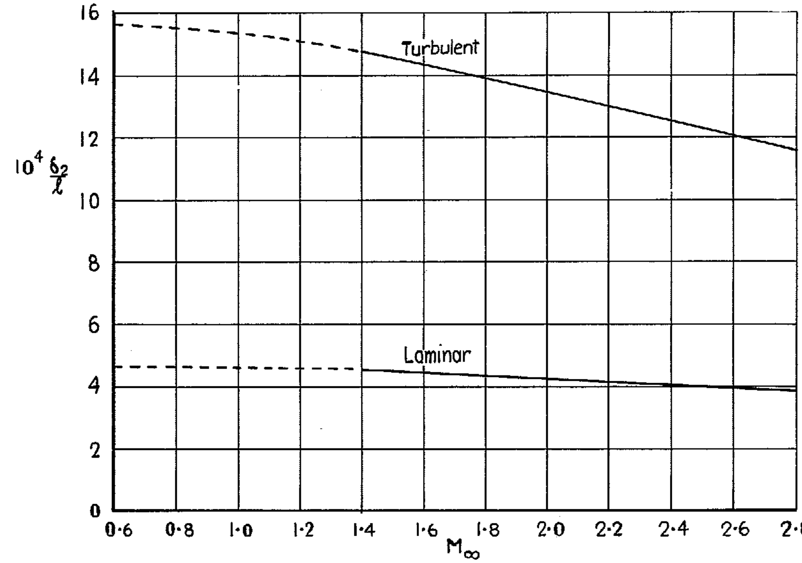

FIG. 13. Calculated momentum thickness $x = 0{\cdot}1416$ $Re_l = 10^7$.

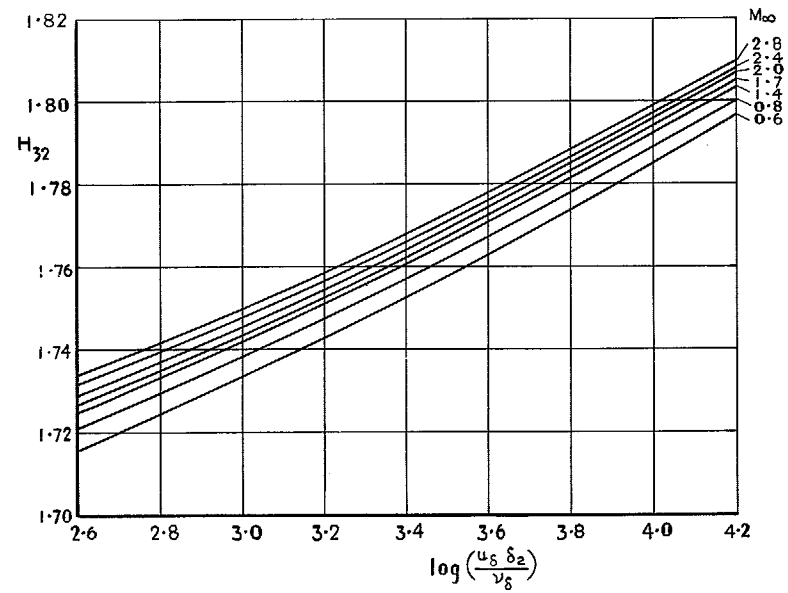

FIG. 14. Chart for determination of H_{32} at $x = 0{\cdot}1416$.

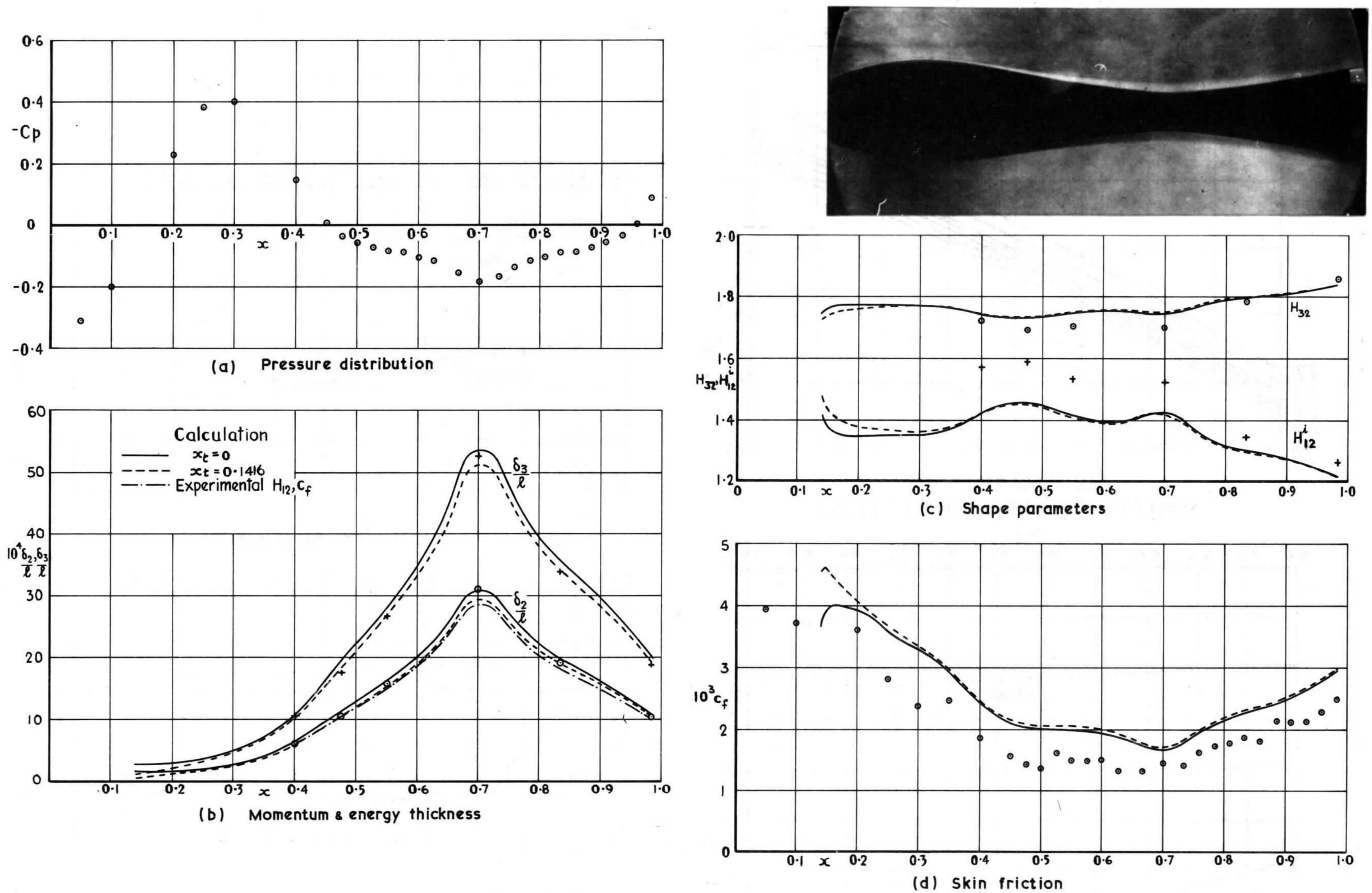

FIG. 15. Comparison of calculation and experiment $M_\infty = 0{\cdot}597$ $Re_l \simeq 10^7$.

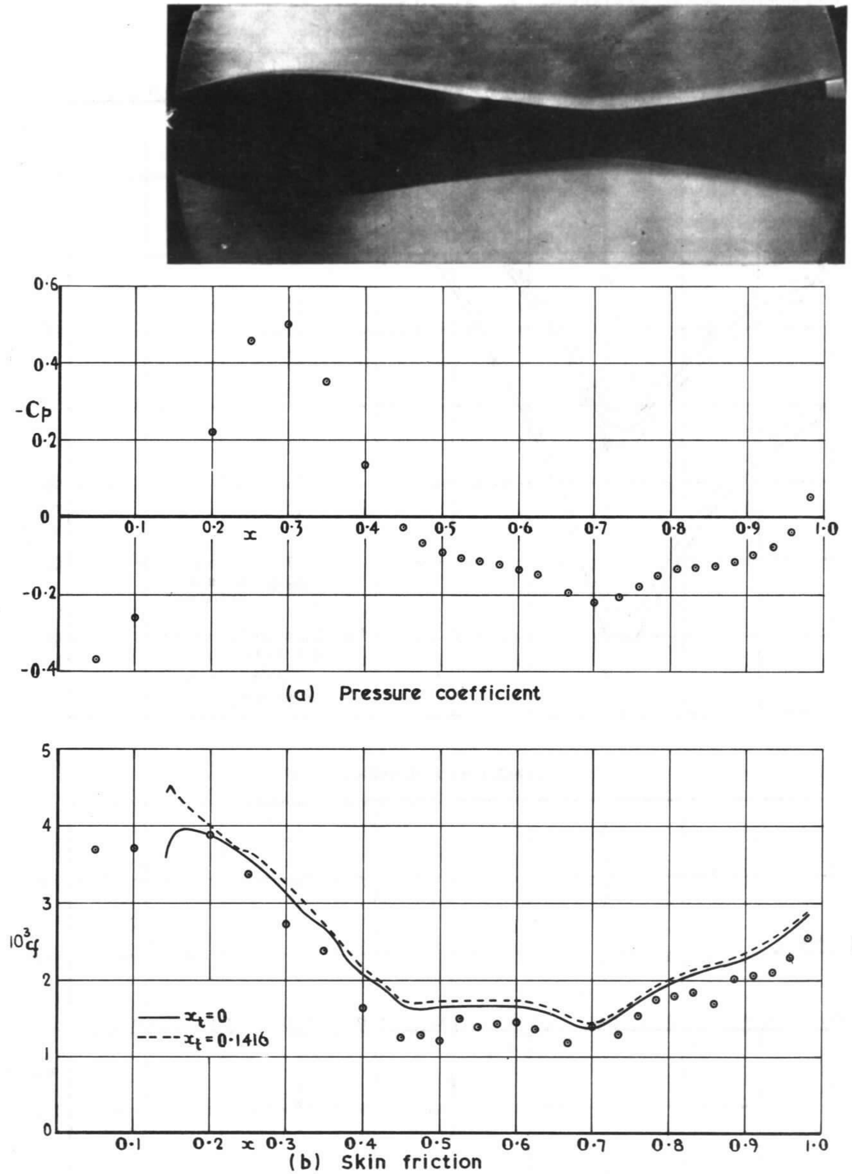

FIG. 16 a & b. Comparison of experiment and calculation $M_\infty = 0{\cdot}801$ $Re_l \simeq 10^7$.

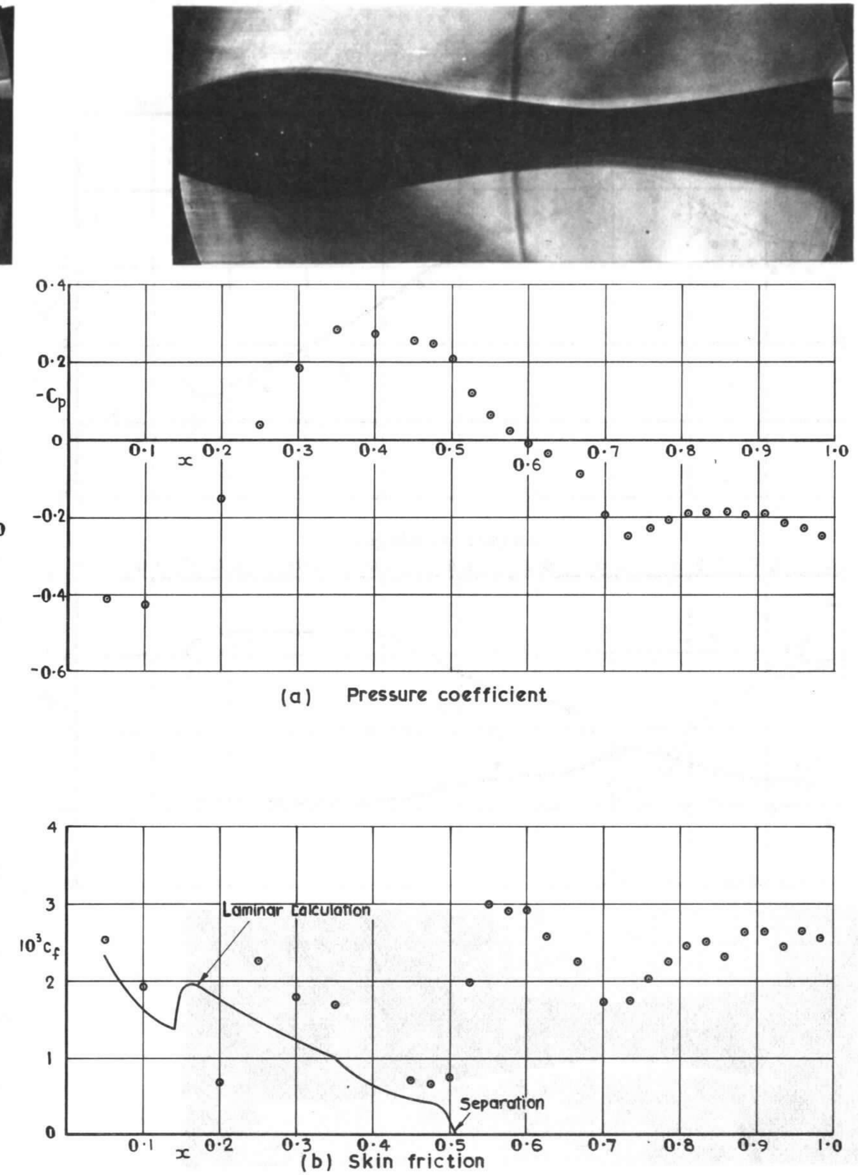

FIG. 17 a & b. Comparison of experiment and calculation $M_\infty = 1{\cdot}390$ $Re_l \simeq 5 \times 10^6$.

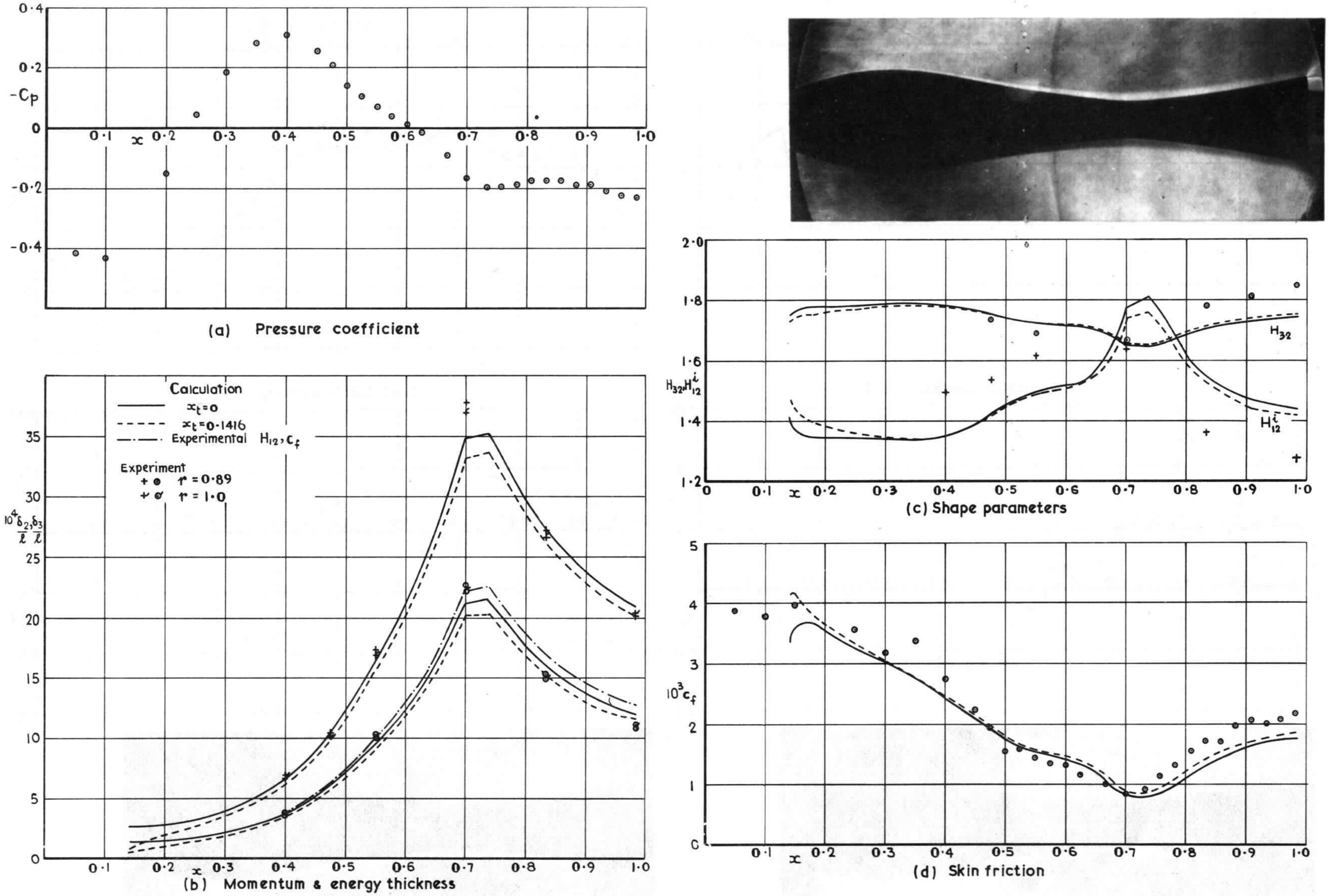

FIG. 18. Comparison of experiment and calculation $M_\infty = 1{\cdot}398$ $Re_l \simeq 10^7$.

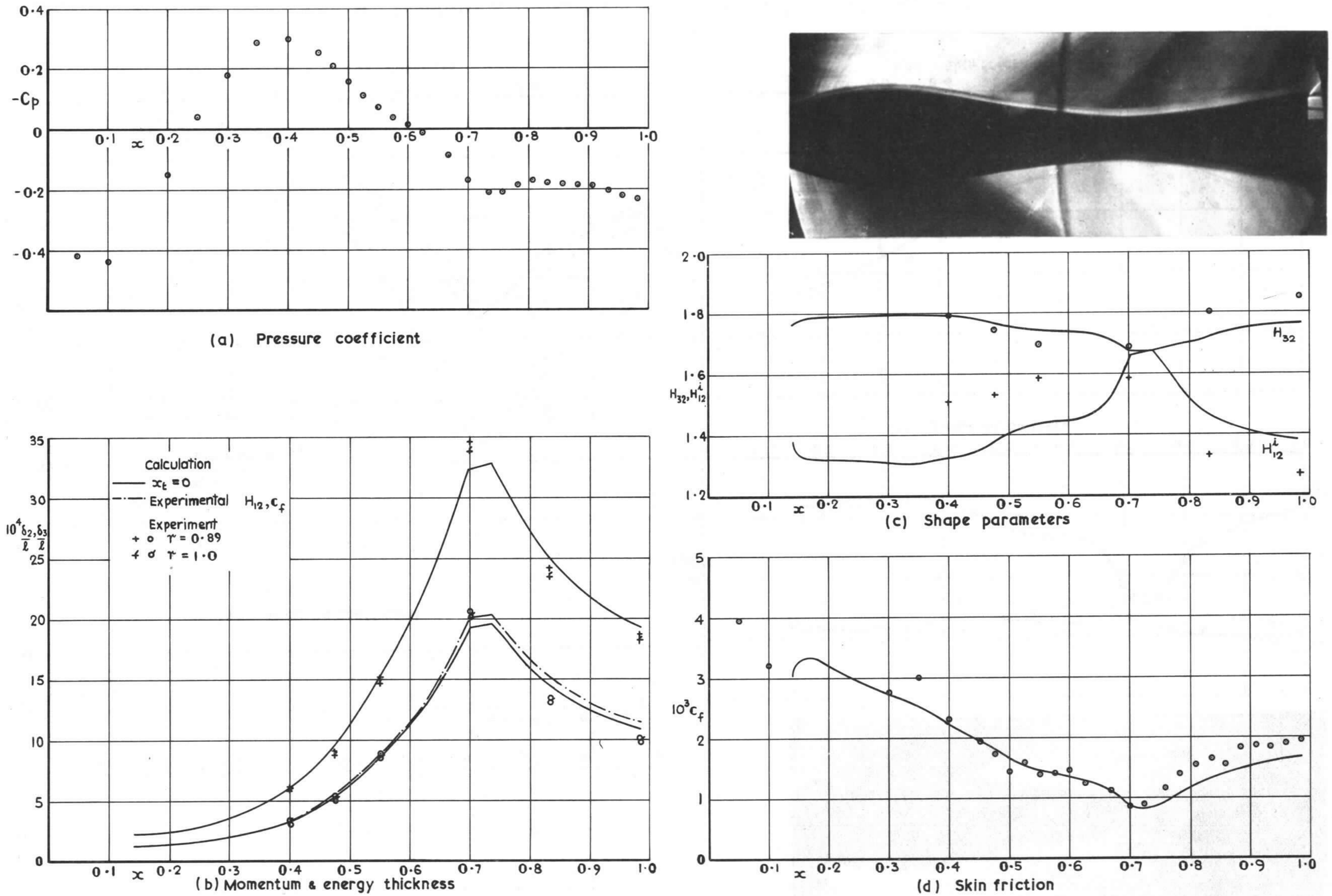

FIG. 19. Comparison of calculation and experiment $M_\infty = 1{\cdot}404$ $Re_l \simeq 2 \times 10^7$.

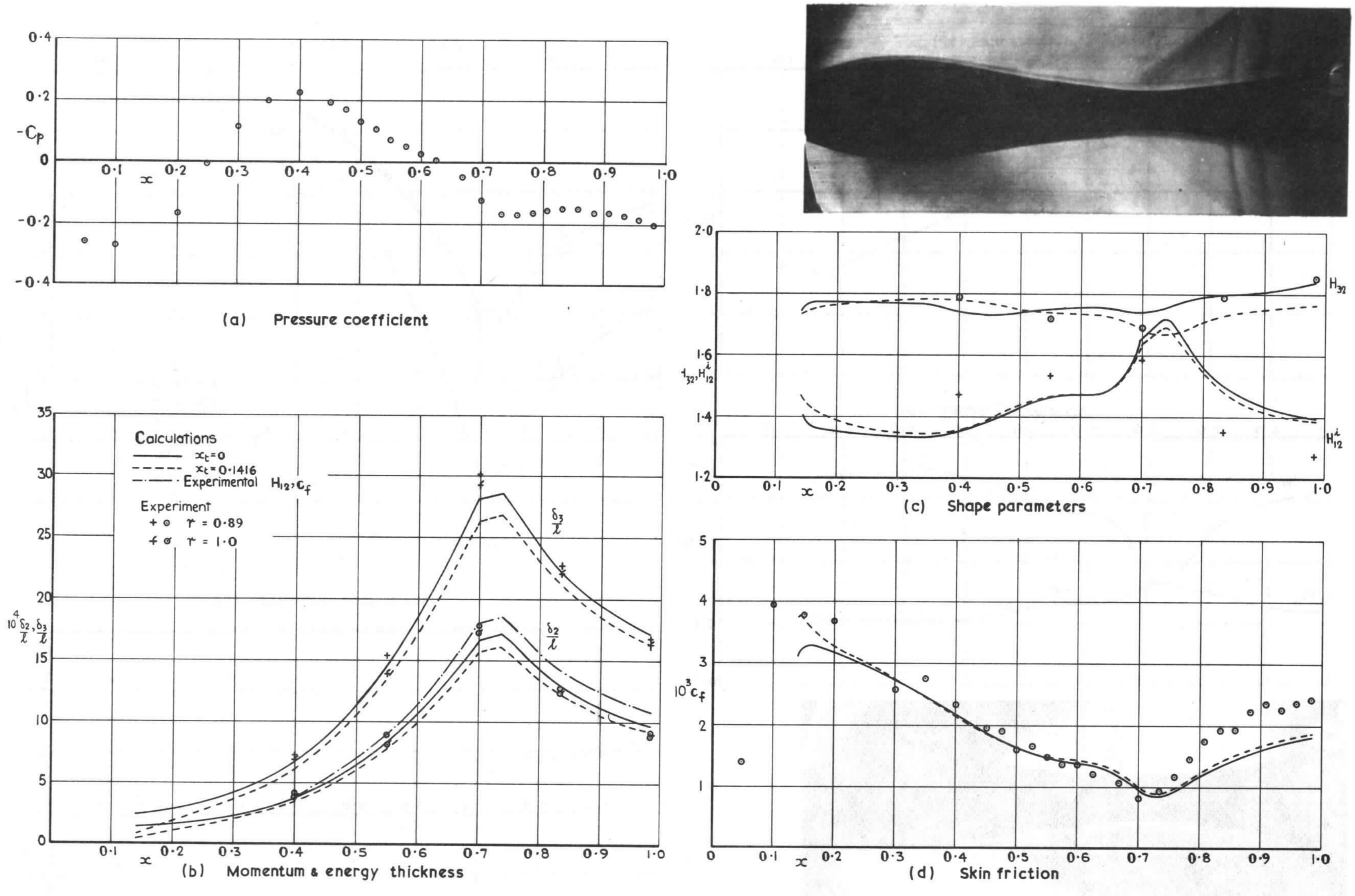

FIG. 20. Comparison of calculation and experiment $M_\infty = 1{\cdot}700$ $Re_l \simeq 10^7$.

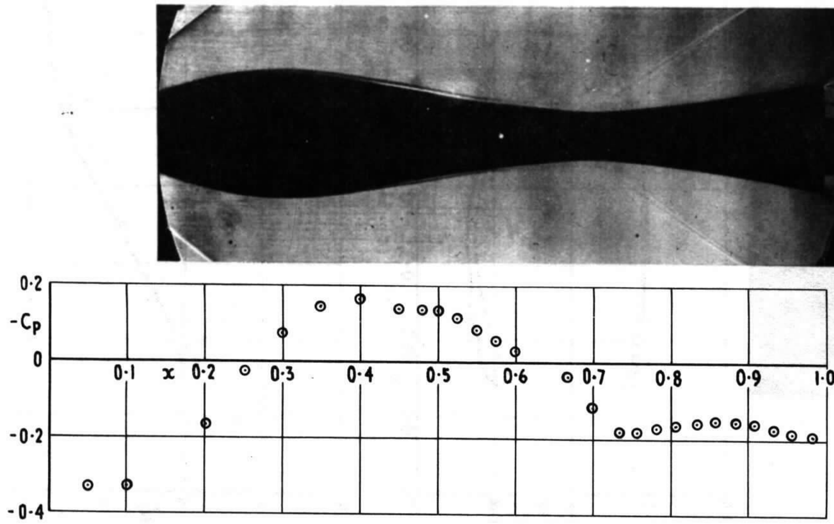

(a) Pressure coefficient

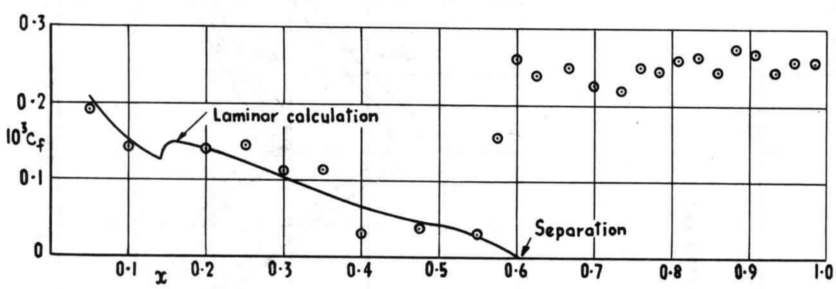

(b) Skin friction

FIG. 21 a & b. Comparison of calculation and experiment $M_\infty = 1{\cdot}996$ $Re_l \simeq 5 \times 10^6$.

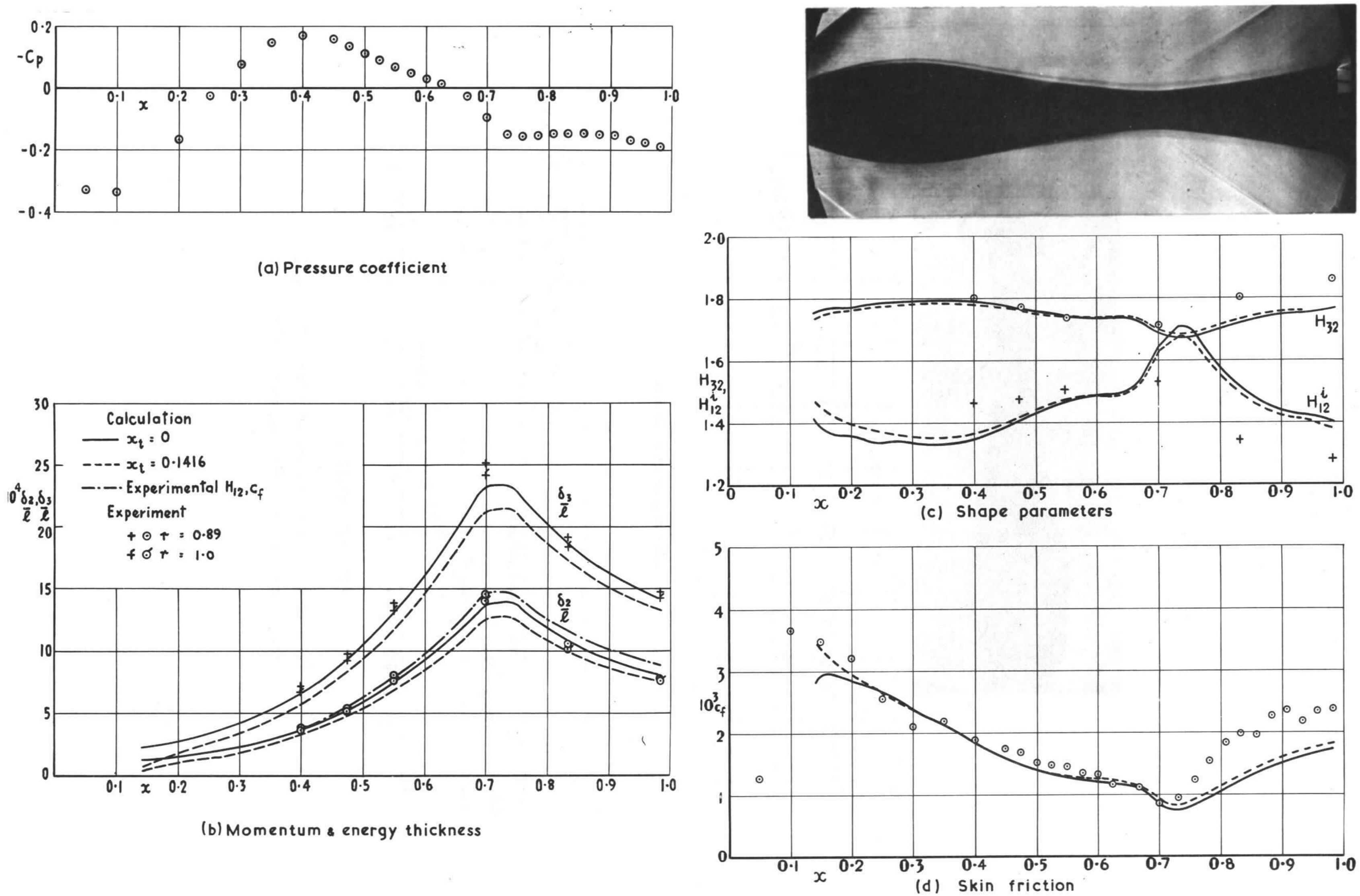

FIG. 22. Comparison of calculation and experiment $M_\infty = 2{\cdot}000$ $Re_l \simeq 10^7$.

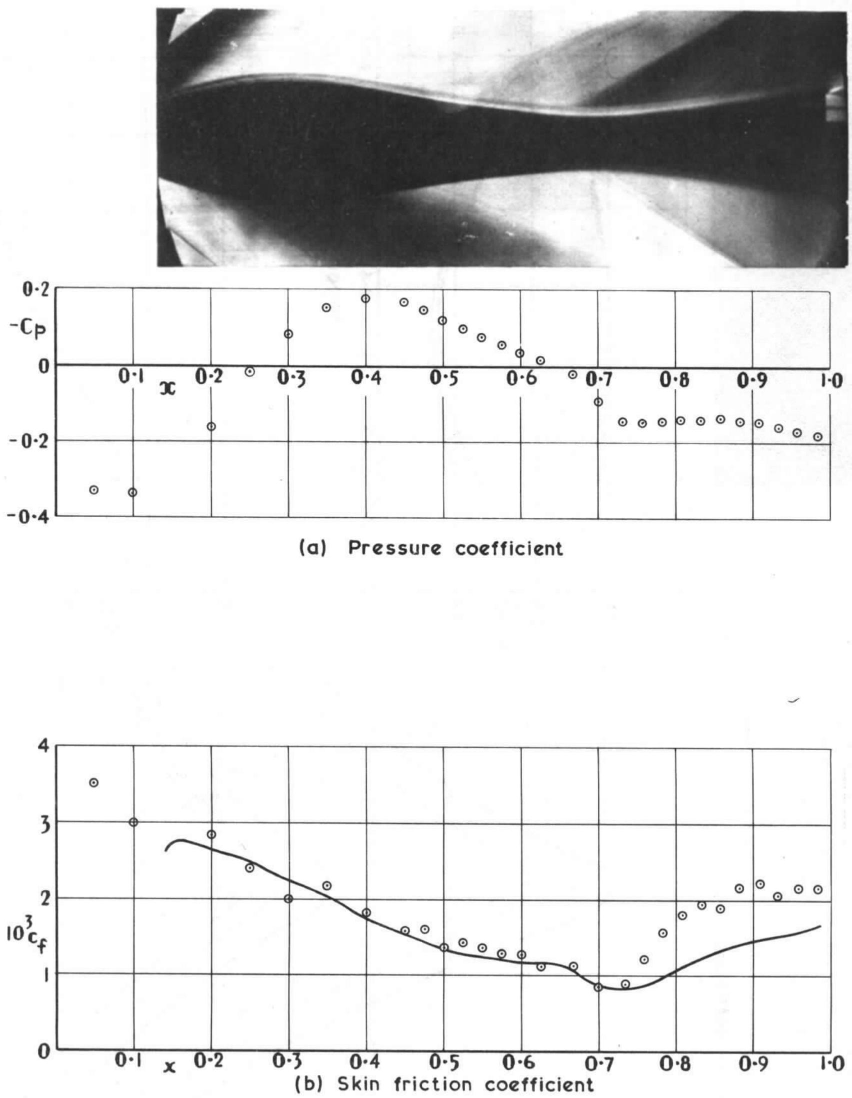

FIG. 23 a & b. Comparison of calculation and experiment $M_\infty = 2{\cdot}002\ Re_l \simeq 1{\cdot}7 \times 10^7$.

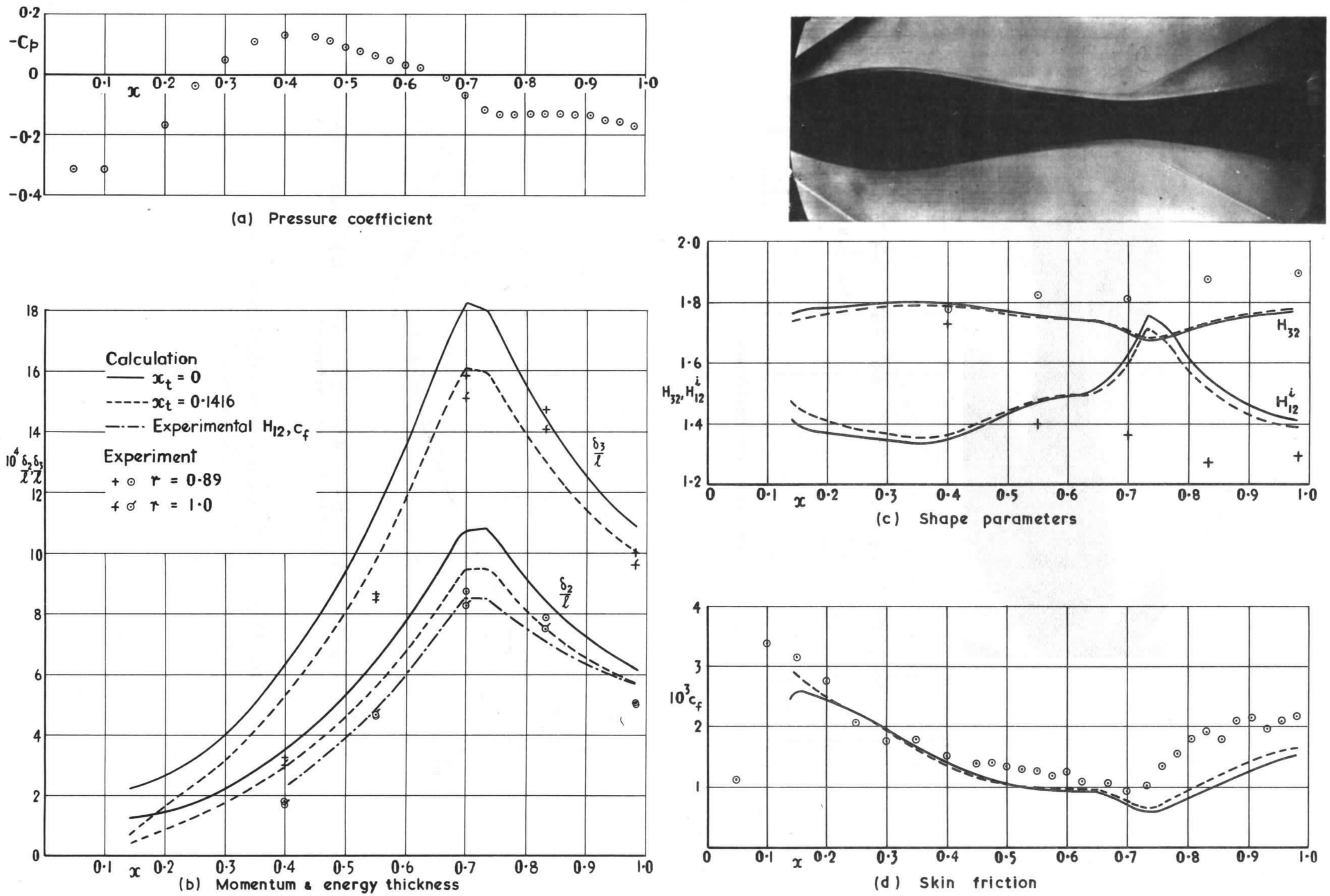

FIG. 24. Comparison of calculation and experiment $M_\infty = 2{\cdot}401$ $Re_l \simeq 10^7$.

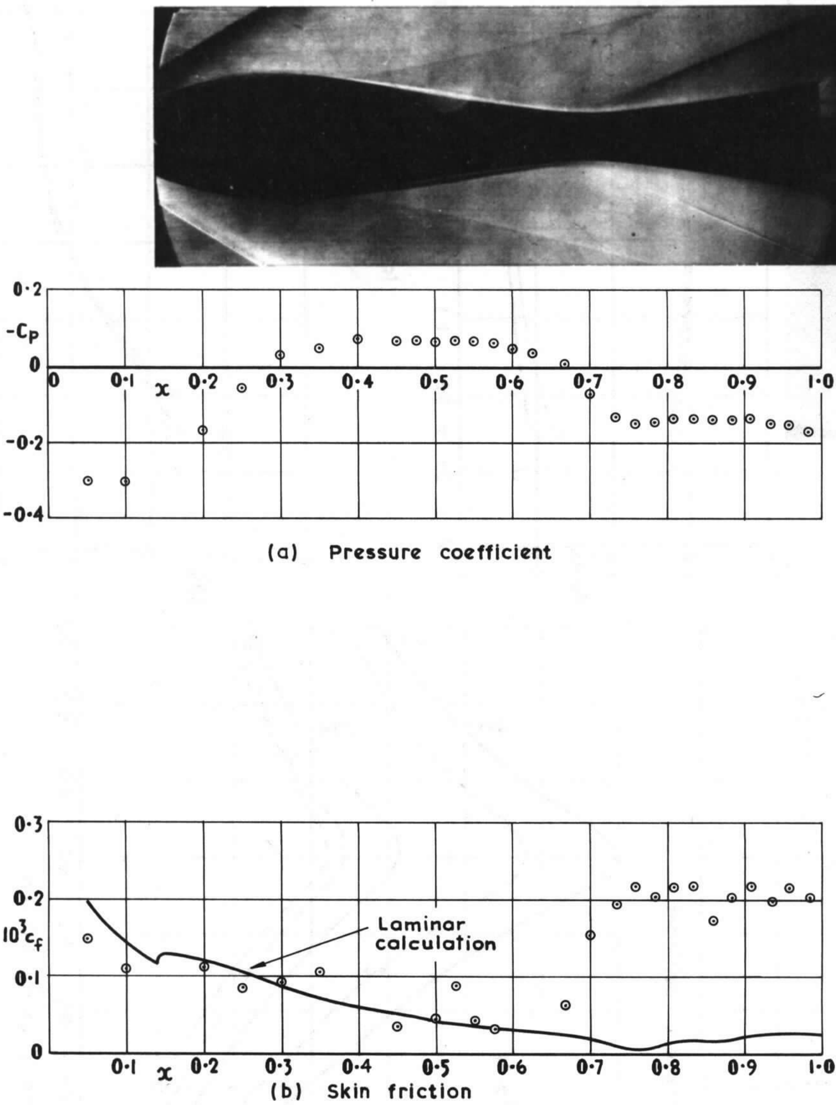

FIG. 25 a & b. Comparison of calculation and experiment $M_\infty = 2{\cdot}793$ $Re_l \doteq 5 \times 10^6$.

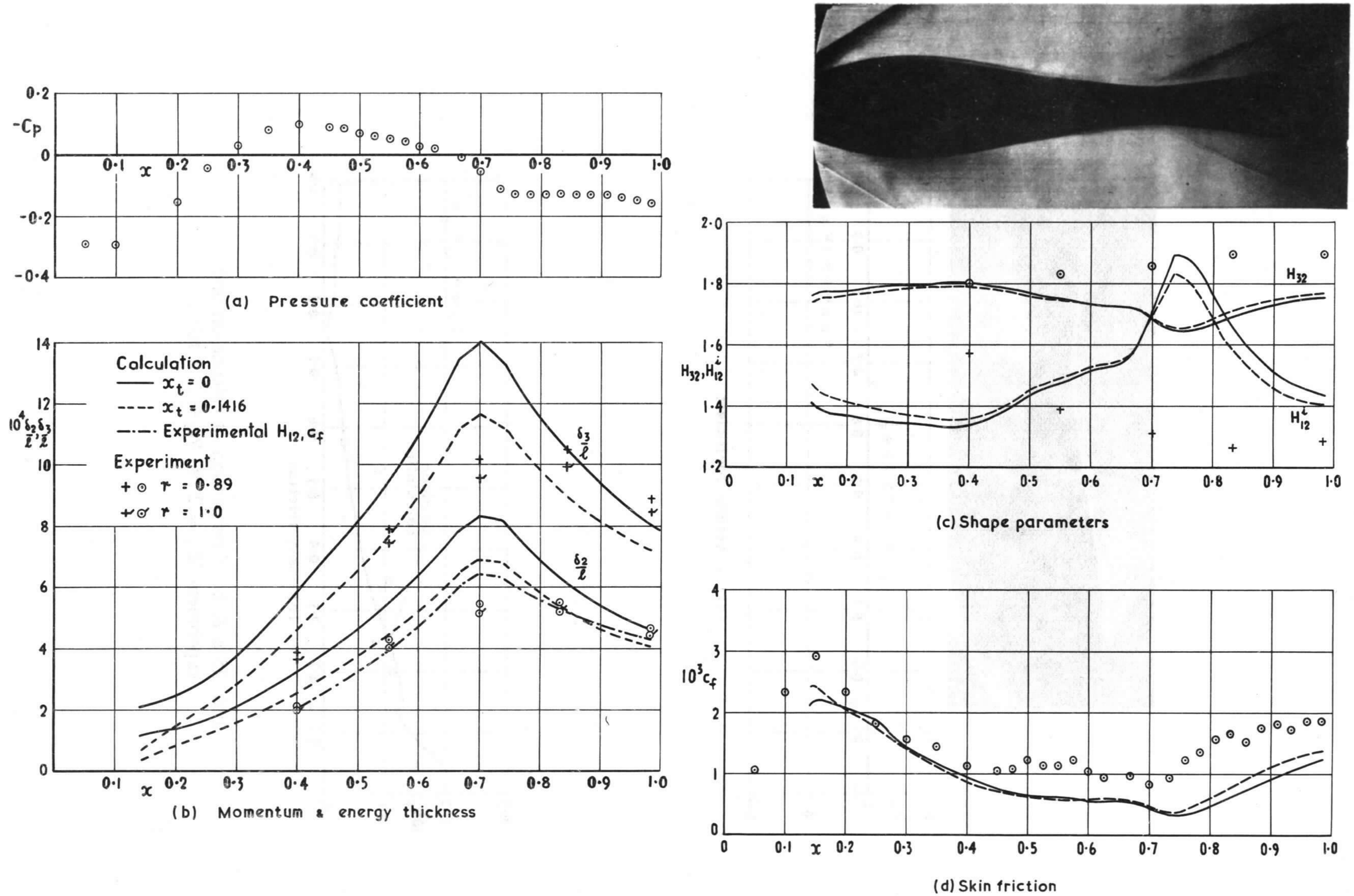

FIG. 26. Comparison of calculation and experiment $M_\infty = 2{\cdot}799$ $Re_l \simeq 10^7$.

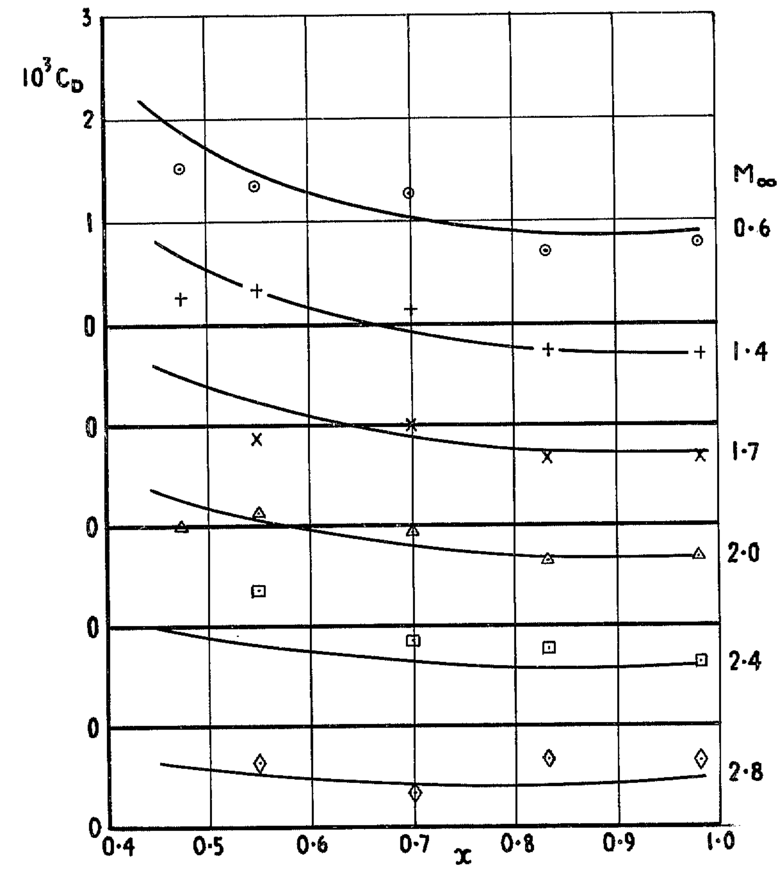

FIG. 27. 'Mean' dissipation coefficient $Re_l \simeq 10^7$.

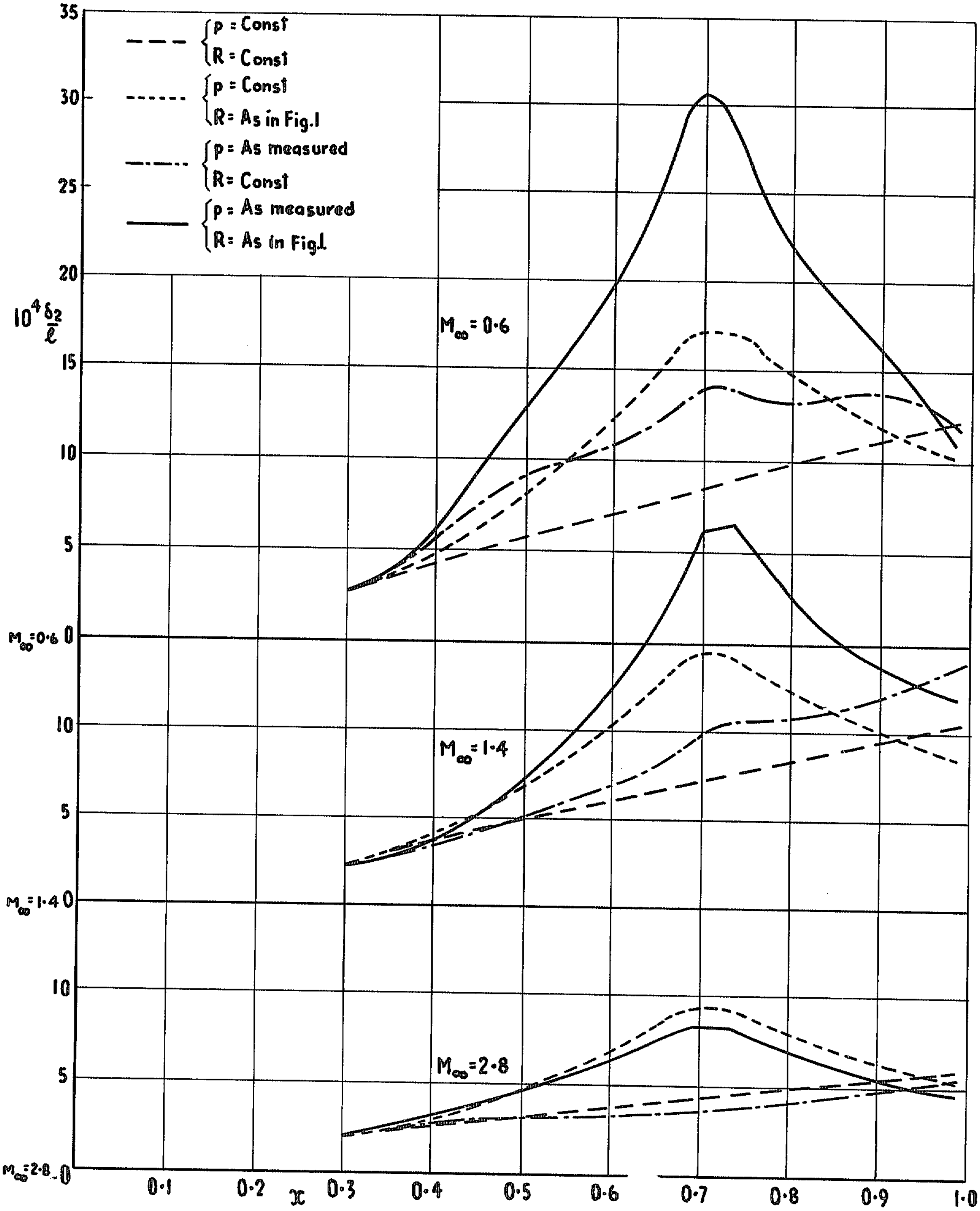

FIG 28. Influence of pressure gradient and streamline convergence on momentum thickness $Re_l = 10^7$.

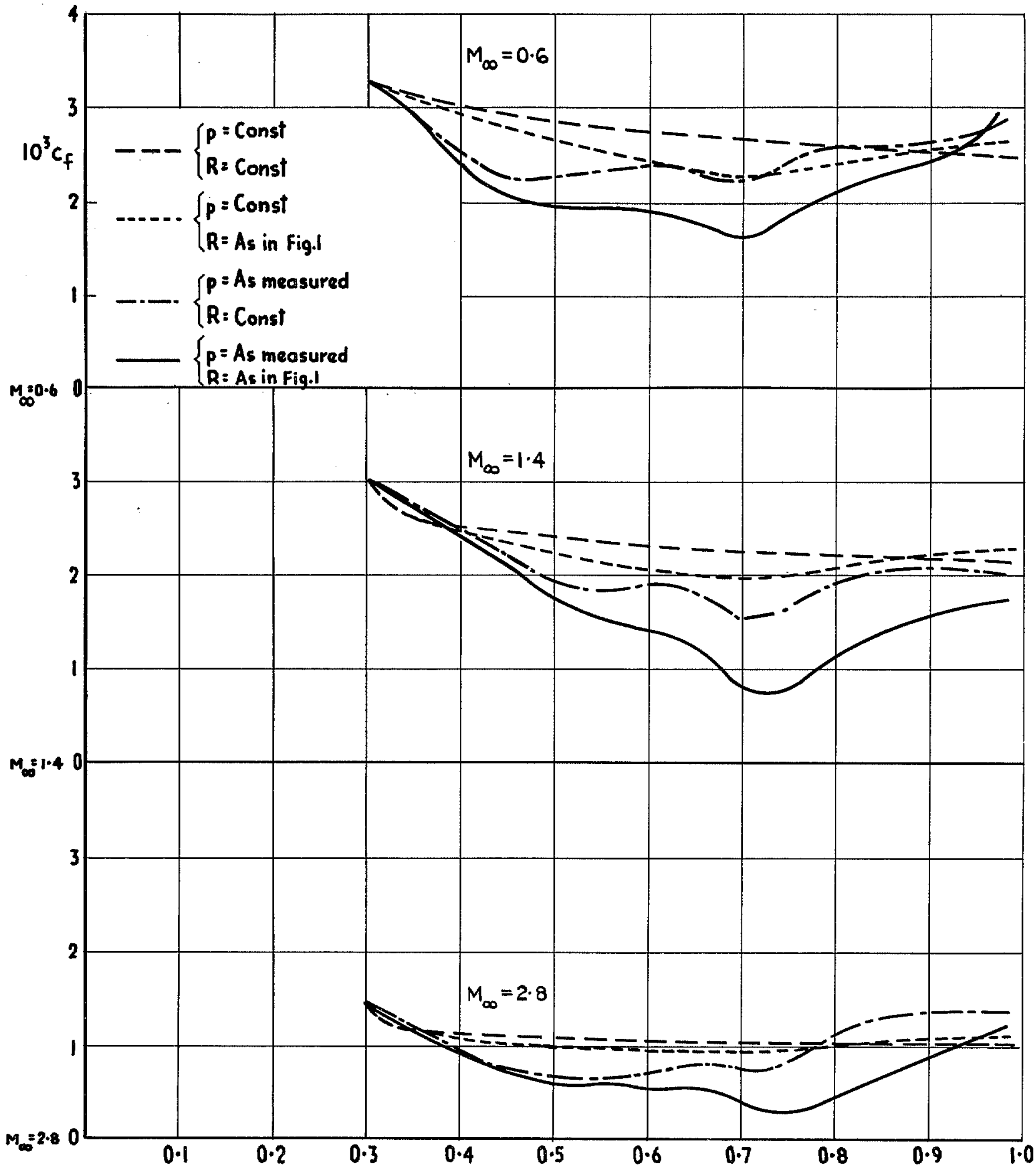

FIG. 29. Influence of pressure gradient and streamline convergence on skin friction $Re_l = 10^7$.

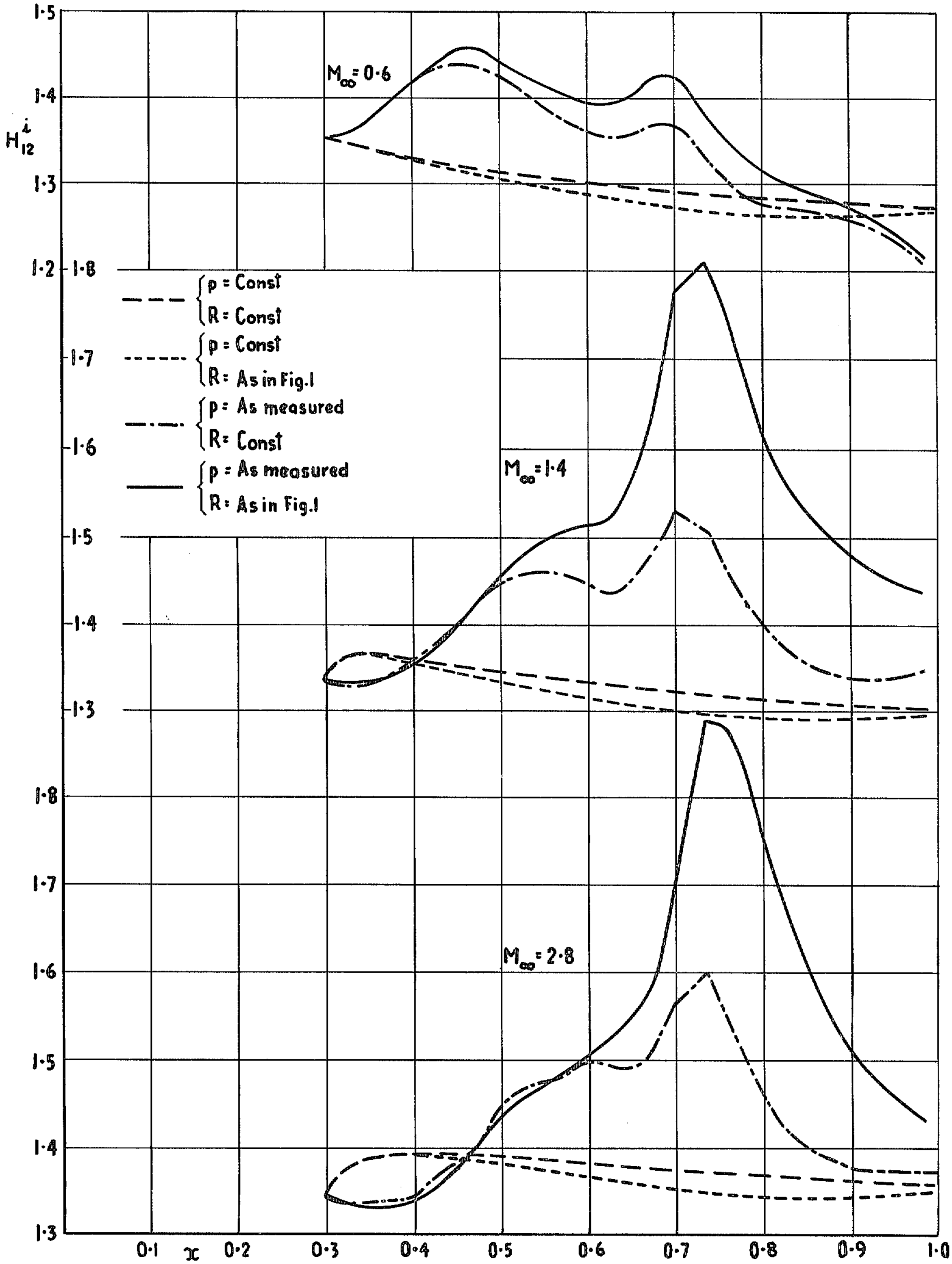

FIG. 30. Influence of pressure gradient and streamline convergence on shape parameter H^i_{12} $Re_l = 10^7$.

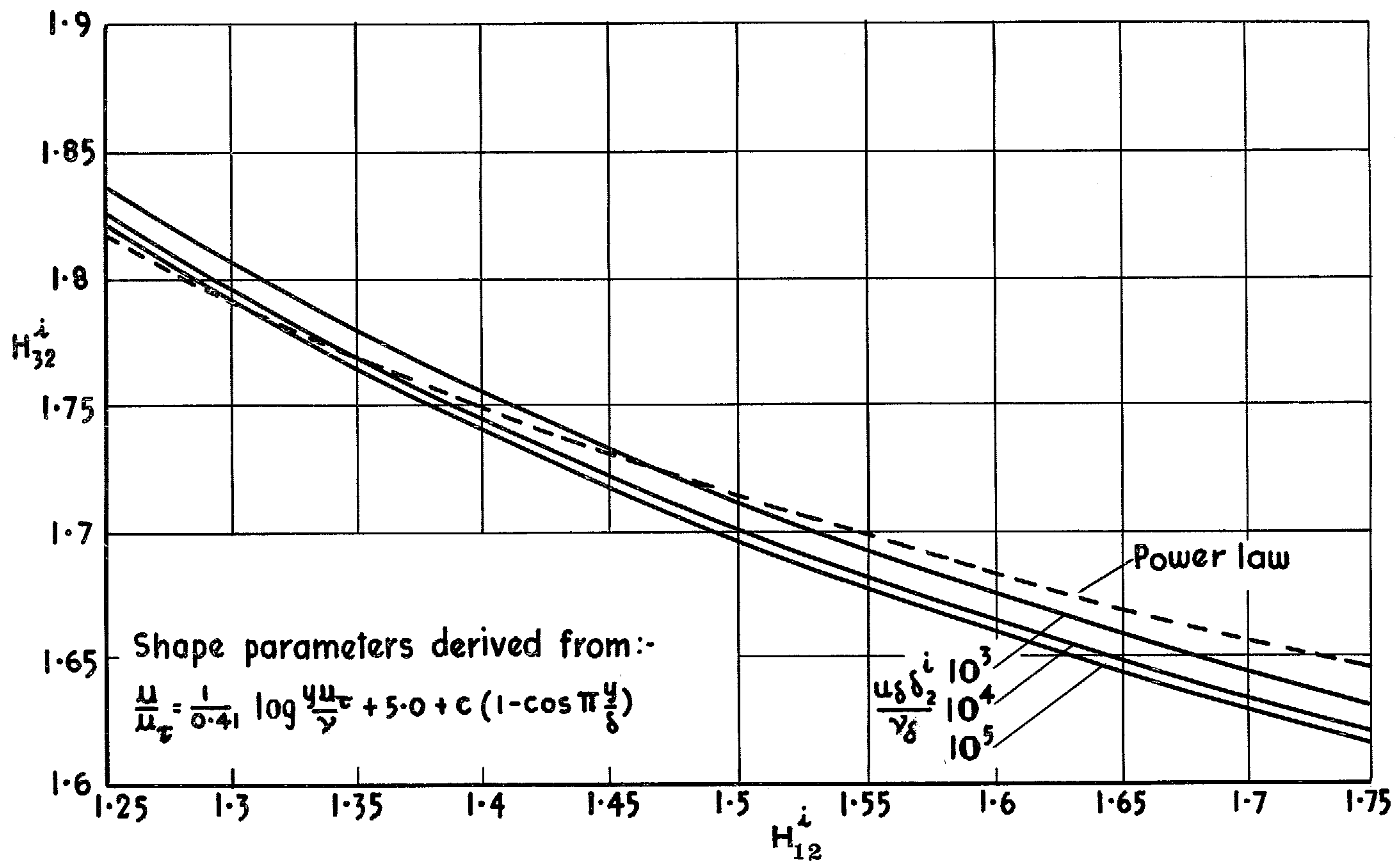

FIG. 31. Alternative shape parameter correlation.

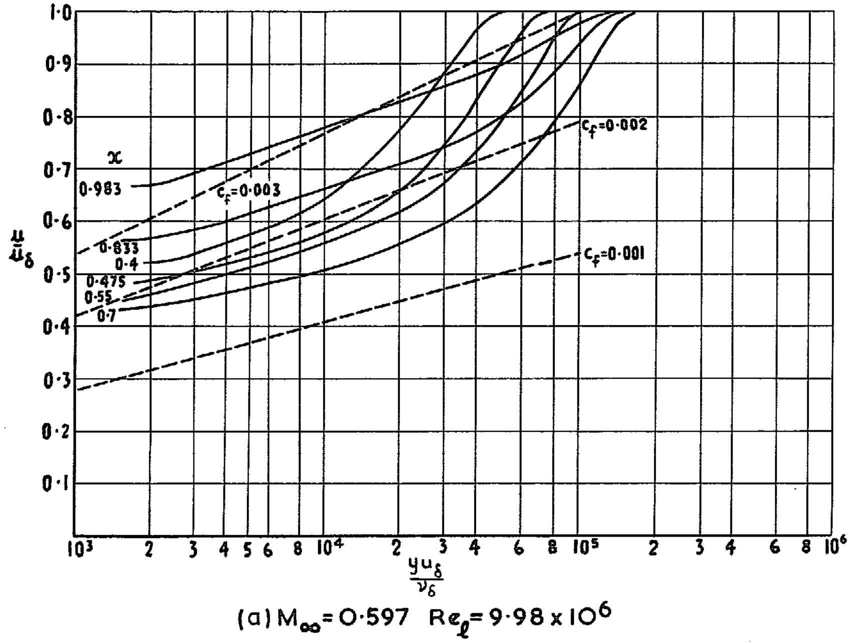

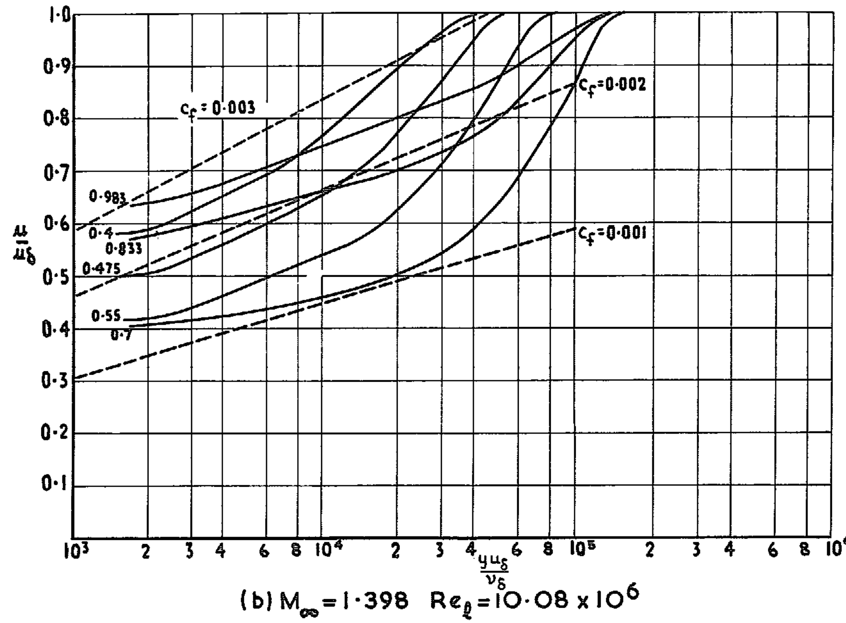

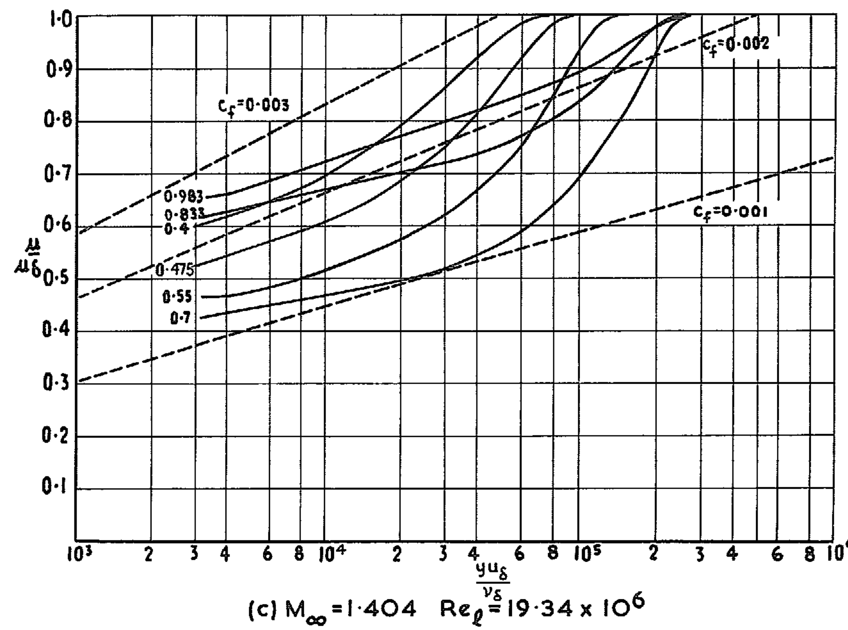

FIG. 32 a to c. Semi-logarithmic plot of velocity profiles.

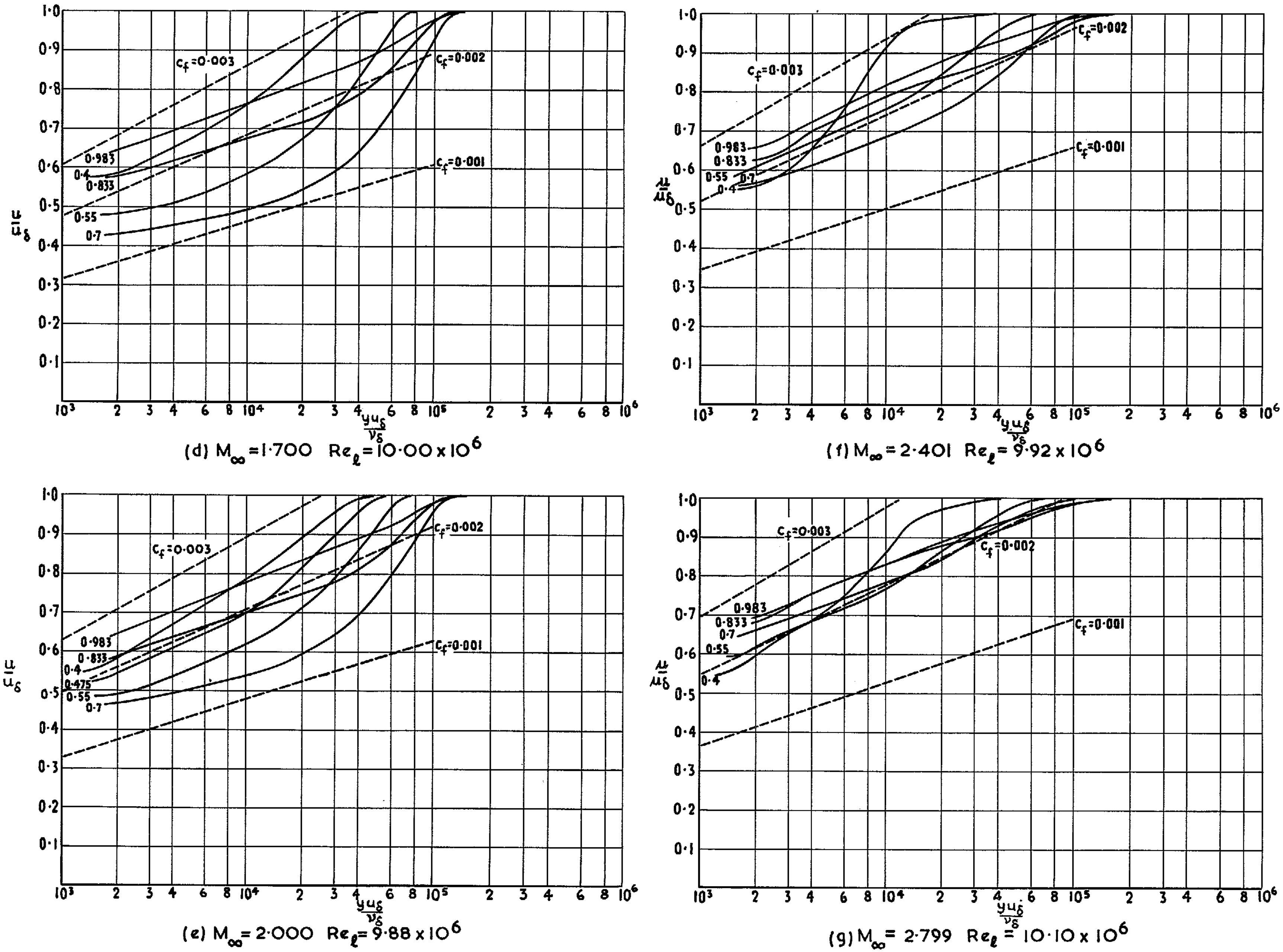

FIG. 32d to g. Semi-logarithmic plot of velocity profiles.

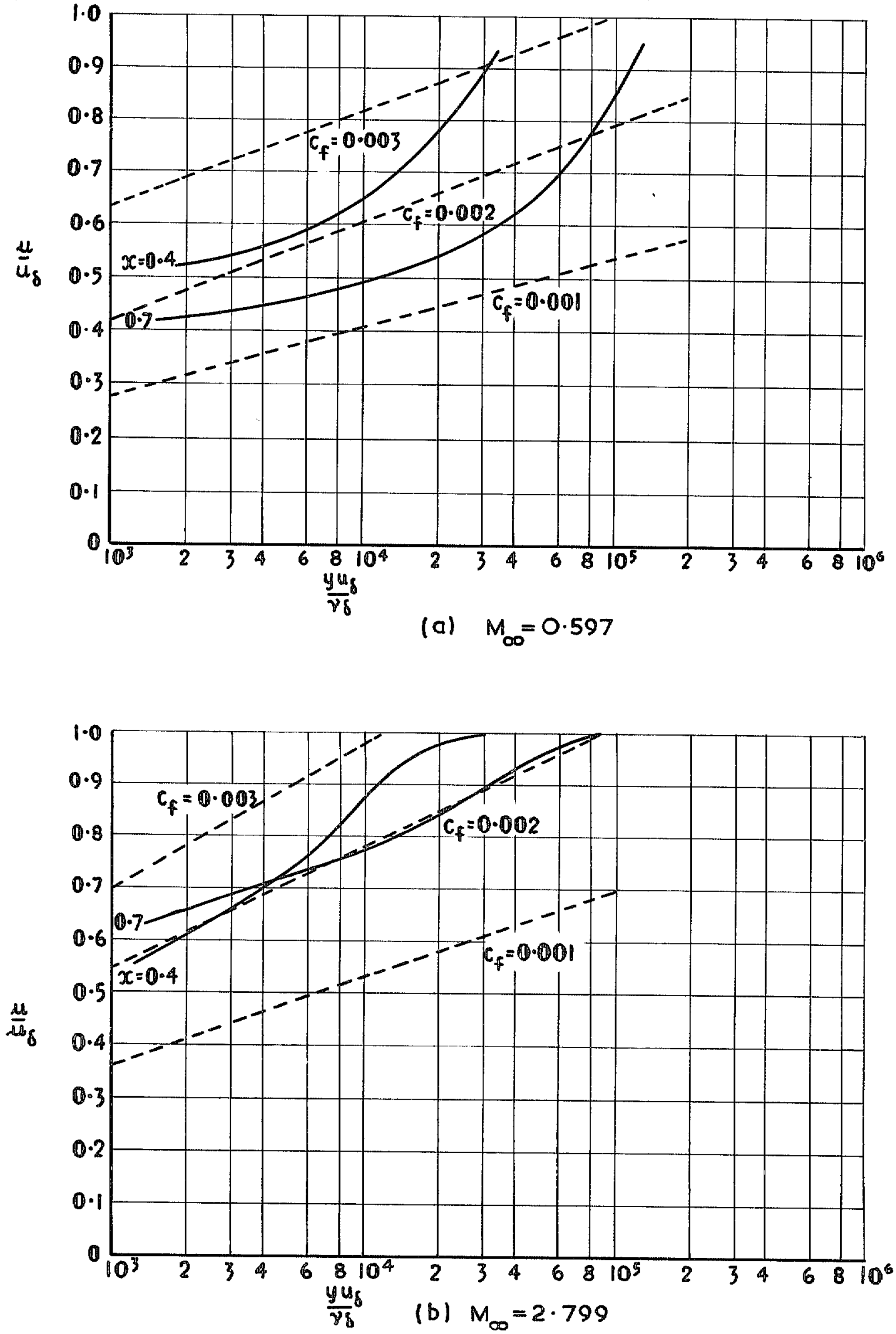

FIG. 33 a & b. Velocity profiles corrected for normal pressure gradient.

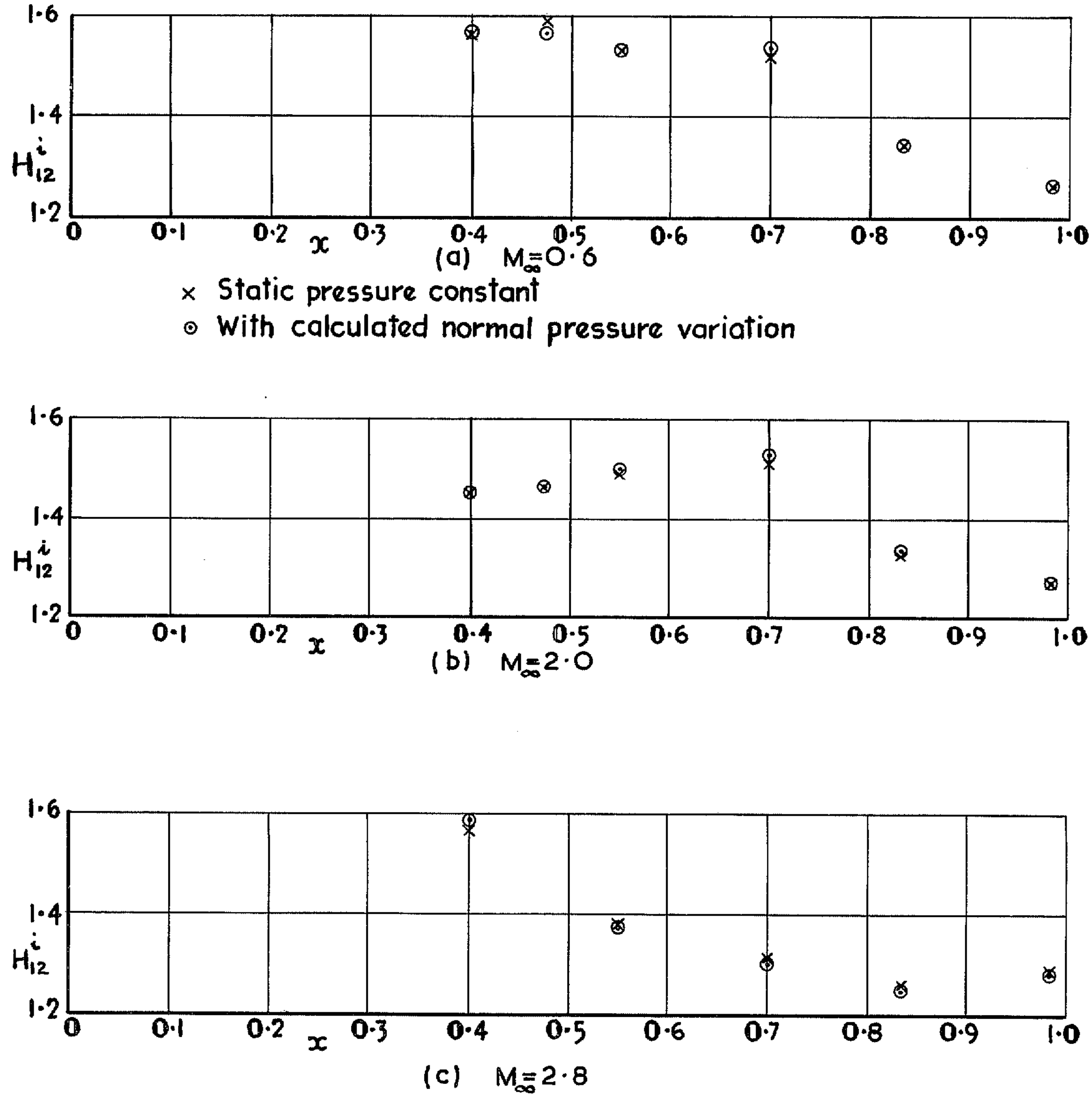

FIG. 34 a to c. Calculated effect of normal pressure gradients on shape parameter H^i_{12} ($r = 1$).

Printed in Wales for Her Majesty's Stationery Office by Allens Printers (Wales) Limited

Dd. 146916 K.5.

Published by
HER MAJESTY'S STATIONERY OFFICE

To be purchased from
49 High Holborn, London WC1
13a Castle Street, Edinburgh EH2 3AR
109 St Mary Street, Cardiff CF1 1JW
Brazennose Street, Manchester M60 8AS
50 Fairfax Street, Bristol BS1 3DE
258 Broad Street, Birmingham 1
7 Linenhall Street, Belfast BT2 8AY
or through any bookseller

R. & M. No. 3633
SBN 11 470333 7